Oxygen transfer of fine-bubble aeration systems in wastewater treatment: Influence of diffuser design on oxygen transfer at increased salt concentrations

vom Fachbereich 13

Bau- und Umweltingenieurwissenschaften

der Technischen Universität Darmstadt

zur Erlangung des akademischen Grades eines

Doktor-Ingenieurs (Dr.-Ing.)

genehmigte

DISSERTATION

von

Justus Behnisch, M. Sc.

aus Berlin

Erstgutachter:	Prof. Dr.-Ing. habil. Martin Wagner
Zweitgutachter:	Prof. Dr.-Ing. Markus Engelhart
	Prof. Dr.-Ing. Norbert Jardin

Darmstadt 2022

Justus Behnisch

Oxygen transfer of fine-bubble aeration systems in wastewater treatment: Influence of diffuser design on oxygen transfer at increased salt concentrations

Darmstadt, Technische Universität Darmstadt
Jahr der Veröffentlichung der Dissertation auf TUprints: 2023

URN: urn:nbn:de:tuda-tuprints-229405

URI: https://tuprints.ulb.tu-darmstadt.de/id/eprint/22940

Erstgutachter	Prof. Dr.-Ing. habil. Martin Wagner
Zweitgutachter:	Prof. Dr.-Ing. Markus Engelhart Prof. Dr.-Ing. Norbert Jardin

Tag der mündlichen Prüfung: 14.10.2022

Zusammenfassung

Das Thema dieser kumulativen Dissertation ist die Untersuchung des Einflusses des Belüfterdesigns auf den Sauerstoffeintrag feinblasiger Druckbelüftungssysteme bei der Behandlung salzhaltiger Abwässer. Beim Belebungsverfahren, dem gängigen aeroben biologischen Behandlungsverfahren, werden heutzutage zur Deckung des Sauerstoffbedarfs der Mikroorganismen bevorzugt feinblasige Druckbelüftungssysteme eingesetzt. Dabei hat die Belüftung mit 50 % bis 80 % den größten Anteil am Gesamtenergieverbrauch des Belebungsverfahrens. Zur Sicherstellung einer hohen Energieeffizienz des Belüftungssystems und damit des gesamten biologischen Reinigungsprozesses müssen bei dessen Planung alle Prozessbedingungen berücksichtigt werden. Einer der maßgebenden Faktoren ist die Salzkonzentration, deren Anstieg zu einer Hemmung der Koaleszenz und damit zu einer Verringerung der Blasengröße führt. Mit der dadurch vergrößerten Gas-Flüssig-Grenzfläche geht ein massiver Anstieg des Sauerstoffeintrags einher.

Im Rahmen dieser Arbeit wurde der Sauerstoffeintrag verschiedener, konventioneller feinblasiger Belüfterelemente in Trink- und Salzwasser sowie in salzhaltigem Belebtschlamm gemessen. Ziel dabei war die Identifizierung und Bewertung wie Belüftermembrandesign, Belüftertyp, Belegungsdichte und Salzart bei unterschiedlichen Salzkonzentrationen den Sauerstoffeintrag beeinflussen. Parallel wurde in Trink- und Salzwasser mittels Bildanalyse die Blasengröße an verschiedenen Stellen des aufsteigenden Blasenschwarms gemessen. Die Untersuchungen in Trink- und Salzwasser fanden in einer 250 L Blasensäule sowie in einem 17.100 L Glasbecken statt. Für die Sauerstoffeintragsmessungen in salzhaltigem Belebtschlamm wurde eigens eine mit salzhaltigem Industrieabwasser beschickte Belebungsanlage im Pilotmaßstab mit einem belüfteten Beckenvolumen von 2.250 L über 269 d betrieben. Der Sauerstoffeintrag wurde dabei kontinuierlich mittels Abluftmethode erfasst.

Die Ergebnisse zeigen, dass in Trinkwasser der Sauerstoffeintrag vorwiegend von der Belegungsdichte und dem Belüftertyp sowie von der Einblastiefe abhängt. Hingegen hat das Belüftermembrandesign in Trinkwasser keinen Effekt auf den Sauerstoffeintrag, obwohl Blasengrößenvermessungen eine deutliche Abhängigkeit zwischen der Schlitzgröße und der Größe der Primärblasen zeigen. Ursache der fehlenden Einflussnahme ist die rasche Koaleszenz der Blasen während ihres Aufstiegs. Der Einsatz feingeschlitzter Belüfter führt also in Trinkwasser gegenüber dem Einsatz grobgeschlitzter Belüfter gleichen Typs nicht zu einer Veränderung oder gar zu einer Verbesserung des Sauerstoffeintrags. Vielmehr verschlechtert sich der Sauerstoffertrag infolge des höheren Druckverlustes der feingeschlitzten Belüfter.

Erhöht sich jedoch die Salzkonzentration, führt die zunehmende Hemmung der Koaleszenz dazu, dass die Blasengröße ab- und der Sauerstoffeintrag deutlich zunimmt. Erreicht die Salzkonzentration die sog. kritischen Koaleszenzkonzentration (engl. *crictial coalescence concentration*; CCC) ist die Koaleszenz gar vollständig gehemmt und der Sauerstoffeintrag erreicht sein Maximum. Die CCC ist dabei unterschiedlich für jedes Salz bzw. Salzgemisch. Mit einem eigens neu entwickelten Ansatz konnten erstmals für konventionelle feinblasige Druckbelüfter die CCC für verschiedene Salze bestimmt werden. Ist die Koaleszenz vollständig gehemmt entspricht die Blasengröße etwa dem der Primärblasen, wodurch mit feingeschlitzten Belüftern im Vergleich zu gröber geschlitzten Belüftern gleichen Typs ein höherer Sauerstoffeintrag erreicht wird. So wurde ein Anstieg des Sauerstoffeintrags um bis zu 23 % erreicht. Trotz des höheren Druckverlustes der feingeschlitzten Belüfter, stieg der Sauerstoffertrag um bis zu 17 %. Bei erhöhten Salzkonzentrationen kann die Effizienz des feinblasigen Belüftungssystems also durch eine Anpassung des Belüftermembrandesigns signifikant erhöht werden, ein Fakt, den es künftig auch bei der Bemessung zu berücksichtigen gilt. Ein optimierter Bemessungsansatz wird im Rahmen der Thesis vorgestellt, welcher eine bedarfsgerechte Bemessung feinblasiger Druckbelüftungssysteme bei erhöhten Salzkonzentrationen ermöglicht.

Abstract

The topic of this cumulative thesis is to investigate the influence of diffuser design on the oxygen transfer of fine-bubble aeration systems in wastewater treatment at increased salt concentrations. In the activated sludge process, as the common aerobic biological treatment process, fine-bubble aeration systems are preferred to satisfy the oxygen demand of microorganisms. Thereby, aeration is usually the most energy-intensive part of the activated sludge process, accounting for 50 % to 80 % of total requirement. To ensure high energy efficiency of aeration and thus of the entire treatment process, designers of WWTP must therefore consider all influencing factors including salinity. When salinity rises, coalescence is increasingly inhibited. The resulting decrease in bubble size leads to an increase in the gas-liquid interface, followed by a tremendous increase in oxygen transfer.

Within this thesis, the oxygen transfer of various conventional fine-bubble aeration diffusers in tap- and saline water as well as in saline activated sludge was measured. The scope was to assess the effect of diffuser membrane design, diffuser type, diffuser density and salt type on oxygen transfer at different salt concentrations. Simultaneously, bubble size along the ascent of the bubble swarm were measured via image analyses at different levels of ascending bubble swarm in tap water and in saline water. The measurements in tap- and saline water took place in a 250 L glazed bubble column and in a 17,100 L glass-steel-frame tank. Oxygen transfer tests in saline activated sludge were conducted in a pilot scale activated sludge tank with an aerated water volume of 2.250 L. The plant was operated for 269 days with saline industrial wastewater influent. The oxygen transfer into the activated sludge was measured continuously by off-gas method.

The results show, that in tap water the oxygen transfer depends predominantly on diffuser density and type of diffuser as well as on the depth of submergence. In contrast, the diffuser membrane design has no effect on oxygen transfer in tap water, although bubble size measurements showed that the slit length of diffuser membrane affect the size of bubbles close to the diffuser (primary bubbles). The reason is, that bubbles coalescence rapidly during their ascent. Therefore, using fine-slitted diffusers in tap water does not lead to an improved oxygen transfer compared to large-slitted diffusers of the same type. Rather, the aeration efficiency decreases due to the higher pressure drop of fine-slitted diffusers.

However, when the salt concentration increases, the increasing inhibition of coalescence leads to a decreasing bubble size and a tremendously rising oxygen transfer. When the salt concentration exceeds the critical coalescence concentration (CCC), coalescence is completely inhibited and the oxygen transfer reaches its maximum. The CCC is specific for each salt or salt mixture. Using a new self-developed analytical approach, for the first time CCC was determined for various single salt solutions for conventional fine-bubble diffusers. If coalescence is completely inhibited, the bubble size equals the size of primary bubbles, which results in an improved oxygen transfer using fine-slitted diffusers. Oxygen transfer measurements in saline water as well as in saline activated sludge show, that oxygen transfer increases up to 23 % compared to large-slitted diffusers of the same type. Despite higher pressure drop of fine-slitted diffusers, aeration efficiency increases up to 17 %. Thus, at elevated salt concentrations, the efficiency of fine-bubble aeration systems can be significantly improved by adjusting the diffuser membrane design, a fact, that must also be considered in the future in the design of aeration systems. Therefore, an optimized design approach is proposed, which enables an appropriate design of fine-bubble aeration systems at increased salt concentrations.

Danksagung

Die vorliegende Arbeit ist Ergebnis meiner Zeit als wissenschaftlicher Mitarbeiter am Institut IWAR der Technischen Universität Darmstadt. An dieser Stelle möchte ich allen Menschen danken, die mich bei der Entstehung dieser Arbeit unterstützt haben. Allen voran Herrn Prof. Dr.-Ing. habil. Martin Wagner für die Übernahme der Betreuung meiner Dissertation, die großen Freiheiten und die Förderung die er mir zuteilwerden lies sowie für die vertrauensvolle und stets zuverlässige Zusammenarbeit. Herrn Prof. Dr.-Ing. Peter Cornel danke ich dafür, dass er während meines Studiums mein Interesse an der Abwassertechnik weckte und damit den Grundstein dieser Dissertation und meines weiteren beruflichen Werdegangs legte. Bei Prof. Dr.-Ing. Norbert Jardin und Prof. Dr.-Ing. Markus Engelhart bedanke ich mich für die freundliche Übernahme der Korreferate.

Ein besonderer Dank richtet sich auch an meine ehemaligen Kolleginnen und Kollegen. Stephan Sander danke ich für die Einführung in die Welt der Belüftungstechnik. Für legendäre B-Runden und den anregenden Gedankenaustausch auch über das Für und Wider von Staubsaugrobotern danke ich Maximilian Schwarz. Thomas Fundneider danke ich für die immerwährende Versorgung mit kulinarischen Leckereien bei den gemeinsamen Grillabenden. Sinem Kale danke ich dafür, dass sie mich auf der gemeinsamen Reise nach Fernasien nicht allein gelassen hat. Johannes Rühl danke ich für die stets kontroversen Diskussionen, die wir bereits seit unserer gemeinsamen Schulzeit führten. Pia Herrling danke ich für die Zusprache den Mut zu finden auch mal einen Schlusspunkt unter ein Paper zu setzen. Luisa Barkmann danke ich für die stets angenehme und gutgelaunte Tischgesellschaft. Bernhard Düppenbecker, Jochen Sinn, Tobias Blach, Jana Trippel und Phillipp Bunse danke ich dafür, dass sie maßgeblich zum freundschaftlichen Arbeitsumfeld am Institut beigetragen haben. Julian Mosbach und Jessica Beck danke ich für die hervorragende Zusammenarbeit dabei jedes Semester hunderte von Studierenden durch die Prüfungen bekommen zu haben. Anna Dell und Sonja Bauer danke ich für die vergnügliche Reisegemeinschaft und für die tolle Zeit bei den gemeinsamen Wanderungen.

Zu Dank verpflichtet bin ich auch Vera Soedradjat und Renate Schäfer, die immer ein waches Auge auf den Institutsalltag und den Kaffeevorrat haben. Dem Werkstattteam Arno Beck, Ewa Freitag und Christian Georg danke ich für die stets schnell helfenden und geschickten Hände, auch wenn es mal „ganz dringend“ war. Dem Laborteam Ute Kopf, Renate Benz und Harald Grund danke ich für die detaillierte Einführung in die Laborarbeit, Wissen von dem ich weit über meine Zeit an der Uni zehren kann.

Die vorliegende Arbeit wäre auch nicht ohne die Unterstützung zahlreicher Studierender entstanden. Ganz besonders möchte ich mich bei Anja Ganzauge für das Zählen und Vermessen tausender Luftbläschen bedanken. Bei Nils Strohmenger bedanke ich mich für die zuverlässige Hilfe bei den zahlreichen Versuchen, auch wenn es uns manchmal Blut, Schweiß und Tränen abverlangt hat. Anna Lena Heinz danke ich dafür, dass sie mir als tatkräftige stellvertretende Betriebsingenieurin zur Seite stand.

Von ganzem Herzen bedanke ich mich auch bei meinen Eltern, die mir immer jegliche Unterstützung haben zuteilwerden lassen. Für die außeruniversitäre Ablenkung bei dem einen oder anderen Kaltgetränk danke ich meinen Freunden Christine, Sabrina, Jenny, Magdalena, Marcell, Thore und Jens. Herzlichst bedanken möchte ich mich auch bei meiner Freundin und besseren Hälfte Hanna, die es klaglos toleriert hat, wenn ich mich mal wieder zum Schreiben zurückzog oder mich auch mal abends ins Labor verabschiedete. Auf deinem Weg zur Dissertation hoffe ich mich angemessen revanchieren zu können, auf das wir danach zusammen mehr Zeit für die handfesteren Dinge im Leben haben werden.

List of contents

List of Figures

List of Tables

List of Abbreviations

a	m^2/m^3	liquid/gas interfacial area
A_A	m^2	active (perforated) membrane area
A_g	m^2	total gas surface
A_P	m^2	projected media surface area
AS		activated sludge
BSD		bubble size distribution
CCC	g/L; mol/L	critical coalescence concentration
CCIS		critical coalescence ionic strength
COD	mg/L	chemical oxygen demand
c_S	mg/L	oxygen saturation concentration
$c_{S,20}$	mg/L	oxygen saturation concentration at STP
$c_{S,atm}$	mg/L	oxygen saturation concentration at process atmospheric pressure
$c_{S,md,20}$	mg/L	mid-depth dissolved oxygen saturation concentration
$c_{S,Saline\ water}$	mg/L	oxygen saturation concentration in saline (waste)water
$c_{S,T}$	mg/L	oxygen saturation concentration at process temperature
c_{Salt}	g/L	salt concentration
c_X	mg/L	actual dissolved oxygen concentration in water
D	m^2/s	diffusion coefficient
d_{32}	mm	sauter mean diameter
d_B	m; mm	bubble diameter
DCCC		dynamic cost comparison calculation
DD	%	diffuser density
DO		dissolved oxygen
DOF	mm	depth of field
d_S	mm	slit length
d_W	m	water depth
E	MWh/a	annual energy demand
EC	mS/cm	electrical conductivity
EPDM		ethylene propylene diene terpolymer
EPS		extracellular polymeric substances
F/M ratio	g/g/d	food-to-mass ratio
f_B	1/s	bubble formation frequency
f_D		water depth correction factor
f_S		salt correction factor for volumetric mass transfer coefficient
$f_{S,max}$		maximum f_S

h_D	m	depth of submergence
IS		ionic strength
k		empirical parameter for calculating f_S
k_L	m/h	liquid-side mass transfer coefficient
k_La	1/h	volumetric mass transfer coefficient
k_La_{20}	1/h	k_La at 20° water temperature
k_N		normalized k-value
MLSS	g/L	mixed liquor suspended solids
NPC	€	net presence costs
OTR	kg/h	oxygen transfer rate
OUR	kg/m³/h	oxygen uptake rate
OV_h	kg/h	OTR required under process conditions
P	kW	required power requirement
p_0	kPa	elastic pressure
p_{atm}	kPa	atmospheric pressure
p_C	kPa	pressure in the gas chamber
p_d	kPa	pressure drop of diffusers
PD		positive displacement blower
PE		population equivalent
p_h	kPa	hydrostatic pressure
P_R	mm	distance between rows of diffuser membrane
P_S	mm	distance between slits of diffuser membrane
p_S	kPa	pressure drop of pipes and valves
p_T	kPa	total air supply pressure
PU		Polyurethane
p_σ	kPa	surface tension
Q_1	m³/h	blower inlet airflow rate
Q_A	m³/h	airflow rate
$Q_{A,Aa}$	m³/m²/h	Q_A per total area covered by the grids of diffusers
$Q_{A,Da}$	m³/m²/h	Q_A per diffuser membrane area
$q_{A,Disc}$	m³/Disc/h	Q_A per disc diffuser
$q_{A,dS}$	dm³/mm/h	Q_A per slit and slit length of diffuser membrane
$q_{A,Plate}$	m³/Plate/h	Q_A per plate diffuser
$q_{A,Slit}$	m³/Slit/h	Q_A per slit of diffuser membrane
$q_{A,Tube}$	m³/Tube/h	Q_A per tube diffuser
$Q_{A,VAT}$	m³/m³/h	Q_A per aerated tank volume
Q_{ave}	m³/h	average airflow rate

Q_{max}	m^3/h	maximum airflow rate
Q_{min}	m^3/h	minimum airflow rate
R^2		coefficient of determination
RH	%	relative humidity
r_N	1/s	renewable rate
s	%	relative deviation
SAE	kg/kWh	standard aeration efficiency
sAS		saline activated sludge
SBR		sequencing batch reactor
SD	$1/cm^2$	slit density
SGV	m/h	superficial gas velocity
SMP		soluble microbial products
SOTE	%	standard oxygen transfer efficiency
SOTR	kg/h	standard oxygen transfer rate
$SOTR_{PW}$	kg/h	SOTR in process water
$SOTR_{VAT}$	$g/m^3/h$	SOTR per aerated tank volume
SRT	d	sludge retention time
SSOTE	%/m	specific standard oxygen transfer efficiency
STP		standard temperature and pressure
SVI	mL/g	sludge volume index
SW		saline water
t	s	contact time
T_0	°C	inlet temperature of blower
T_A	°C	ambient temperature
t_B	s	total bubble formation time
$t_{B,time\text{-}out}$	s	time-out between two consecutive bubbles generated
$t_{B,growth}$	s	bubble growth time
TC	g/L	transition concentration
t_d	a	life cycle of diffusers
TOC		total organic carbon
T_P	°C	air-pipe temperature
T_W	°C	water-temperature
TW		tap water
V	m^3	aerated liquid volume
v_S	m/s	slip velocity
WAS		waste activated sludge
WWTP		wastewater treatment plant

α		interface factor
β_{St}		salt correction factor for oxygen saturation concentration at standard conditions
β_{α}		salt correction factor for oxygen saturation concentration at process conditions
Δp	kPa	overall pressure drop
ε	%	gas holdup
η		overall efficiency of blower
Θ		temperature correction factor
ρ	kg/m^3	air density
σ	%	standard deviation

1 Introduction

The topic of this cumulative thesis is to investigate the influence of diffuser design on oxygen transfer of fine-bubble aeration systems in wastewater treatment at increased salt concentrations. Elevated salt concentration is quite common in industrial wastewater as well as in the municipal wastewater of some cities, such as in Macau or Hong-Kong (Sander 2018), which are close to the ocean and where seawater infiltrates into the leaky sewage system or it is used directly for toilet flushing to substitute fresh water. Increased salt concentration inhibit bubble coalescence. Therefore, the average bubble size of an ascending bubble swarm decreases. The smaller bubbles offer a larger gas-liquid interfacial area, which leads to an increasing oxygen transfer of fine-bubble aeration systems at elevated salt concentration. Depending on the aeration devices and salt concentration, the oxygen transfer is up to twice as high as in tap water. Despite numerous studies of this phenomenon, it was often neglected in the design of aeration systems in wastewater treatment. As a result, aeration systems are often being constructed with too high capacity, which results in unnecessarily high investment and operating costs. If the aeration system cannot be regulated down sufficiently, there is also a risk of excessive oxygen concentration in the activated sludge. This can lead to a decrease in denitrification capacity and thus to insufficient nutrient elimination.

With the revision of the German design recommendation DWA M 229-1 (DWA 2017a), a first approach was included, so that the design engineers are able to consider the influence of increased sea salt concentration on oxygen transfer of fine-bubble aeration systems. However, the new design approach is insufficient, because it does not consider the influence of diffuser design on oxygen transfer at increased salt concentration, nor it is applicable to other salts than sea salt.

This knowledge gap is closed with the present thesis. Comprehensive experiments were carried out in tap water, saline water and saline activated sludge to show the differences in oxygen transfer and bubble size of fine-bubble diffusers of different designs and of different types. The experimental setup being used for the experiments ranges from a 250 L small bubble column (1 m depth of submergence) via an 2.250 L aeration tank of a pilot scale activated sludge plant (3.6 m depth of submergence) to a 17,100 L pilot scale glass-steel frame test tanks (3.8 m depth of submergence). During the different experiments the oxygen transfer, the bubble size in the bubble swarm, the pressure drop of diffusers, salt concentration and, in case of the experiments with a pilot scale activated sludge plant treating saline industrial wastewater, operating parameters such as F/M ratio, MLSS, COD elimination etc. were measured.

2 Outline and structure of the thesis

This thesis is a cumulative research work on the influence of fine-bubble diffuser design on oxygen transfer in saline conditions and comprises four peer-reviewed articles published in international scientific journals. The scope was to assess the effect of diffuser membrane design, diffuser type, diffuser density and salt type on oxygen transfer at different salt concentrations. Chapter 3 of the thesis contains the corresponding theory and background, including a brief description of the functionality and components of modern fine-bubble aeration systems, the basics of oxygen transfer and its manifold influencing factors and common theories about bubble formation as well as bubble coalescence process. Furthermore, an overview is given of the occurrence and biological treatment of saline wastewater.

The articles, this thesis is based on, are reprinted in chapter 4. They are arranged following the medium in which the oxygen transfer and bubble formation was investigated (tap water; saline water; saline activated sludge) and the scale of the experimental setup (see Figure 1). Each paper describes a step in investigating the influence of fine-bubble-diffuser design on oxygen transfer at elevated salt concentrations.

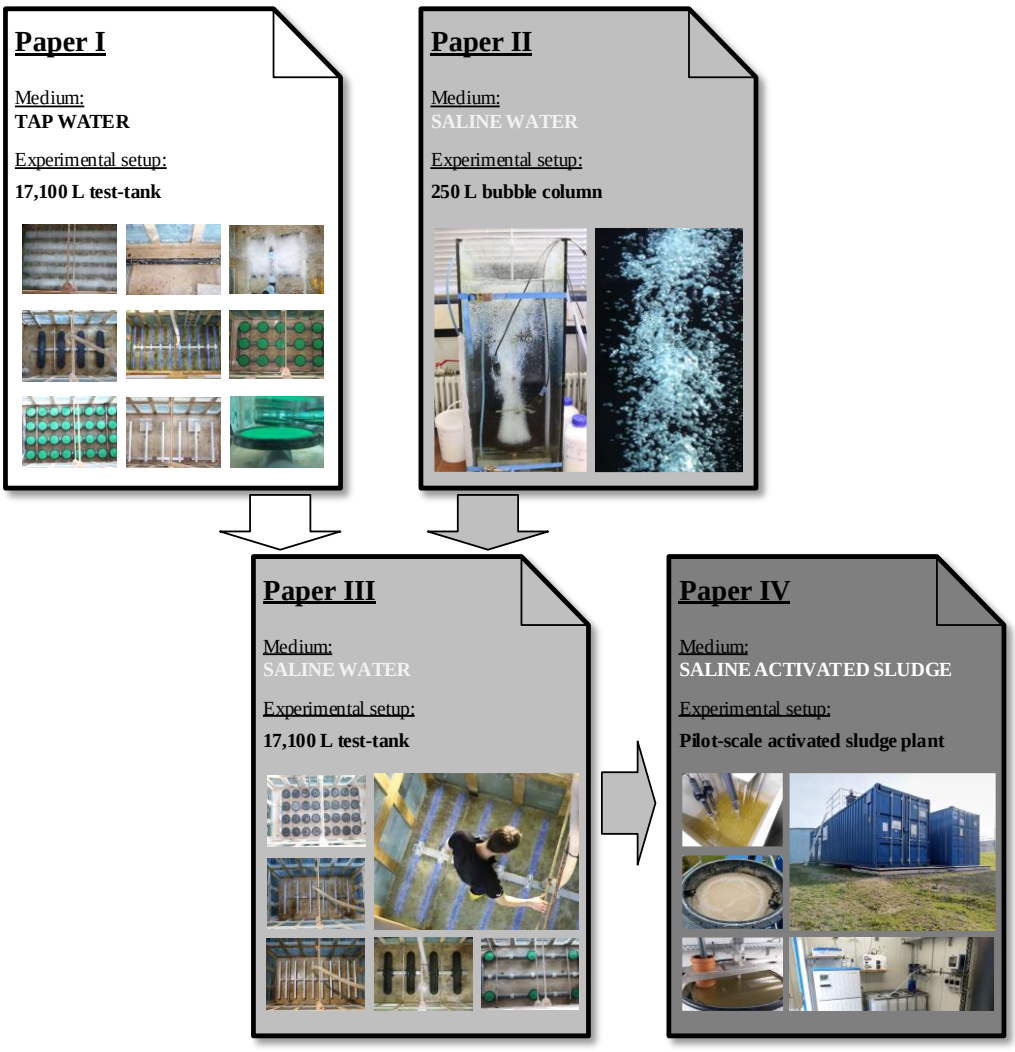

Figure 1: Overview of the four peer-reviewed scientific journals this thesis is based on

Conventional aeration equipment is rated in terms of its oxygen transfer in tap water. Nevertheless, corresponding published data of modern fine-bubble membrane diffusers are rare and mostly not up to date. However, current tap water performance data are necessary to assess the expected increase in oxygen transfer at elevated salt concentration. Furthermore, such data are also essential in design of

aeration systems, also in none-saline conditions. Therefore, Paper I deals with the performance of modern fine-bubble aeration systems in tap water. In detail, the experience from three decades of oxygen transfer testing and aeration research at Technical University of Darmstadt were summarized, including results of 306 oxygen transfer tests of 65 different fine-bubble diffusers carried out in a 17,100 L pilot-scale test tank in tap water.

Paper II addresses the effect of diffuser membrane design on bubble size and bubble size distribution at different salt concentrations. By using a new analytical approach, oxygen transfer and the bubble size along the ascent of the bubble swarm were measured simultaneously and in real time in lab-scale experimental setup. While the influence of an increased salt concentration on oxygen transfer of rigid diffusers has been described in several scientific publications, there are only insufficient references to modern fine-bubble membrane diffusers as they are used today. Investigations of bubble size distribution of fine-bubble membrane diffusers at different salt concentrations do not exist at all and were described for the first time in the present paper.

Accordingly, with the results from the lab-scale experiments, the general influence of the diffuser membrane design on oxygen transfer and the bubble size could be described. However, the lab-scale setup neither enabled the investigation of the oxygen transfer of diffuser types other than the disc diffusers used, nor was it possible to vary the diffuser density during the experiments. However, as tap water results in Paper I showed, diffuser density as well as diffuser type influence oxygen transfer.

Therefore, lab-scale experiments were repeated in the pilot-scale test tank as used during tap water experiments and by conducting additional tests with tube and plate diffusers, it was possible to demonstrate the transferability to large scale as well as assess the effect of diffuser type and diffuser density on oxygen transfer at elevated salt concentration. Furthermore, by additional lab-scale experiments and using a new analytical approach, the so-called critical coalescence concentration (CCC) of various salts ($MgCl_2$; $CaCl_2$; Na_2SO_4; NaCl; KCl) were measured. Exceeds the salt concentration CCC, the coalescence is fully inhibited and oxygen transfer reaches its maximum. CCC is specific for each salt and depends significantly on the bubble size and thus on the diffuser design. With the results presented in Paper III, CCC of various salts for conventional fine-bubble membrane diffusers were published for the first time.

The experiments in saline water show, in lab- as well as in pilot-scale experimental setup, that fine-slitted diffusers and corresponding smaller primary bubble size are to be recommended in saline conditions, because the oxygen transfer improves significantly compared to large-slitted diffusers and corresponding larger primary bubble size. However, it was not known whether an improvement in aeration of saline activated sludge also occurs. The coalescence behaviour in the aerated tank as well as the fouling of the diffusers could be influenced by the activated sludge. A concern was, for example, that fine-slitted diffusers would have a higher fouling rate. The associated increase in pressure drop of diffusers and the corresponding increase in energy requirement for air supply could negate the improvement in oxygen transfer.

Therefore, Paper IV handles experiments in a pilot-scale activated sludge plant, which was operated for 269 d with saline industrial wastewater influent. Same disc diffusers as used in tap water and saline water experiments were successively installed in the aeration tank and the oxygen transfer was measured continuously by off-gas method. Additionally, a modified design approach for considering salt-effect on oxygen transfer is described.

In chapter 5 the main conclusions from the different papers are summarized. Finally, the thesis closes with chapter 6, in which an outlook is given which further investigations are required regarding oxygen transfer at elevated salt concentrations.

3 Theory

3.1 Aeration System

The aeration system is one of the most important system components in aerobic biological wastewater treatment. Its main task is to ensure the oxygen demand of the microorganisms, which degrade the wastewater ingredients (EPA 1989).

In case of fine-bubble aeration systems, air is introduced via diffusers installed at the bottom of the aeration tank (Mueller et al. 2002). The oxygen transfers via diffusion from the small ascending bubbles into the liquid phase. Besides oxygen supply, the aeration system prevents sludge sedimentation in the aeration tank and provides optimal contact between wastewater ingredients and activated sludge flocs (Wagner and Stenstrom 2014). Furthermore, gaseous metabolic by-products of microorganisms like CO_2 are removed from liquid phase. Depending on the mean bubble size, a distinction is made between fine- and coarse bubble aeration system. Although there is no exact definition, it can be said, that mean bubble size of fine-bubble aeration systems is up to 5 mm (Hendricks 2011). Bubbles of coarse bubble aeration systems are bigger. The use of coarse bubble systems has rapidly declined over the past decades, due to their low efficiency and high power costs (Rosso et al. 2018).

A fine-bubble aeration system essentially consists of the blowers, the air-pipes and the diffusers installed in the aeration tank. In addition, there are various measuring devices (DWA 2017b). Relevant monitoring and control parameters are the airflow rate (Q_A; m³/h), total air supply pressure (p_T; kPa) and air-pipe temperature (T_P, °C) as well as environmental parameters such as ambient temperature (T_A; °C), relative humidity (RH; %) and atmospheric pressure (p_{atm}; kPa).

For air-supply different blower types are available. These include turbo compressors, screw compressors or positive displacement blowers (Rosso et al. 2018). During the operation of the wastewater treatment plants, the amount of air provided must be adjusted to the fluctuating loads of the wastewater. Accordingly, a distinction is made in dimensioning of aeration systems between maximum, minimum and average airflow rate (Q_{max}, Q_{min}, Q_{ave}), that need to be provided. With municipal wastewater composition common in Germany, Q_{max}/Q_{min} ratio of 1:10 to 1:5 is usual (Wagner and Stenstrom 2014).

The energy of blower operation makes the aeration system the main energy consumer of the activated sludge process. Even replacing the former used coarse bubble diffusers by more efficient fine-bubble technology in most WWTP of Europe and USA, aeration is still the most energy-intensive process of total electricity usage, accounting for 50 to 80 % of total WWTP demand (Amaral et al. 2018). The number and capacity of the blowers depends on the efficiency of the oxygen transfer and the corresponding required airflow rate for oxygen supply in the aeration tank. A high oxygen transfer means a lower required airflow rate, which reduces the necessary blower capacity and thus the total power consumption of the aeration system.

Besides the blowers, the diffusers are an essential part of a fine-bubble aeration system (EPA 1989). There are many different diffuser types available (plates, tubes, discs), made out of different material such as Ethylene propylene diene terpolymer (EPDM), silicone or polyurethane (PU). For a high oxygen transfer, it is important during operation that the air is released over the entire membrane surface of the diffuser as far as possible. Therefore, manufacturers often define operating ranges for their diffusers with a minimum and a maximum airflow rate, also to prevent fouling if the airflow rate is too low.

Fouling results from the deposition of organic as well as inorganic wastewater ingredients on the surface of the diffuser and in the slits from which the air escapes (Loock 2009). An increasing air supply pressure at constant airflow rate is a typical indication of diffuser fouling. In some cases, the deposits can be removed by abruptly expanding and relaxing the diffuser, also known as ‘bumping’. Otherwise, only

chemical or mechanical cleaning or replacement of the diffusers can reduce the total air supply pressure sustainably (DWA-M 299-2).

3.2 Oxygen transfer of fine bubble aeration systems

In case of fine-bubble aeration systems, the oxygen transfers via diffusion from ascending gas bubbles to the liquid phase. This transfer is described by the volumetric mass transfer coefficient (k_La; 1/h) and is proportional to the difference between the oxygen saturation concentration (c_S; mg/L) and the oxygen concentration in the water (c_X; mg/L). Therefore, the oxygen transfer increases when aerating with pure oxygen instead of air. The greater the difference the higher the driving force of oxygen transfer:

$$\frac{dC}{dt} = k_L a \cdot (c_S - c_X) \quad (1)$$

The k_La represents the product of the liquid-side mass transfer coefficient (k_L; m²/s) and the liquid/gas interfacial area (a; m²/m³), where a is defined as ratio of total gas surface (A_g; m²) to aerated liquid volume (V, m³):

$$k_L\mathrm{a} = k_L \cdot a = k_L \frac{A_g}{V} \quad (2)$$

There are several theories to describe the liquid-side mass transfer coefficient (Mueller et al. 2002). The penetration model according to Higbie (1935) assumes small fluid elements that are brought into contact with the interface where the diffusion of oxygen takes place. Accordingly, k_L is a function of diffusion coefficient (D; m²/s) and contact time (t; s). Thereby *t* can be expressed as the ratio of slip velocity (v_S; m/s) and bubble diameter (d_B; m) (Wagner 2002; Motarjemi and Jameson 1978). The slip velocity is defined as the difference between bubble velocity and liquid velocity.

$$k_L = 2 \cdot \sqrt{\frac{D}{\pi \cdot t}} = 2 \cdot \sqrt{\frac{D \cdot v_S}{\pi \cdot d_B}} \quad (3)$$

The reciprocal of the contact time is known as the renewable rate (r_N; 1/s):

$$r_N = \frac{1}{t} \quad (4)$$

The liquid/gas interfacial area is defined as the ratio of A_g to aerated liquid volume (V; m³). Obviously, it depends on the gas holdup (ε; -) and d_B (Akita and Yoshida 1974):

$$\mathrm{a} = \frac{A_g}{V} = \frac{6 \cdot \varepsilon}{d_B} \quad (5)$$

3.3 Design of aeration system

Since the wastewater ingredients and other different parameters, which affect the oxygen transfer, are different for every WWTP, commercial aeration equipment is rated in terms of oxygen transfer in clean water under standard conditions. Properties of ‘clean water’ is not defined in detail but is usually equated with the quality of the local tap water. The definition of standard conditions varies among industries and geographical areas. The definition used in the following is defined according to the European standard EN 12255-15 as follows:

- Water temperature = 20 °C
- Atmospheric pressure = 101.3 kPa
- Oxygen concentration = 0 mg/L

The main design parameter of an aeration system is the standard oxygen transfer rate (SOTR; kg/h), which expresses the amount of oxygen that dissolves in clean water at standard conditions. SOTR of an aeration system is calculated as a function of k_La, V and c_S at standard conditions ($c_{S,20}$; mg/L) and a conversion factor of 1,000 g/kg :

$$SOTR = \frac{V \cdot k_L a \cdot c_{S,20}}{1{,}000} \tag{6}$$

Other important parameters are the standard oxygen transfer efficiency (SOTE; %) and the standard aeration efficiency (SAE; kg/kWh). SOTE describes the fraction of oxygen of injected air that dissolves at standard conditions in clean water (Jolly et al 2010), and is calculated as a function of SOTR, the injected airflow rate (Q_A; m³/h) and the density of oxygen in the ambient air of 0.299 kg/m³:

$$SOTE = \frac{100 \cdot SOTR}{Q_A \cdot 0.299} \tag{7}$$

Usually, SOTE is referred to depth of submergence (h_D; m). This ratio is known as specific SOTE (SSOTE; %/m) and is helpful to compare different aeration systems with each other (EN 12255-15):

$$SSOTE = \frac{SOTE}{h_D} \tag{8}$$

SAE is defined as the ratio of SOTR to the required power requirement (P; kW) of blowers and, if applicable, the mixing devices (EN 12255-15):

$$SAE = \frac{SOTR}{P} \tag{9}$$

To design an aeration system, the required SOTR must be obtained by applying factors to the oxygen transfer rate required under process conditions (OV_h; kg/h). These factors reflect the different effects on the oxygen transfer, such as water temperature ($\theta^{(TW-20)}$), pressure (f_D; $p_{atm}/101.3$), wastewater ingredients and activated sludge (α) as well as salinity (β_{St}; β_α; $f_{S,St}$; f_α). The required SOTR is calculated as follows (DWA 2017a):

$$SOTR = \frac{f_D \cdot \beta_{St} \cdot c_{S,20} \cdot f_{S,St}}{\alpha \cdot f_{S,\alpha} \cdot \left(f_D \cdot \beta_\alpha \cdot c_{S,T} \cdot \frac{p_{atm}}{101.3} - c_X\right) \cdot \theta^{(T_W-20)}} \cdot OV_h \tag{10}$$

The various correction factors are explained in the following chapter 3.4. The large number of these factors shows that the oxygen transfer is subject to a variety of influencing effects. Understanding and describing these effects is essential in the design of aeration systems. Otherwise, the calculated SOTR does not match the actual required SOTR, which leads to an inefficient or even insufficient wastewater treatment process.

After the required SOTR, the required airflow rate is of interest for the design engineer of an aeration system. The airflow rate determines the required blower capacity as well as the number of diffusers that

need to be installed. It is calculated as a function of the calculated SOTR and the estimated SSOTE (DWA 2017a):

$$Q_A = \frac{100 \cdot SOTR}{3 \cdot SSOTE \cdot h_D} \quad (11)$$

Here it becomes evident, that proper estimation of SSOTE is crucial for efficient aeration system design (Stephenson et al. 2010), as the dimensioning of air pipes and selection of type and number of blowers depends on the calculated airflow rate. Therefore, Pöpel and Wagner (1989) published a table with standard values for SSOTE and SAE differentiated for different aeration system designs. Due to the further development of aeration equipment and improvement in the efficiency in aeration in particular, the recommendations were continuously revised and adapted (Wagner 1992; Wagner and Loock 2006; Wagner et al. 2011; Wagner and Stenstrom 2014). The actual version of the table is shown below. A proposal for a new revision of this table was published as part of this thesis (see chapter 4.2).

Table 1: Standard values for diffused aeration system according to Wagner and Stenstrom (2014)

	Favorable		**Average**	
System:	**SSOTE [%/m]**	**SAE [kg/kWh]**	**SSOTE [%/m]**	**SAE [kg/kWh]**
Full-floor coverage	8.0 – 8.7	4.2 – 4.5	6.0 – 7.0	3.3 – 3.4
Circulation and aeration	6.7 – 8.0	3.7 – 4.2	5.0 – 7.0	3.2 – 3.3

3.4 Factors affecting oxygen transfer

Oxygen transfer can be affected in different ways, either by influencing c_S, k_La or both. These includes water temperature, wastewater contaminants and salinity. These major influencing factors are discussed below.

3.4.1 Water temperature

Water temperature affects c_S and k_La. With increasing water temperature, c_S decreases, which leads to a lower concentration gradient and thus decreasing oxygen transfer. The oxygen saturation concentration at process temperature ($c_{S,T}$; mg/L) can be taken from tables, to be found e.g. in ISO 5814, or can be calculated as a function of the water-temperature (T_W; °C) according to (DWA 2017a):

$$c_{S,T} = \frac{2{,}234.34}{(T_W + 45.93)^{1.31403}} \quad (12)$$

With increasing temperature, diffusion coefficient rises as viscosity of water drops. From eq. (3) it can be seen, that this leads to an increase of k_La. Due to the impact of water temperature, the k_La is usually corrected to 20 °C water-temperature as a function of the temperature correction factor (θ; -) by the following equation (DWA-M 209):

$$k_La_{20} = k_La_T \cdot \theta^{(20-T)} = k_La_T \cdot 1.024^{(20-T)} \quad (13)$$

3.4.2 Pressure

With increasing pressure (atmospheric and hydrostatic) the oxygen saturation concentration rises. Thereby, both the atmospheric as well as the hydrostatic pressure must be considered. The saturation concentration therefore changes along the ascent of the air bubble. Therefore, the theoretical mid-depth dissolved oxygen saturation concentration ($c_{S,md,20}$; mg/L) is used, which is calculated for standard conditions according to (DWA M 299-1):

$$c_{S,md,20} = c_{S,20} \cdot \left(1 + \frac{h_D}{2 \cdot 10.35}\right) \quad (14)$$

The atmospheric pressure must be considered, especially if it deviates significantly from the standard conditions (101.3 kPa). For example, when the WWTP is located at high altitudes. Then, the oxygen saturation concentration can be corrected to standard conditions according to:

$$c_{S,patm} = c_{S,20} \cdot \frac{p_{atm}}{101.3} \quad (15)$$

3.4.3 Wastewater ingredients and activated sludge

Different dissolved and suspended substances present in the mixture of activated sludge and wastewater inhibit oxygen transfer. Therefore, k_La in activated sludge compared to k_La in tap water is usually lower. The inhibiting substances include surfactants, the activated sludge flocs and dissolved organic substances present in the activated sludge-wastewater mixture.

The effect of surfactants on oxygen transfer is subject of many different studies (Eckenfelder and Barnhart (1961), Wagner and Pöpel (1996), Steinmetz (1996), Chern et al. (2001), Painmanakul et al. (2005), Rosso et al. (2006), Sardeing et al. (2006), Hebrard et al. (2009)). Due to their simultaneously hydrophilic (polar) and hydrophobic (non-polar) nature, surfactants tend to adsorb at the gas-liquid interfacial area. Such substances are used in soaps and detergents and find their way into wastewater and thus into WWTPs. Experiments show that in case of fine-bubble aeration, surfactants usually leads to a reduction of the ascension velocity and bubble diameter. The smaller bubbles lead to an increase in interfacial area and it would be assumed, that the oxygen transfer therefore increases. Indeed, surfactants also immobilize the bubble surface so that the bubbles behave more and more like rigid particles, which leads to a reduction in the interfacial renewable rate and reduces the internal gas circulation (Rosso et al. (2006)). Furthermore, due to their accumulation at the interfacial area, they act as a barrier for the diffusion of oxygen from gas into the liquid phase. Therefore, the net effect of increasing surfactants concentration is usually a decreasing oxygen transfer (Wagner 1991).

The negative effect of surfactants is commonly accepted as an explanation for the positive correlation between oxygen transfer and activated sludge tanks operating parameters such as sludge retention time (SRT; d) or food to mass (F/M) ratio, whereby both parameters are reciprocal to each other. With increasing SRT or decreasing F/M ratio, the oxygen transfer improves, because there is also an improvement in treatment, which leads to a lower surfactant's concentration in the activated sludge. This phenomenon is also observed in plug flow reactors, where oxygen transfer is lowest for the influent and increases to a maximum at the effluent. (Kayser (1967), EPA (1989))

Like surfactants, the physical presence of solids has a detrimental effect on the oxygen transfer. The sludge flocs accumulate at the interfacial area, lower permeability and block oxygen transfer. Therefore, the oxygen transfer has been considered inversely related to the mixed liquor suspended solids concentration (MLSS; g/L) (Krampe and Krauth 2003), or mixed liquid volatile suspended solids (MLVSS) concentration (Henkel 2010). Furthermore, as the solids concentration increases, the gas hold-

up decreases compared to two-phase systems with the same gas input and the bubble velocity is reduced due to hydrodynamic forces and mutual collisions. This again favours coalescence and therefore lowers interfacial area and k_La, respectively.

Organic substances originated by the microorganisms like extracellular polymeric substances (EPS) or soluble microbial products (SMP) are also suspected to inhibit oxygen transfer (Wagner 1991; Schwarz et al. 2021). EPS represent a significant component when discussing microbial aggregates because they hold the aggregates together in a three-dimensional matrix (Sheng et al. 2010). EPS in wastewater treatment is produced during metabolism of the bacterial cell or comes from the wastewater influent. Main components of EPS are proteins, carbohydrates, nucleic acids and lipids (Henkel 2010). Steinmetz (1996) observed a decrease in oxygen transfer with increasing EPS concentration in the sludge and concluded that bacterial metabolism products may influence oxygen transfer. However, EPS mainly occurs inside the sludge floc and consequently does not get directly into contact with the interfacial area (Henkel 2010). Therefore, Germain et al. (2007) focused on the analyses of SMP, which are ostensibly soluble and thus part of the liquid phase. They found that increasing SMP concentration decreases oxygen transfer.

The reduction in oxygen transfer caused by ingredients present in activated sludge-wastewater mixture is governed by the alpha factor (α; -), which is defined as the ratio of k_La in non-saline activated sludge and k_La in tap water at standard conditions (k_La_{20}; 1/h):

$$\alpha = \frac{k_L a_{non\ saline\ activated\ sludge}}{k_L a_{tap\ water}} \tag{16}$$

The α factor is reported as the most uncertain aeration process parameter (Rosso et al. 2018), since it is highly dynamic and cannot predict with certainty the aeration efficiency under different process conditions, either in a single WWTP or across different WWTP. Therefore, recommendation ranges for α are often given in literature, such as by Günkel-Lange (2013). He recommends values for minimum, average and maximum α-factors in fine bubble diffuser aeration systems for various load cases and treatment goals accordingly (see Table 2). Due to the high dynamics of the α-factor, it is recommended to calculate the required amount of oxygen with minimum, maximum and average α to achieve the necessary flexibility of the aeration system in operation (DWA 2017a).

Table 2: Recommended α-values for maximum, average and minimum load cases process variants for fine-bubble aeration systems (Günkel-Lange 2013)

	α_{min}	α_{ave}	α_{max}
	(maximum load case)	(average load case)	(minimum load case)
continuously operated denitrification (simultaneous, intermittent, alternating, upstream)	0.60	0.75	0.85
SBR process for nutrient removal	0.50	0.65	0.80
Membrane Bioreactor (MLSS ~ 12 g/L, SRT = 25 d)	0.50	0.60	0.70
Simultaneously aerobic stabilization	0.70	0.80	0.90
Carbon removal	0.35	0.50	0.60

3.4.4 Salinity

It is generally assumed, that the presence of salts due to their hydration reduces the activity of water and the space available for the solution of oxygen molecules, and thus diminishes the solubility of oxygen in water (Henkel 2010). This effect is considered in design of aeration systems by the salt correction factor (β; -), which is defined as the ratio of oxygen saturation concentration in saline (waste)water ($c_{S,Saline\ water}$) to clean water (Mueller et al. 2002):

$$\beta = \frac{c_{S,saline\ water}}{c_S} \tag{17}$$

The oxygen saturation concentration for different water temperatures and salt concentrations can be taken from tables, to be found e.g. in ISO 5814. How β can be calculated as a function of salt concentration is shown in chapter 4.4. As seen in eq. (1), due to the reduced oxygen saturation concentration increased salinity has a negative effect on oxygen transfer. Nevertheless, this effect is usually overlapped by another (positive) effect: the inhibition of bubble coalescence.

As shown in Figure 2, if salinity rises, the coalescence of a fine-bubble aeration system will be increasingly inhibited, which leads to a tremendous reduction in bubble size. Common theories how salts inhibit bubble coalescence are described in more detail in chapter 3.7.

With inhibition of bubble coalescence, the bubble size decreases and the interfacial area and k_La rises, respectively. Since the negative effect of reduced oxygen saturation concentration is quite low in comparison to the positive effect of coalescence inhibition, k_La rises with increasing salinity. The inhibiting effect of salts due to reduced oxygen saturation concentration is only relevant at very high salt concentration, as Dinkel et al. (2019) showed in their experiments in a small bubble column. They registered a decrease in k_La not until the salt concentration reaches 130 g NaCl/L. With further increase in salinity, k_La decreases until the salt saturation concentration was reached.

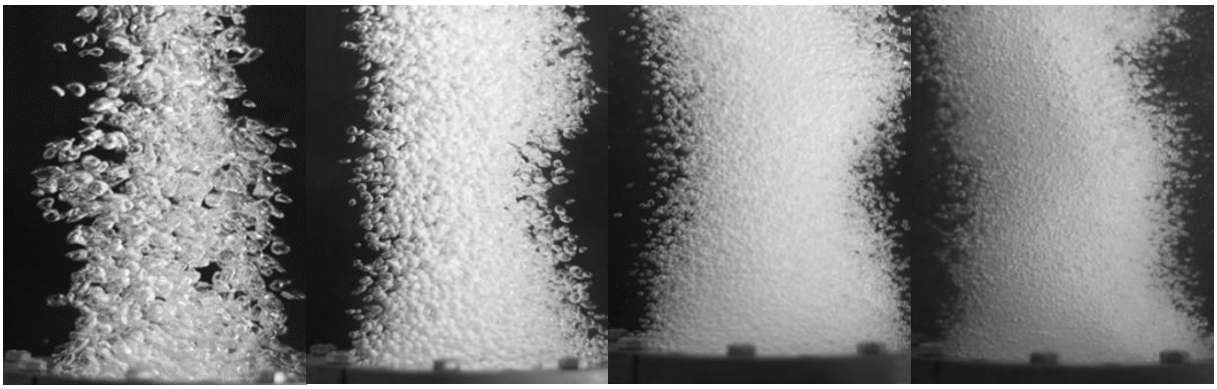

Tap water | 5 g/L NaCl | 10 g/L NaCl | 15 g/L NaCl

Figure 2: Pictures of bubble swarm of same airflow rate at different salt concentrations

The change in oxygen transfer caused by salts present in wastewater is governed by the f_S value, which is defined as the ratio of k_La in saline (waste)water (k_La_{20SW}; 1/h) to k_La in tap water at standard conditions (k_La_{20}; 1/h):

$$f_S = \frac{k_L a_{saline\ water}}{k_L a_{tap\ water}} \tag{18}$$

In the following, the effect of salt on oxygen transfer is shown exemplarily based on own measurements. Figure 3 shows f_S as a function of $MgCl_2$ and $CaCl_2$ concentration, measured in a lab-scale bubble column with the same fine-bubble diffuser and with identical airflow rate. With increasing salt

concentration f_S rises linearly (Zone 1). Here the coalescence is more and more inhibited and bubble size decreases. At a certain salt concentration the coalescence is completely inhibited and f_S reaches its maximum ($f_{S,max}$). A comparison of the two graphs shows, that f_{Smax} is reached at different salt concentrations ($MgCl_2$: 0.063 mol/L or 6 g/L; $CaCl_2$: 0.080 mol/L or 10 g/L). Furthermore, it can be seen, that f_S or k_La is more than doubled compared to tap water for each salt, which shows the tremendous effect of salt on oxygen transfer. If the salt concentration increases further, no change in k_La is recognisable and f_S is therefore constant (Zone 2).

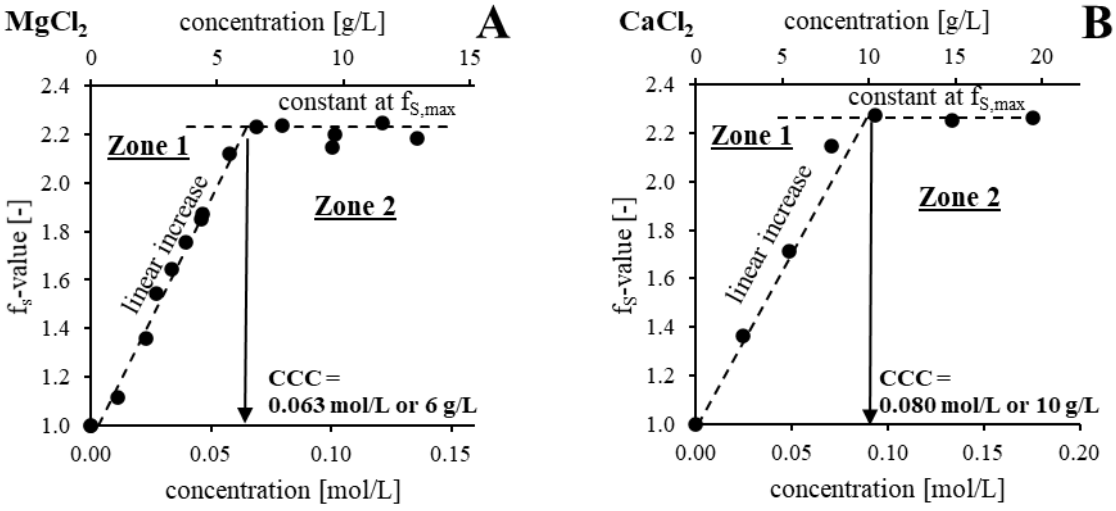

Figure 3: f_S as a function of $MgCl_2$- concentration (A) and $CaCl_2$-concentration (B)

According to Quinn et al. (2014), the concentration at which bubble coalescence is fully inhibited (and f_S reaches its maximum) is called the critical coalescence concentration (CCC; g/L). Figure 3 shows, that CCC is different for each salt or mixed salt solution, respectively. CCC as well as $f_{S,max}$ is affected by the bubble formation system and the bubble size. The rule of thumb is: the smaller the bubbles the higher CCC and $f_{S,max}$ is. As part of this thesis, CCC of different salts were determined for the first time for conventional fine-bubble aeration systems and then compared with literature data (see chapter 4.4).

3.5 Bubble Formation

Because of its relevance in many technical applications, the bubble formation with its influencing factors has been studied many times (Loubière and Hébrard (2003); Kumar and Kuloor (1970); Bals (2002); Painmanakul et al. (2004)). The bubble formation begins, when pressure in the gas chamber (p_C) balances the sum of resistances due to hydrostatic pressure (p_H), surface tension (p_σ) and, in case of flexible membrane diffusers, "elastic" pressure (p_0) (Painmanakul et al. 2004):

$$\Delta p < p_C - p_H - p_\sigma - p_0 \qquad (19)$$

Kumar and Kuloor (1970) described the bubble formation process in two stages:

a) Expansion stage, in which the bubble volume increases as long as the downward forces exceed the upward one. The bubble rises during bubble growth, and the bubble neck is formed.

b) Detachment stage, in which the bubble detaches itself when the bubble neck is closed.

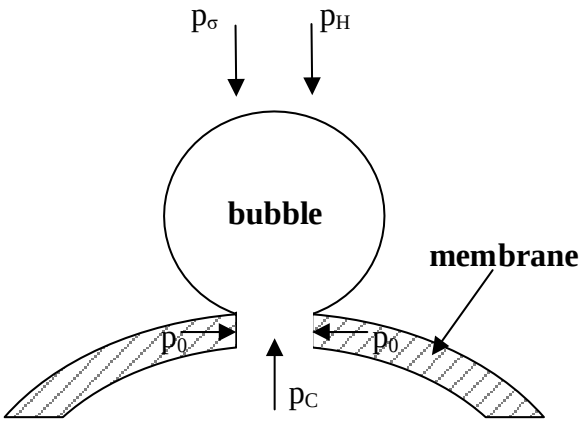

Figure 4: Balance of forces during bubble formation at an elastic orifice or "slit" adapted from Painmanakul et al. (2004)

The bubble formation process is affected by the diffuser material, the size of the orifice from which the air escapes and the airflow rate. With rigid diffuser materials, bubble formation takes place at constantly open orifices of fixed diameter. In the case of flexible membrane diffusers, it takes place at elastic orifices. If the pressure in the gas chamber is insufficient, these elastic orifices close themselves and thus prevent that liquid enters the gas chamber (Painmanakul et al. 2004). Due to their elasticity, the orifices of flexible membrane diffusers are therefore often termed "slits".

Studies investigating bubble formation on flexible membrane diffusers are rare. One of the few studies dealing with bubble formation on both rigid and flexible membrane diffusers is Loubière and Hébrard (2003). They defined the total bubble formation time (t_B), which is the sum of bubble growth time ($t_{B,growth}$) and of a time-out between two consecutive bubbles generated ($t_{B,time\text{-}out}$). The bubble formation frequency (f_B) is reciprocal to t_B, from which results:

$$t_B = t_{B,growth} + t_{B,time-out} = \frac{1}{f_B} \tag{20}$$

Loubière and Hébrard (2003) showed, that in the case of rigid diffusers, with rising airflow rate the bubble formation frequency increases initially while the bubble diameter remains constant. Thereby, the increased bubble formation frequency results from a reduced time-out between detachment and a newly forming bubble. The time of bubble formation remains constant. That is because after the gas bubble is released, the pressure in the orifice drops and liquid enters. The pressure of the gas phase must first overcome the hydrostatic pressure so that a new bubble can form. If airflow rate increases further, the bubble diameter and bubble formation frequency increases until jet regime begins, and the bubbles already coalesce during their formation process (Kumar and Kuloor 1970).

In case of flexible membrane diffusers, the bubble diameter increases logarithmically with increasing airflow rate (Loubière and Hébrard 2003). In parallel, bubble formation frequency increases linearly until a maximum is reached and remains almost constant. In contrast to rigid diffusers, the bubble growth time is equal to the total bubble formation time ($t_B = t_{B,growth}$). That means there is no time out between two bubbles formed successively. When a bubble detaches from a slit of a flexible membrane diffuser, a new bubble grows and pushes up the previous one.

3.6 Bubble coalescence

Bubble coalescence is a process by which two (or more) gas bubbles in a liquid medium collide and form one larger bubble. Firouzi et al. (2015) describes the bubble coalescence in four steps:

A) Approaching of two bubbles

B) Hydrodynamic interaction between the bubbles which can cause deformation on the bubbles

C) Thinning (or "Drainage") of the liquid film between the bubbles, which is 200 to 300 nm thick

D) Rupture of the liquid film at a critical thickness of 10 to 200 nm with subsequent coalescence of the bubbles.

In pure air-water mixture, the step of thinning (step C) is extremely fast and is in the range of milliseconds (Zlokarnik 1980; Gnotke 2005). On the other hand, in solutions that tend to foam, the step of thinning takes place extremely slowly (Mersmann 2013). The critical film thickness between bubbles before coalescence occurs (step D) depends on the concentration of surface-active substances or salts in the liquid phase and on the approach speed of both bubbles (Orvalho et al. 2021). If the contact time of the bubbles is insufficient and the critical film thickness is not reached, the bubbles do not coalesce.

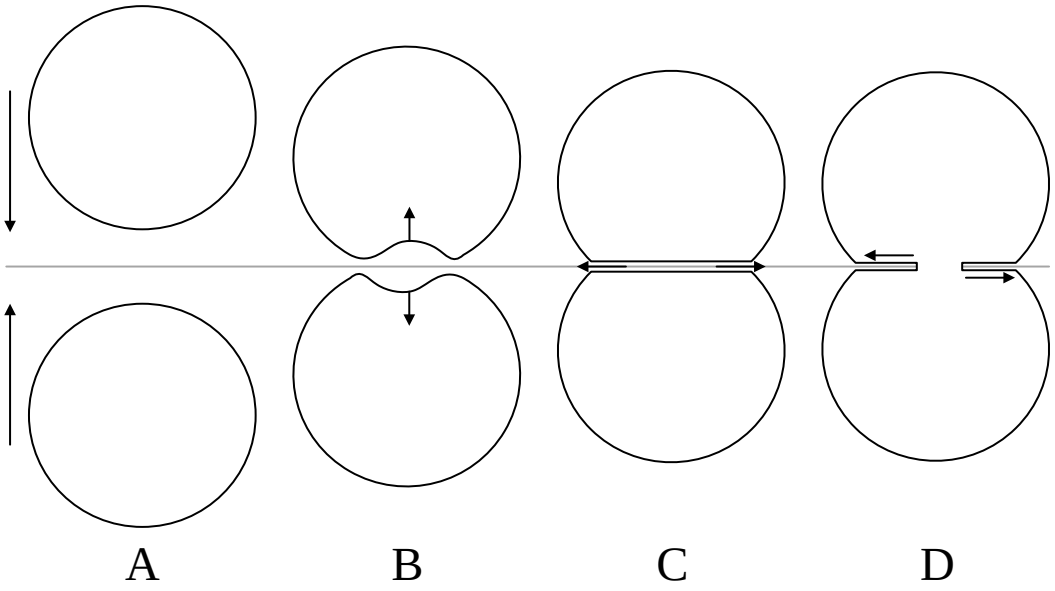

Figure 5: Four steps of bubble coalescence: Approaching of two bubbles (A); Hydrodynamic interactions (B); Thinning of liquid film (C); Rupture of the liquid film (D) (Firouzi et al. 2015)

Studies of bubble size distribution in a bubble swarm which escapes from aeration devices commonly used in wastewater treatment show, that coalescence preferably takes place close to the diffusers (Hasanen et al. 2006). Often coalescence occurs in a vertical direction of the ascent of the fine bubbles. The ascending bubble accelerates a following bubble in its wake, which subsequently collides with the first one. That is particularly common when the subsequent bubble is smaller than the first one (Drogaris and Weiland 1983).

The mean bubble size under conventional conditions in clean or tap water (without salt) of fine-bubble aeration system is between 2 and 5 mm (Hendricks 2011). Nevertheless, the bubble size is not constant along their ascent. The minimum bubble size can be found near to the diffuser (Hasanen et al. 2006). Here, bubble size corresponds to the size of bubbles detaching from the diffuser (primary bubbles). Then, due to the high bubble density and turbulence near to the diffuser, bubbles coalescence very quickly and often several times (Wagner 1992). Bubble density decreases and with it the number of bubble collisions and thus the coalescence rate. Due to the change from high bubble density to low bubble density, the shape of the bubble swarm escaping from a disc diffuser (see Figure 6) is therefore appropriately described as that of an hourglass (Hasanen et al. 2006).

Figure 6: Hourglass shape of a bubble swarm

In tap water with minor salt concentration, the diameter of the primary bubbles has only a minor effect on the resulting bubble diameter of the bubbles in the bubble swarm. In coalescence inhibited system (e.g. due to increased salt concentration) the diameter of bubbles equals the diameter of primary bubbles (Räbiger and Schlüter 2013). Marrucci and Nicodemo (1967) investigated the influence of different salts on the coalescence behaviour in a bubble swarm of porous diffusers. They showed that bubbles detaching from the distributor always have the same size, irrespective of airflow rate and salt concentration. They defined the diameter of the detaching bubbles as quasi-static bubble diameter. By increasing the salt concentration, the mean bubble size of the bubble swarm aspired asymptotically to the observed quasi-static value, which es exemplary illustrated in Figure 7.

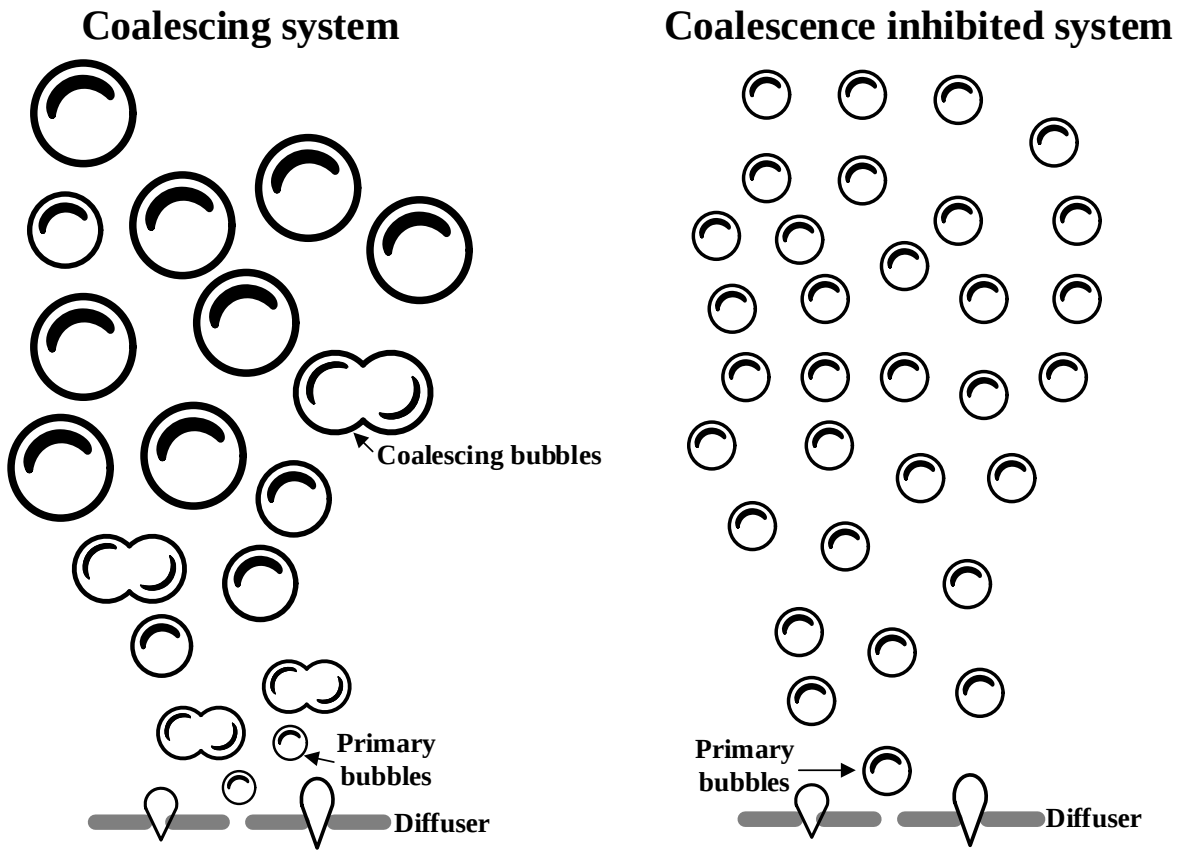

Figure 7: Ascent of bubble swarm in coalescing system (left) and coalescence inhibited system (right)

The opposing process of coalescence is bubble breakup (Wagner 2002). Bubble breakup occurs, if available disruptive forces (hydrodynamic forces) overcome the stabilising forces due to surface tension and viscosity (Henkel 2010). It only occurs in highly turbulent systems, if the bubble exceeds a critical size. In addition, bubble-bubble collision can result in a bubble breakup. This is typically the case in coarse bubble aeration systems.

3.7 Effect of salts on bubble coalescence

Whether two colliding bubbles coalesce or break up depends on many interfacial forces that become significant at small separation distance, such as van der Waals forces, electrostatic and capillary forces. Salts and other ingredients of the medium surrounding the bubbles may influence these interactions (Wagner 2002). However, although bubble coalescence and its influencing factors have been studied and described many times (Craig et al. 1993; Lessard and Zieminski 1971; Prince and Blanch 1990; Quinn et al. 2014; Orvalho et al. 2021), the inhibiting effect of salts on bubble coalescence is still not well understood. A detailed review of various common theories on this subject is given by Firouzi et al. (2015).

The most likely explanation is the Gibbs-Marangoni effect or Marangoni convection. Due to the rapid stretching of the liquid film of salt solution between two bubbles during its thinning and drainage causes a non-uniform distribution of ions at the interface (Firouzi et al. (2015). The resulting surface concentration gradient leads to a surface tension gradient along the gas-liquid interface. This surface tension gradient leads to a mass transfer, also known as Marangoni convection, which opposes the film drainage and immobilizes the interface (Gnotke 2005).

However, Henry et al. (2007) argued that the Marangoni effect alone cannot explain ion-specific coalescence inhibition. As alternative mechanism they suggested the ion-specificity and prevention of

film rupture owing to the short-range double layer repulsion arising from the location of ions at the interface. Nevertheless, it is questionable how is short-ranged and weak electrostatic double-layer repulsion can inhibit bubble coalescence at a transition concentration in order of 0.1 M and rupture thicknesses of tens of nanometres (Firouzi et al. 2015).

Craig and Henry (2010) studied the effect of bubble coalescence and concluded that some salt combinations have an effect, some not. Based on different ion affinities to the gas-liquid interface, they assigned the property α and β to each anion and cation (see Table 3), not to be mistaken with the factors used in design of aeration systems. They suggested that α anions and β cations are attracted to the gas-liquid interface, while α cations and β anions do not. Therefore, salts with ion combination of αα or ββ inhibit coalescence whereas salts with αβ or βα ion combination do not affect bubble coalescence.

Table 3: Effect of selected ion combinations on the inhibition of bubble coalescence (Craig und Henry 2010)

Ions		**Li^+**	**Na^+**	**K^+**	**Cs^+**	**Mg^{2+}**	**Ca^{2+}**	**NH_4^+**	**H^+**	**$(CH_3)NH_3^+$**	**$(CH_3)_2NH_2^+$**	**$(CH_3)_3NH^+$**	**$(CH_3)_4N^+$**
Assignment		**α**	**α**	**α**	**α**	**α**	**α**	**α**	**β**	**β**	**β**	**β**	**β**
OH^-	**α**		+	+					0				
Cl^-	**α**	+	+	+		+	+		0	0	0	0	0
Br^-	**α**		+	+	+				0				0
NO_3^-	**α**	+	+	+			+		0				
SO_4^{2-}	**α**	+	+	+		+			0				
$(COO_2)^{2-}$	**α**			+					0				
IO_3^-	**α**		+										
ClO_3^-	**β**		0										
ClO_4^-	**β**		0			0		0	+				
CH_3COO^-	**β**		0	0	0	0		0	+				+
SCN^-	**β**		0										

+ = inhibition; 0 = no effect; blank = not determined

3.8 Saline wastewater

In municipal wastewater the salt concentration is usually below 2.0 g/L. Nevertheless, in some cases the salt concentration is increased. In the influent of a municipal WWTP located on the cost of South-China, Sander (2018) observed daily fluctuation of conductivity between 1.1 and 7.5 mS/cm. He found that the fluctuation correlates with the daily tidal cycle of the nearby sea. His explanation is quite easy: Seawater infiltrates into the leaky sewer system and leads to increased sea salt concentration in the municipal wastewater. But this is not the only possible way for increased (sea)salt concentration in municipal wastewater. Even the global trend towards saving fresh water, e.g. through wastewater reuse or by using seawater for toilet flushing, will raise the volume of saline wastewater that needs to be (biologically) treated.

In contrast to municipal wastewater, increased salt concentration is quite common in industrial wastewater (Lefebvre and Moletta 2006; Behnisch et al. 2020a). In 2016, the manufacturing industry in Germany discharged 4,980 million cubic metres of wastewater (Statistisches Bundesamt 2018). The most significant sources of wastewater in industry are chemical synthesis, off-gas treatment, cooling water blowdown, backflush of filters and ion exchangers, as well as landfill leachate and rainwater from contaminated areas (Canova et al. 2018).

Some of these wastewater streams are highly contaminated with salts as well as with organic substances. For instance, generated wastewater during plastic production such as polycarbonate show high sodium chloride concentration of 50 to 100 g NaCl/L (Huber and Rische 2017). Günther et al. (2017) report about wastewater from off-gas treatment, which is highly contaminated with various salt types (~ 120 g Na_2SO_4/L and 12 g NaCl/L) and organic contaminants (~ 4,000 mg COD/L). During the production of

methylcellulose, concentrations of 80 g NaCl/L are achieved on average in the wastewater generated, with very high COD concentrations of about 31,900 mg/L (Sterger and Köppke 2013). These and other examples show, that predominantly the salts Na_2SO_4 or NaCl are present in industrial wastewater.

All these wastewater streams need to be biologically treated, preferably by activated sludge process as it is economic and effective (Engelhart et al. 2020). Therefore, a deeper understanding of the effects of increased concentration of different salts and salt mixtures is crucial to enhance the (energy) efficiency of aerobic biological wastewater treatment.

3.9 Influence of salt on activated sludge

The adaption of microorganisms to saline conditions is designated as halotolerance (Stolz 2017). An important criterion in assessing the viability of the microorganisms under saline conditions is the growth rate as a function of salt concentration. Microorganisms are not capable to accumulate in the WWTP when their growth range does not cover the actual salt concentration in the wastewater (Lay et al. 2010).

In the literature, there is a distinction between halophilic and halotolerant microorganisms, but this distinction is not precise (Lay et al. 2010). True halophilic microorganisms or halophiles microorganisms are those that grow in saline environment and require a certain minimum level of salt to survive. Halotolerant microorganisms are those that grow better in tap water but tolerate higher salt concentrations and can be found in saline environment too. A more detailed definition gives Rodriguez-Valera et al. (1981). They categorise microorganisms according to the sodium chloride concentration that is optimal for growth (see Table 4)

Table 4: Categories of microorganisms according to the optimal growth range in NaCl (Rodriguez-Valera et al. 1981; Lay et al 2010)

Category	**NaCl range for optimal growth [g/L]**
Non-halophilic	< 10
Slightly halophilic	10 – 30
Moderately halophilic	30 – 150
Extremely halophilic	> 150

The majority of microorganisms that exists in activated sludge of conventional WWTP are non-halophilic (Woolard and Irvine 1995). These microorganisms are not able to cope with the osmotic stress exerted by increased salt concentration. The osmotic stress would cause an outward flow of intracellular water, resulting in cell dehydration and finally, plasmolysis and loss of activity of the microorganisms (Uygur 2006).

The ability to deal with osmotic stress by maintaining osmotic balance between the intracellular cytoplasm and the increased salt concentration of the environment is therefore an essential attribute of the halophilic and halotolerant microorganisms. Two strategies are known to cope with osmotic stress: The "Salt-in" strategy involves the accumulation of potassium (K^+) and chloride (Cl^-) ions within the cytoplasm for osmotic balance (Oren 1999). This strategy of osmotic adaption is found to be bioenergetically less expensive, but it requires the intracellular enzymatic systems to remain functional at high salt concentration. The use of this strategy is therefore confined only to a few specialised groups of extreme halophilic microorganisms. Their metabolic processes (i.e. especially their enzymes) are adapted to high salt concentration in such a way that their functionality is lost when the salt concentration decreases.

The other strategy to deal with osmotic stress is known as the “organic-osmolyte” strategy (Lay et al. 2010). This strategy is more widely used among the larger group of moderately halophilic and halotolerant microorganisms. It involves the accumulation of compatible organic osmotic solutes such as glycerol, glycine betaine, ecotin and various sugar alcohols and amino acids within the cytoplasm for osmotic balance. This mode of osmotic adaption is found to be bioenergetically more expensive, but it does not require the intracellular enzymatic systems to adapt to high concentrations of inorganic salts.

The influence of increased salt concentration on the biological treatment of wastewater is subject of numerous scientific publications. In most of the studies a wide range of salt concentrations was investigated. Some of the studies were conducted with real wastewater, such as from olive processing (Ferrer-Polonio et al. 2015), seafood processing (Moon et al. 2003) or fishing industry (Khannous et al. 2003). However, most of the studies are conducted with synthetic wastewater. For salting up mostly NaCl was used. Only Campos et al. (2002) and Jia et al. (2014) have also investigated the influence of other salts than NaCl on the biological treatment process.

Increased salt concentration affects aerobic biological wastewater treatment in different ways. In the following a short summary is given about the impact on treatment performance, the microbial community structure, sludge settling behaviour and microbial respiration activity. A more detailed review can be found in He et al. (2017) or Lefebvre and Moletta (2006).

The COD elimination as well as nitrification performance is negatively affected by increased salt concentrations, as different experimental studies show (Dinçer and Kargi 2001; Ferrer-Polonio et al. 2015; Kargi and Dincer 1997; Ng et al. 2005; Panswad and Anan 1999; Wang et al. 2005; Jia et al. 2014; Rene et al. 2008). In a comparison of adapted and non-adapted biomass, Panswad and Anan (1999) observed a decrease in COD elimination, when the salt concentration was increased to 30 g/L. Thereby the adapted biomass shows significantly lower reduction performance than the non-adapted biomass. Even after being subject to shock loading of a salt concentration of 70 g/L, the adapted biomass was found to be more resistant. Wang et al. (2005) investigated in batch tests the effect of shock loads on the total organic carbon (TOC) elimination performance. They observed a decrease of 7 % in TOC elimination already at a salt concentration of 2 g/L. A shock load of 5 g/L led to a decrease of 30 %. However, the biomass used by Wang et al. (2005) was not adapted to high salt concentrations. Jia et al. (2014) increased the concentration of sodium chloride and sodium sulphate up to 30 g/L in each of two separately observed sequencing batch reactors (SBR). Up to a salt concentration of about 18 g/L, the COD elimination remained almost constant at about 90 %. With a further increase in salt concentration, the COD-elimination reduced to 65 %. As the salt concentration was then gradually lowered again, the COD-elimination was further reducing to about 45 %. Thereby, they could not observe any difference of SBR dosed with NaCl or Na_2SO_4.

The effect of increased salt concentration on nitrification is similar. In several cases, a decreasing performance could be observed (Bassin et al. 2012; Campos et al. 2002; Moussa et al. 2006; Panswad and Anan 1999; Rene et al. 2008; Jia et al. 2014). Some experimental results indicate that ammonium-oxidizing bacteria are more sensitive to changing salt concentration than nitrite-oxidizing bacteria (Moussa et al. 2006; Jia et al. 2014). A difference in effect of the salt type does not seem to exist (Campos et al. 2002; Jia et al. 2014). As already the results of salt effect on COD elimination shows, the adapted biomass also promises a more stable nitrification performance (Panswad and Anan 1999).

As clear as the negative effect of increased salinity on COD elimination and nitrification is, as ambivalent are the experimental results on the influence on sludge settling properties. Many studies report, that sludge settling properties improve with rising salt concentration (Bassin et al. 2012; Campos et al. 2002; Ferrer-Polonio et al. 2015; Linarić et al. 2013; Ng et al. 2005; Jia et al. 2014). A possible explanation suggested by Linarić et al. (2013) is that the repulsive forces between the predominantly negatively charged sludge flocs is overcome by compacting the electrical double layer. Nevertheless,

other studies report a negative effect of increased or changing salt concentration on sludge settling properties (Lefebvre and Moletta 2006; Kara et al. 2008; He et al. 2017). Jia et al. (2014) could even observe both in their SBR treating saline wastewater. With increasing salt concentration, they observed a drop in sludge volume index (SVI; mL/g) from 137 mL/g to 71 mL/g. With subsequent decreasing salt concentration, the SVI increased to 298 mL/g, and therefore poorer SVI than at the beginning of the experiment. Furthermore, they detected sludge bulking. Bassin et al. (2012) increased salt concentration in two SBR stepwise over 35 d. They observed a gradual improvement in SVI with rising salt concentration, but also a considerable washout of cells and high turbidity in the effluent. Similar observations were made by Ferrer-Polonio et al. (2015) and Ng et al. (2005). Using electron microscopy, Ng et al. (2005) showed, that the increased turbidity in effluent is caused by undissolved cellular components which are released due to plasmolysis of microorganisms. Again, adapted biomass shows a better performance. i.e. less turbidity and solids concentration in the effluent, than non-adapted biomass (Ferrer-Polonio et al. 2015). A hint how microorganism adapt to the changing salt concentration is shown by the experimental results of Jia et al. (2014). They found an increase in extra polymeric substances (EPS) in the activated sludge both with increasing and decreasing salt concentration. He et al. (2017) suggest that this is a stress mechanism of the activated sludge to adapt to changing environmental conditions by producing such substances. These results are of interest for aeration research, as these substances are known for inhibiting oxygen transfer (see chapter 3.4.3).

Increasing salt concentration is also associated with a reduction in the respiratory activity of microorganisms (Linarić et al. 2013; Moussa et al. 2006; Wang et al. 2005), whereby no influence of the type of salt is recognizable (Campos et al. 2002). Furthermore, most studies report an impoverishment of diversity in the biocenosis (Bassin et al. 2012; Moussa et al. 2006; Ng et al. 2005). Especially the protozoa population is significantly reduced or even disappear at salt concentration of 5 g/L or higher (Wang et al. 2016).

In summary, increased salt concentration in aerobic wastewater treatment affects overall treatment performance negatively. Lower organic elimination, poorer nitrification and a change in biocenosis are to be expected. Thereby, the degree of the effect is smaller the more adapted the biocenosis is. In addition, shock loads and therefore stress for the microorganisms should be avoided. Otherwise, the EPS-production increases and cell-plasmolysis occurs. These leads to poorer effluent quality and likely to a decreasing oxygen transfer.

4 Cumulative Part

4.1 Summary of Publications

Paper I

Behnisch, J.; Schwarz, M.; Wagner, M. (2020):

Three decades of oxygen transfer tests in clean water in a pilot scale test tank with fine-bubble diffusers and the resulting conclusions for WWTP operation.

In: *Water Practice and Technology*, 15(4), 910–920.

Paper II

Behnisch, J.; Ganzauge, A.; Sander, S.; Herrling, M.P.; Wagner, M. (2018):

Improving aeration systems in saline water: measurement of local bubble size and volumetric mass transfer coefficient of conventional membrane diffusers.

In: *Water Science and Technology*, 78(4), 860–867.

Paper III

Behnisch, J.; Schwarz, M.; Trippel, J.; Engelhart, M.; Wagner, M. (2021):

Improving aeration systems in saline water (Part II): Effect of different salts and diffuser type on oxygen transfer of fine-bubble aeration systems.

In: *Water Science and Technology*, 83(11), 2278–2792.

Paper IV

Behnisch, J.; Schwarz, M.; Trippel, J.; Engelhart, M.; Wagner, M. (2022):

Oxygen transfer of fine-bubble aeration in activated sludge treating saline industrial wastewater.

In: *Water*, 14(12), 1964.

4.2 Paper I

Title: **Three decades of oxygen transfer tests in clean water in a pilot scale test tank with fine-bubble diffusers and the resulting conclusions for WWTP operation**

Published: ©IWA Publishing 2020. The definitive peer-reviewed and edited version of this article is published in *Water Practice and Technology* 15(4), 910 – 920, 2020, doi:10.2166/wpt.2020.072 and is available at www.iwapublishing.com

First author: Behnisch, J., M.Sc.

Co-authors: Schwarz, M., M.Sc.

Wagner, M., Prof. Dr.-Ing. habil.

Abstract: We summarized the experience from three decades of oxygen transfer testing and aeration research at Technical University of Darmstadt to validate the oxygen transfer efficiency of modern fine-bubble diffusers. 306 oxygen transfer tests in clean water of 65 different fine-bubble diffusers, carried out in the same test tank under identical test conditions, were analyzed and compared with previous results. As a result, we could show that the performance of fine-bubble aeration systems has increased by 17 % over the last three decades. Therefore, modern well designed and operated aeration systems can achieve SSOTE values between 8.5 and 9.8 % · m^{-1}. Additionally, a comparison of various diffuser types and diffuser densities was done. Based on the new results an exemplary cost/benefit analyses for a 100,000 PE WWTP shows the calculation of an optimized diffuser density with respect to investment and operating costs.

Keywords: aeration system, oxygen transfer efficiency, dynamic cost comparison calculation

4.3 Paper II

Title: **Improving aeration systems in saline water: measurement of local bubble size and volumetric mass transfer coefficient of conventional membrane diffusers**

Published: ©IWA Publishing 2018. The definitive peer-reviewed and edited version of this article is published in *Water Science and Technology* 78(4), 860 – 867, 2018, doi:10.2166/wst.2018.358 and is available at www.iwapublishing.com

First author: Behnisch, J., M.Sc.

Co-authors: Ganzauge, A., M.Sc

Sander, S., Dr.-Ing.

Herrling, M. P., Dr.-Ing.

Wagner, M., Prof. Dr.-Ing. habil.

Abstract: In this study, for the first time, the influence of the design of conventional membrane diffusers on the volumetric mass transfer coefficient (k_La) and bubble size in tap water (TW) and saline water (SW) was investigated (up to 15 g/L NaCl). By using a new analytical approach, k_La and the bubble size along the ascent of the bubble swarm were measured simultaneously and in real time. The results show that in TW, after collision bubbles merge into larger bubbles by coalescence. In SW, coalescence is inhibited by salt. Due to the smaller bubble size, k_La increases to more than double compared to TW. The results show that in SW, membrane diffusers with dense slit patterns and smaller slit lengths are to be recommended in order to enable improved utilization of oxygen in saline water.

Keywords: Aeration; flexible membrane diffuser; image analysis; oxygen transfer; bubble size distribution; volumetric mass transfer coefficient

4.4 Paper III

Title: **Improving aeration systems in saline water (Part II): Effect of different salts and diffuser type on oxygen transfer of fine-bubble aeration systems**

First author: Behnisch, J., M.Sc.

Co-authors: Schwarz, M., M.Sc.

Trippel, J., M.Sc.

Engelhart, M., Prof. Dr.-Ing.

Wagner, M., Prof. Dr.-Ing. habil.

Abstract: The objective of the present study is to investigate the different effects on the oxygen transfer of fine-bubble aeration systems in saline water. Compared to tap water, oxygen transfer increases due to the inhibition of bubble coalescence. In Part I of the present study, we investigated in lab-scale experiments the effect of design of diffuser membrane. The objective of Part II is the assessment of effects of different salts, diffuser type and diffuser density. We measured the concentration of various salts (MgCl2; CaCl2; Na2SO4; NaCl; KCl) above which coalescence is fully inhibited and oxygen transfer reaches its maximum (referred to as the critical coalescence concentration; CCC). For this purpose, we developed a new analytical approach, which enables to investigate the coalescence behaviour of any aeration system and (mixed) salt solution quickly and easily by evaluating the results of oxygen transfer tests. To investigate the transferability to large scale and the effect of diffuser type and density, we repeated lab-scale experiments in a 17,100 L pilot scale test tank and carried out additional tests with tube and plate diffusers at different diffuser densities. The results show, that despite the higher pressure drop, diffusers with dense slit density and smaller slits are to be recommended in order to improve efficiency of aeration systems in saline water.

Keywords: Critical Coalescence Concentration; Transition Concentration; SSOTE; SAE; flexible membrane diffuser

Introduction

Today, in biological wastewater treatment plants, mainly fine-bubble aeration systems are used to satisfy the oxygen demand of microorganisms in activated sludge (Wagner and Stenstrom 2014). Air is introduced via diffusers installed at the bottom of the aeration tank. From the rising air bubbles, the oxygen is transferred to the liquid phase. There are different diffuser types available (Discs, Plates, Tubes) made out of various materials. Oxygen transfer from ascending air bubbles to the liquid phase is described by the volumetric mass transfer coefficient (k_La), which represents the product of the liquid-side mass transfer coefficient (k_L) and the liquid/gas interfacial area (a). The k_La mainly depends on water quality parameters (e.g. salt concentration, temperature) and diffuser design. Today, mainly some industrial wastewaters show increased salt concentration (Lefebvre and Moletta 2006; He et. al. 2017). Nevertheless, the global trend towards saving fresh water, e.g. through (industrial)-wastewater reuse or by using seawater for toilet flushing (Sander 2018), will raise the volume of saline wastewater that needs to be (biologically) treated. Depending on the origin of the wastewater, the dissolved salt and salt mixture will change. Therefore, a deeper understanding of the effects of increased concentration of different salts and salt mixtures is crucial to enhance the (energy) efficiency of aerobic biological wastewater treatment.

For fine-bubble aeration systems, increased salt concentration (c_{Salt}) reduces k_L, but increases a due to the inhibition of bubble coalescence. The increase is enough resulting in a net increase of k_La (Baz-Rodríguez et al. 2014). The increase of k_La in saline water (SW) is described by the f_S value, which is the ratio between k_La in SW to k_La in tap water (TW). In Part I of the present work, we could show in lab-scale experiments with different conventional disc diffusers by combining bubble size measurement and oxygen transfer tests, that the length and density of the slits in the diffuser membrane influences f_S (Behnisch et al. 2018). In this case, the smaller the bubbles detaching from the diffuser (primary bubbles) the higher is f_S. Early 1980s, Zlokarnik (1980) investigated the coalescence behaviour of different aeration devices commonly used at that time. He also concluded that the more the coalescence is inhibited, the more advantageous it is to use aeration devices, which produce small primary bubbles.

Sander et al. (2017) carried out oxygen transfer tests at varying sea salt concentrations with disc diffusers in a pilot-scale test tank. They found the simple relationship $f_S = k \cdot c_{Salt} + 1$, whereby k mainly depends on the airflow rate per disc diffuser. Nevertheless, f_S does not increase infinitely. At a certain c_{Salt} the coalescence is completely inhibited and f_S reaches its maximum ($f_{S,max}$). This concentration is called the critical coalescence concentration (*CCC*) and is specific for each salt(solution) and bubble formation system (Cho and Laskowski 2002; Firouzi et al. 2015).

Sovechles and Waters (2015) as well as Quinn et al. (2014) determined *CCC* of varying salts in a lab-scale flotation cell by measuring the bubble size (given as Sauter mean diameter (d_{32})) via image analyses of the bubble swarm at different c_{Salt}. Due to the inhibition of bubble coalescence with increasing c_{Salt}, d_{32} decreases linearly (Zone 1) up to *CCC* (Grau et al. 2005). Here (Zone 2), d_{32} reached its minimum ($d_{32,min}$), called quasi-static-bubble diameter or initial bubble diameter (Marrucci and Nicodemo 1967; Sovechles and Waters 2015). According to Grau et al. (2005), the point at which the fitted lines for Zone 1 and Zone 2 meet defines the *CCC*.

There are other methods to investigate the coalescence of a system than with image analyses. Craig et al. (1993) measured the coalescence by detecting the change of light intensity from an expanded beam of light, which was passed through the bubble swarm produced by a sinter at the base of the transparent test column. Prince and Blanch (1990) used a model-based approach to predict *CCC* for different salts using test results of Marrucci and Nicodemo (1967) and Lessard and Zieminski (1971). While Marrucci and Nicodemo (1967) also applied image analyses to determine the bubble size in a bubble swarm produced by a bronze porous plate, Lessard and Zieminski (1971) observed bubble pairs detaching at

the end of two adjacent capillaries. Similar to *CCC*, some researchers also use the transition concentration (TC_X) to quantify the grade of decrease of bubble size with increasing c_{Salt}. The index *X* indicates the grade at which the bubbles size reduces X % from that in pure water to the constant bubble size at high salt concentration. Accordingly, TC_{100} and *CCC* are synonymous (Sovechles and Waters 2015). Currently, there is no definitive agreement in explaining the inhibiting effect of salts on bubble coalescence. Firouzi et al. (2015) gives a detailed review of all proposed theories, which include colloidal forces, gas solubility, Gibbs-Marangoni effect, surface rheology and ion specific effects.

Experiments show that bubble formation as well as bubble size affect *CCC* (Firouzi et al. 2015; Sander 2018). Since the bubbles in a flotation cell as used by Sovechles and Waters (2015), are very small and are formed by cavitation and not by a diffuser, the validity of the results for fine-bubble diffusers is questionable. Furthermore, to investigate the influence of salt on oxygen transfer, previous studies used only disc diffusers (Sander et al. 2017; Behnisch et al. 2018) or porous plates and frits (Marrucci and Nicodemo 1967; Zlokarnik 1980), which are no longer used today for wastewater treatment. Additionally, only the influence of NaCl and sea salt has been investigated so far.

Therefore, we determined for the first time *CCC* for different salts with conventional fine-bubble diffusers. Because measuring bubble size in a bubble swarm is laborious, we transferred the method of Grau et al. (2005) for determining *CCC* to our results of oxygen transfer tests. To do so, we took advantage of the fact that f_S behaves similarly to d_{32} with increasing c_{Salt}, only with reversed sign. The f_S value increases linearly instead of a linear decrease in d_{32}. In order to investigate the transferability of the results to large scale as well as the influence of the diffuser type and diffuser density on f_S, we also carried out oxygen transfer tests with disc, tube and plate diffusers in a 17,100 L fully glazed steal frame tank at c_{Salt} between 0 and 20 g/L NaCl. Finally, we show the large improvement of aeration in SW by comparing specific standard oxygen transfer efficiency (*SSOTE*) and standard aeration efficiency (*SAE*) with TW conditions, and give some additional design considerations.

Material and Methods

Membrane diffusers

Six different conventional membrane diffusers (2 disc diffusers, 2 plate diffusers, 2 tube diffusers) with different slit densities (*SD*) and slit lengths (d_S) were used (Table 7). *SD* is defined as the number of slits relative to the active (perforated) membrane area (A_A). Tube diffusers used here, perforation is only on the side of the diffuser and top and bottom are not perforated (Figure 18). For plates and discs A_A is similar to the projected media surface area (A_P). Depending on the percentage of perforated membrane area, for tube diffusers applies $A_A >> A_P$. According to Behnisch et al. (2020), diffuser density (*DD*) is the total membrane area (including unperforated area) divided by area of the tank floor.

Table 7: Properties of the tested diffusers

Name	Material	A_A [cm²] per diffuser	A_P [cm²] per diffuser	d_S [mm]	P_R/d_S [-]	P_S/d_S [-]	SD [slits/cm²]	slits per diffuser [-]	$q_{A,XXX}$ operation range
Disc 1	EPDM	324	550	0.75	4.07	2.15	15.5	5,028	1.5 – 8.0[a]
Disc 2	EPDM	306	550	1.25	2.44	1.80	10.0	3,063	1.5 – 8.0[a]
Plate 1	EPDM	1,867	2,000	0.7	14.3	14.3	0.88	1,636	1.0 – 3.0[b]
Plate 2	EPDM	1,867	2,000	1.2	2.50	3.75	5.5	10,285	25.0 – 35.0[b]
Tube 1	Silicon	1,450	665	0.6	3.30	3.33	14.5	21,031	1.0 – 6.0[c]
Tube 2	Silicon	1,450	665	1.2	1.70	2.08	11.3	16,317	4.0 – 8.0[c]

EPDM: Ethylene-Propylene-Dien-Terpolymere; A_A: active (perforated) membrane area per diffuser; A_P: projected media surface area per diffuser; d_S: slit length; P_R: distance between rows; P_S: distance between slits; SD: slit density
Operation range given by manufacturer in: [a] $q_{A,Disc}$ in (m³/h/disc); [b] $q_{A,Plate}$ in (m³/h/plate); [c] $q_{A,Tube}$ in (m³/h/m)

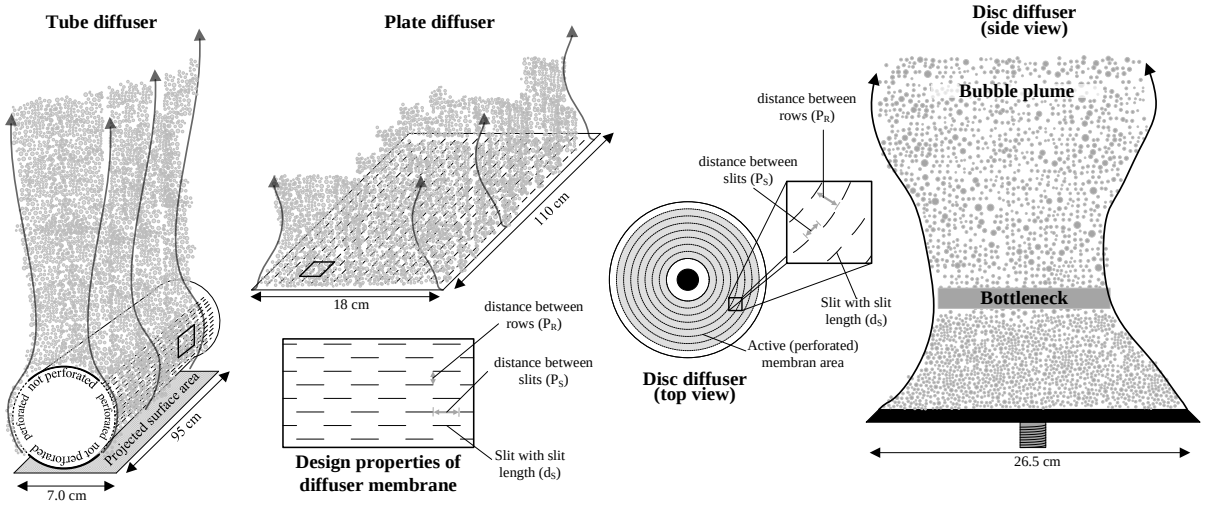

Figure 18: Schematic representation of the tested diffuser types and the definition of parameters of membrane design

Measuring salt concentration (c_{Salt})

Determining the exact salt concentration during the tests, especially in the large pilot scale test tank, faced us with some challenges. Large amounts of salt were needed to achieve the desired concentrations (up to 342 kg for a single test). Additionally, the tests for each salt or diffuser type required several days and a regular addition of TW was necessary to compensate evaporation losses. To ensure constant experimental conditions, an on-line measurement of salinity was necessary. Therefore, we decided to apply a method commonly used in environmental technology and determined c_{Salt} by measuring the conductivity (*EC*) on-site standardized at 20 °C water temperature with standard conductivity cell (TetraCon® 324, WTW, Germany).

The correlation between *EC* and c_{Salt} is usually expressed by a simple linear equation: $c_{Salt} = t \cdot EC$. However, the relationship between *EC* and c_{Salt} is not always linear and depends on the activity of specific dissolved ions, ionic strength (*IS*) and the average activity of all ions in the liquid (Rusydi 2018). Therefore, before starting oxygen transfer tests, we measured *EC* of salt solutions with known concentration in a 500 mL beaker. Our results show, that the relationship in the chosen concentration ranges is always linear. This can be seen, for example, in the calibration line for $MgCl_2$ in Figure 19-A. Therefore, the calibration line is given by the following formula: $EC = b_1 \cdot c_{Salt} + b_0$, being b_0 the *EC* of TW. In all our tests, *EC* of TW was 0.7 mS/cm. With the known calibration lines, we were able to calculate the salt concentration by measuring *EC* on site during oxygen transfer tests. When measuring *EC* in aerated tanks, care must be taken since air bubbles can lead to incorrect measurements.

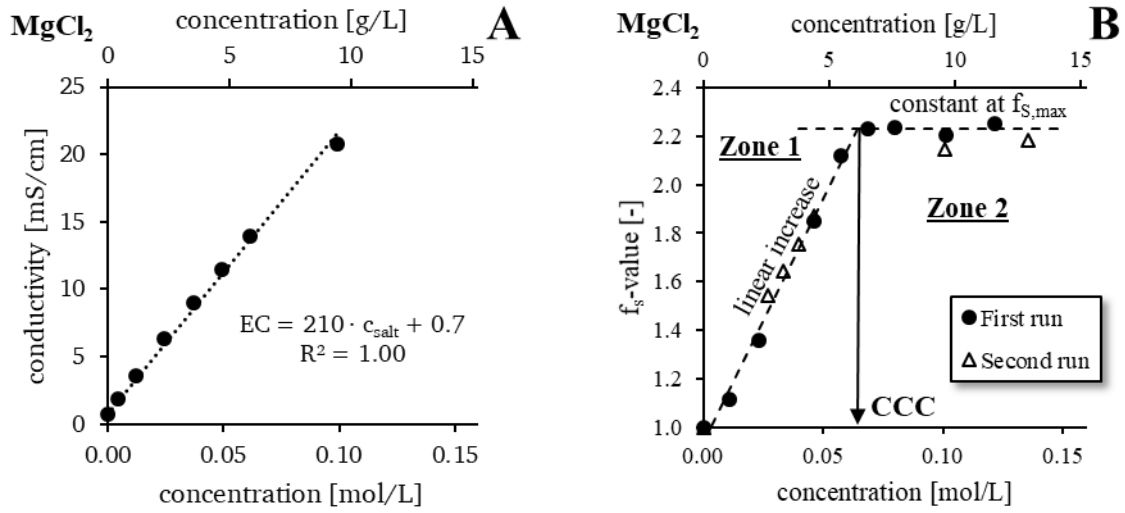

Figure 19: Measuring CCC: calibration line for calculating $MgCl_2$ concentration by measuring conductivity (A); determining *CCC* of $MgCl_2$ by oxygen transfer test results in lab scale experiments (B)

Measuring CCC with oxygen transfer tests in lab-scale experiments

To measure *CCC* for different salts oxygen transfer tests were performed with *Disc 1* in a rectangular tank (0.5 m x 0.5 m) with a water depth of 1.0 m, using the pure oxygen desorption method according to EN 12255-15. With this method, the oxygen concentration is increased 15 – 20 mg/L beyond the oxygen saturation concentration by aerating with pure oxygen gas or oxygen enriched air (Wagner et al. 1998). By switching to aeration with ambient air, the oxygen concentration starts to decreases again until the saturation concentration is reached. From the curve of decreasing oxygen concentration, the k_La for a specific water temperature (*T*) is calculated (k_La_T) by nonlinear regression. Four electrochemical oxygen probes (Oxymax COS51D, Endress + Hauser, Germany) were installed to record dissolved oxygen concentration. Finally, the k_La was standardized to 20 °C (k_La_{20}) according to the equation: $k_La_{20} = k_La_T \cdot 1.024^{(20-T)}$.

Tests were performed at different airflow rates (2.0, 3.5 and 4.5 m³/h) and salt concentrations. The airflow rate was measured at standard temperature and pressure (0 °C; 101.3 kPa; 0 % humidity) with a thermal flow sensor (TA16, Hoentzsch, Germany). The $d_{32,min}$ was only measured during tests with NaCl by image analyses (Behnisch et al. 2018). Several experiments show that regardless of salt type the minimum bubble size is always the same (Lessard and Zieminski 1971; Quinn et al. 2014).The first test was carried out in TW; then salt was added.

Figure 19-B shows how *CCC* was determined using the example of test results with $MgCl_2$. According to the method we adapted from Grau et al. (2005), the *CCC* results from intersection of fitted lines of

Zone 1 (linear increase of f_S) and Zone 2 (constant f_S at $f_{S,max}$). Accordingly, *CCC* for $MgCl_2$ (CCC_{MgCl2}) is 0.065 mol/L or 6.2 g/L. To verify the reproducibility of the measurement, we repeated the experiment with a new disc diffuser of the same design. In the second run, we measured an CCC of 0.061 mol/L or 5.8 g/L, which represents an deviation of 6 %. Therefore, the reproducibility of the results are good.

Oxygen Transfer tests in Pilot Scale Test Tank

The Pilot Scale Test Tank is a fully glazed steal frame tank (L/W/H = 3.0 m/1.5 m/4.0 m) with a water level of 3.8 m, yielding a water volume of 17.1 m³. Ten test series with different diffuser types (Figure 18) and diffuser densities were carried out in the test tank. Therefore, 32 or 6 disc diffusers, 10 or 6 tube diffusers and 4 plate diffusers were installed in the glass tank, respectively. Diffuser depth of submergence is on average 3.65 m and varies negligibly between the individual diffusers.

The oxygen transfer was measured as before in the lab-scale experiments by using the desorption method according to EN 12255-15. As before during lab-scale experiments, dissolved oxygen in water is measured using four electrochemical oxygen probes (Oxymax COS51D, Endress + Hauser, Germany) installed at different positions in the test tank. The compressed air is produced by means of a positive displacement blower (GMA 10.0, Aerzener Machine Factory, Germany). To measure the airflow rate precisely, a calibrated rotary-piston gas meter (Aerzener G 65, type ZB 039.0, Aerzener Machine Factory, Germany) with manometer and thermometer was installed downstream of the blower. The airflow rate (Q_A) was normalized at standard temperature and pressure conditions (0 °C; 101.3 kPa; 0 % humidity). Q_A is indicated per aerated tank volume ($Q_{A,VAT} = Q_A \cdot (\text{tank volume})^{-1}$), per disc diffuser ($q_{A,Disc} = Q_A \cdot (\text{number of disc diffusers})^{-1}$), per plate diffuser ($q_{A,plate} = Q_A \cdot (\text{number of plate diffusers})^{-1}$), per length of tube diffuser ($q_{A,tube} = Q_A \cdot (\text{number of tube diffusers} \cdot \text{length of single tube diffuser})^{-1}$) or per slit of diffuser membrane ($q_{A,slit} = Q_A \cdot (\text{number of diffusers} \cdot \text{slits per diffuser})^{-1}$).

Tests were performed at different airflow rates and NaCl-concentration (c_{NaCl}). The airflow rate set during the tests depends on operational range of diffuser specified by the manufacturer and the capacity of the blower. As described before, c_{NaCl} was calculated by measuring *EC*. Also, the standard oxygen transfer rate per aerated tank volume ($SOTR_{VAT} = \text{SOTR} \cdot (\text{aerated tank volume})^{-1}$) was calculated, being *SOTR* the standard oxygen transfer rate normalized to 20 °C water temperature and atmospheric pressure of 101.3 kPa (EN 12255-15). Here it must be noted, that the solubility of oxygen (c_S) decreases with increasing c_{Salt}. The oxygen saturation concentration for different temperatures and salt concentrations can be taken from tables, to be found e.g. in ISO 5814. According to ASCE/EWRI 18-18, c_S in SW ($c_{S,SW}$) can also be estimated with known c_S in TW ($c_{S,TW}$) and c_{Salt} (in g/L) as follows: $c_{S,SW} = (1.0 - 0.01 \cdot c_{Salt}) \cdot c_{S,TW}$. However, when comparing $c_{S,SW}$ calculated according to the given formula and the tabulated values, we found an increasing deviation with increasing c_{Salt} (see Annex 1). Therefore, we have adjusted the formula to calculate $c_{S,SW}$ as follows: $c_{S,SW} = (1.0 - 0.0059 \cdot c_{Salt}) \cdot c_{S,TW.}$

Results and Discussion

Lab-scale experiments

In Table 8 determined dependencies between *EC* and salt concentration are listed. The coefficients of determination (R^2) close to 1.0 prove the linear dependence between *EC* and c_{Salt} within the chosen concentration range up to maximum selected salt concentration (c_{max}). As previously mentioned, the relationship is influenced by many factors, and therefore the equations shown here are only valid in TW for the specified concentration ranges. To calculate the salt concentration in solutions with other background contamination (i.e. dissolved substances other than the salt to be measured), the equation may have to be adapted.

Table 8: Determined dependencies between *EC* and salt concentration $EC = b_1 \cdot c_{Salt} + b_0$

Salt	**Manufacturer**	**Assay** [%]	**b_1 [(mS · L)/ (cm · mol)]**	**b_0 [mS/cm]**	**R^2 [-]**	**n [-]**	**c_{max} [mol/L]**	**[g/L]**
$MgCl_2$	Zschirmer & Schwarz GmbH	94.5	210	0.7	1.00	7	0.12	11.4
NaCl	Carl Roth GmbH	99.5	98	0.7	1.00	8	0.35	20.6
KCl	Merck KGaA	99.5	119	0.7	1.00	12	0.53	39.9
$CaCl_2$	Zschirmer & Schwarz GmbH	94.0	172	0.7	0.99	8	0.26	28.9
Na_2SO_4	Zschirmer & Schwarz GmbH	99.5	139	0.7	0.98	8	0.36	51.0

EC: conductivity (mS/cm); c_{Salt}: salt concentration (mol/L); n: number of measuring points; c_{max}: Maximum salt concentration at which EC was determined (mol/L or g/L)

Results in Table 9 summarize the determined *CCC* for different salts together with values given in literature supplemented by information of observed $d_{32,min}$, test setup and measurement method of coalescence. Regardless of salt type, $f_{S,max}$ reached during *CCC* measurement varied marginally and was on average 2.2. This confirms several experimental studies (Lessard and Zieminski 1971; Quinn et al. 2014), which show that in coalescence inhibited systems k_La and bubble size reach a fixed value regardless of salt type. During the tests of Sander et al. (2017), the bubble size was not measured and is therefore not available (n.a.). However, since similar fine-bubble diffusers were used, we can assume that similar bubble sizes were achieved as in our tests.

Table 9: Summary of CCC from own measurements and literature references

	own results			**Sovechles and Waters (2015)**			**Quinn et al. (2014)**			**Craig et al. (1993)**			**Prince and Blanch (1990)**		
$d_{32,min}$	1.25 mm			0.60 mm			0.60 mm			n.a.			3.6 - 4.1 mm		
System	bubble swarm			bubble swarm			bubble swarm			bubble swarm			bubble pairs/bubble swarm		
Method	oxygen transfer			measuring bubble size			measuring bubble size			turbidity			measuring bubble size		
Bubble formation	Membrane diffuser			Flotation cell			Flotation cell			Sinter plate			Needles/porous plate		
	CCC	CCC	IS	CCC	CCC	IS	CCC	CCC	IS	CCC	CCC	IS	CCC	CCC	IS
Salt	**[mol/L]**	**[g/L]**	[-]	**[mol/L]**	**[g/L]**	[-]	**[mol/L]**	**[g/L]**	[-]	**[mol/L]**	**[g/L]**	[-]	**[mol/L]**	**[g/L]**	[-]
$MgCl_2$	0.063	6.0	0.19	0.092	8.8	0.28				0.086	8.2	0.26	0.055	5.2	0.17
$CaCl_2$	0.080	8.9	0.27	0.091	10.1	0.27	0.11	12.2	0.33	0.17	18.9	0.51	0.055	6.1	0.17
Na_2SO_4	0.085	12.8	0.27	0.082	11.6	0.25	0.13	18.5	0.39				0.061	8.7	0.18
NaCl	0.18	10.5	0.18	0.22	13.1	0.22	0.31	18.1	0.31	0.23	13.4	0.23	0.18	10.2	0.18
KCl	0.21	15.7	0.21	0.25	18.8	0.25	0.31	23.1	0.31	0.33	24.6	0.33	0.23	17.2	0.23
$MgSO_4$				0.071	8.5	0.28	0.070	8.4	0.28	0.090	10.8	0.36	0.032	3.9	0.13
$AlCl_3$				0.056	7.5	0.34									
$Al_2(SO_4)_3$				0.024	8.2	0.35									
NaBr													0.22	22.6	0.22
K_2SO_4													0.080	13.9	0.24
KOH													0.17	9.5	0.17
$CuSO_4$													0.070	11.2	0.28
KI													0.62	102.9	0.62
KNO_3													0.41	41.5	0.41
Sea Salt	*[0.32*	*10*	*0.19][a]*	0.39	12.4	0.27									

$d_{32,min}$: minimum bubble diameter (also 'quasi-static-bubble diameter' (Marrucci and Nicodemo (1967)) or 'limiting bubble size' (Sovechles et al. (2015))

[a]results from Sander et al (2017), $d_{32,min}$ = n.a. CCC: Critical Coalescence Concentration [in mol/L or g/L]; IS: Ionic Strength [-]

A direct comparison of the *CCC* reported in the different papers is not possible due to the different measurement methods and test conditions. Nevertheless, some tendencies can be identified. For example, with the exception of Na_2SO_4, the *CCCs* reported by other authors are higher than our results. Only the *CCC* determined by Prince and Blanch (1990) are lower, except for KCl. A possible correlation can be seen here with the observed bubble size, which is larger in the case of Prince and Blanch (1990) and smaller in the case of the other papers than in our own experiments. Already Firouzi et al. (2015) and Sander (2018) showed, that the smaller the bubbles the higher the *CCC* of a salt. If only the *CCC* are considered as the molar concentration (i.e., in mol/L) of the salts investigated in all the different studies, the following order emerges for most of the studies reported here:

$$MgCl_2 < CaCl_2 < Na_2SO_4 < NaCl < KCl$$

Already Sovechles and Waters (2015) showed that *CCC* decreases for salts containing multivalent ions. While 1:1 (cation:anion charge) salts had the highest *CCC*; 1:2 and 2:1 salts had intermediate *CCC*; and 2:2, 3:1 and 3:2 salts had the smallest CCC. Therefore, they try to describe the inhibition of coalescence by salt (and multicomponent salt solutions) by calculating *IS*. In analogy to *CCC*, they postulated that coalescence is completely inhibited in their flotation cell when *IS* = 0.28, which they called Critical-Coalescence Ionic Strength (*CCIS*). To verify this, all results in Table 9 were supplemented by the *IS* we calculated. *IS*-values of salt solution by Prince and Blanch (1990) varies between 0.13 and 0.62. Also for our test results *IS* fluctuates between 0.18 and 0.27. This variation is very large, which is why we cannot confirm the approach postulated by Sovechles and Waters (2015) to describe coalescence inhibition by determining the *IS*. Indeed, the *CCC* must be determined for each new (bubble formation) aeration system individually.

So even if the absolute values of the determined *CCC* do not match those from the literature, which is due to the different bubble size, it can still be said that they are in a specific order relative to each other, independent of the aeration system and the measurement method. The validity of the determined *CCC* and thus of the new measurement method is therefore given.

Experiments in Pilot Scale Test Tank

In the following, first we will present the results of the tests in the pilot scale test tank for each individual diffuser type. Then we try to consider all the results together and discuss the different effects on f_S more in detail. At the end, we will discuss other parameters that have to be taken into account in design of aeration systems in SW in addition to k_La (or f_S).

Results from disc diffuser

In Figure 20 f_S-values from test series with disc diffusers are plotted against c_{NaCL} for different airflow rates together with the results from lab-scale experiments described in Part I of the present paper (Behnisch et al. 2018). For *Disc 1* f_S increases up to 10 g/L NaCl, which corresponds to the *CCC* of NaCl (CCC_{NaCl}) previously determined in the lab-scale experiments. Then f_S reaches its peak value ($f_{S,max}$). The same is true for *Disc 2*, although the transition point from Zone 1 (linear increase) to Zone 2 (constant value) is not as obvious as with *Disc 1*. The pilot-scale experiments show, that for both disc diffusers, the level of $f_{S,max}$ is strongly dependent on $q_{A,Disc}$. The highest f_S values could be reached in the middle of the operation range (3.0 – 4.0 Nm³/h per diffuser) given by the diffuser manufacturer (1.5 – 8.0 Nm³/h per diffuser) which corresponds to the results of Sander et al. (2017). In case of *Disc 2* at very low $q_{A,Disc}$ of 0.2 m³/h/disc (Figure 20-D), f_S is only about 1.0. This means that no salt effect can be observed at such low $q_{A,Disc}$ values. The reason for this will discussed below in the present paper, when discussing the influence of airflow rate on f_S.

Comparing the results of both disc diffusers show, that higher $f_{s,max}$ values were reached with *Disc 1* than with *Disc 2*. Considering the results when the full range of airflow rate was tested (Figure 20-A and 3-

B), mean $f_{S,max}$ of *Disc 1* (2.0) is 10 % higher than of *Disc 2* (1.8). In comparison, k_La_{20}-values in TW are in a comparable range for both diffusers (Annex 2). This confirms the results of previous lab-scale experiments with similar disc diffusers (Behnisch et al. 2018). Accordingly, higher f_S values could be reached with smaller slit lengths (*Disc 1* superior to *Disc 2*). Nevertheless, the effect of airflow rate on f_S was not as obvious as in the experiments conducted in the pilot scale test tank, because of the limited blower capacity and reactor volume during the lab scale experiments. Consequently, a scale effect has to be taken into account in order to obtain adequate results during measurement of oxygen transfer in SW. A sufficient reactor volume as well as blower capacity is necessary, to ensure that the full range of airflow rate of diffusers can be set during the tests. If only two diffusers have to be compared relative to each other, a small reactor is sufficient, whereby the test conditions must be identical.

If both the f_S value and the k_La value rises, so does the $SOTR_{VAT}$. While in *TW* there is a linear relationship between $SOTR_{VAT}$ and $Q_{A,VAT}$ (Behnisch et al. 2020), this is not the case in *SW* due to the dependence of f_S (or k_La) on $q_{A,Disc}$. At a salt concentration of 12 g/L NaCl and a $Q_{A,VAT}$ = 1 Nm³/m³/h, almost similar $SOTR_{VAT}$ of 123 g/m³/h and 132 g/m³/h could be achieved with 6 and 32 *Disc 1* diffusers respectively. This represents an increase of 24 % (99 g/m³/h) and 45 % (91 g/m³/h) compared to 6 and 32 *Disc 2* diffusers respectively. Compared to $SOTR_{VAT}$ in *TW* it is an increase of 105 % (6 Diffusers: 60 g/m³/h) or 60 % (32 Diffusers: 84 g/m³/h). The results show, that due to the influence of $q_{A,Disc}$ on f_S, it is possible that in SW with the same $Q_{A,VAT}$ but different number of diffusers, due to the higher f_S-value (or k_La) similar or even more oxygen can be transferred at low than at high diffuser density.

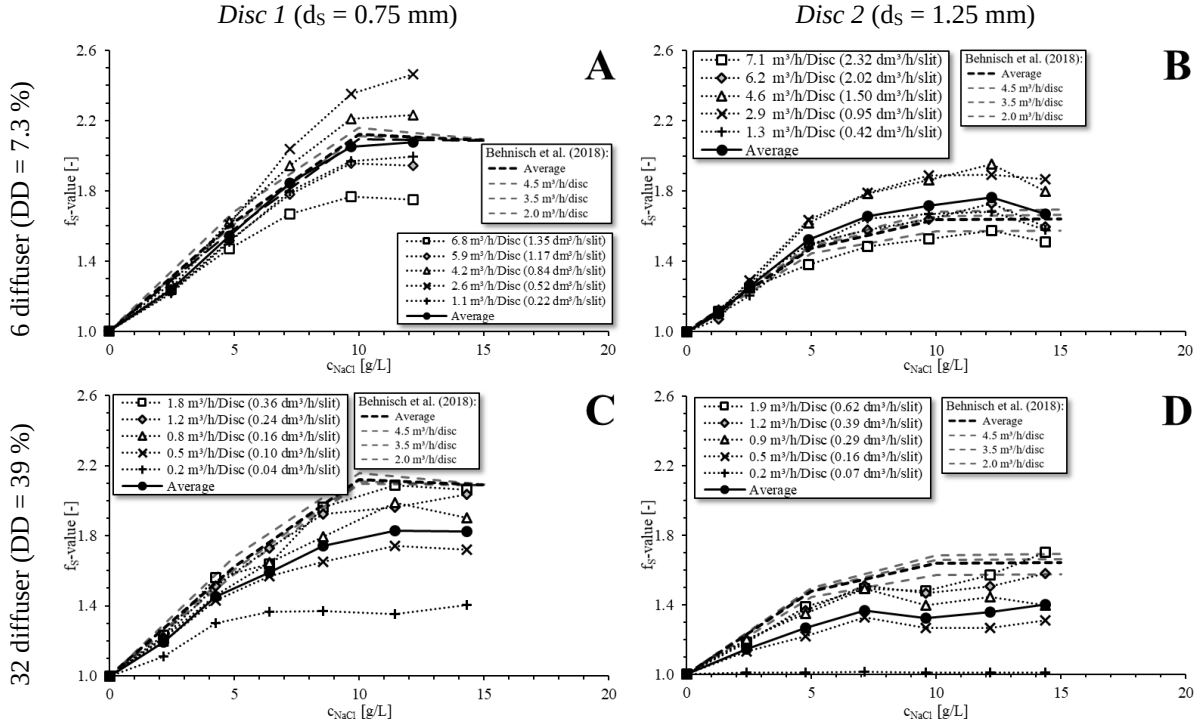

Figure 20: f_S-values as function of c_{NaCl} from disc diffusers for different $q_{A,Disc}$ and $q_{A,Slit}$ supplemented by results of lab-scale experiments described in Part I of the present paper

Results from plate diffuser

In Figure 21 f_S-values from test series with plate diffusers are plotted against c_{NaCl} for different airflow rates. Unexpectedly there are big differences compared to the results of the disc diffusers. For *Plate 1* (Figure 21-A) f_S increases up to a concentration of 5 g/L NaCl, which is quite lower than the measured CCC_{NaCl} in lab-scale experiments. Furthermore, the measured $f_{S,max}$ for *Plate 1* is lower than for *Plate 2* (Figure 21-B), even though *Plate 1* has smaller slits. In comparison, k_La_{20}-values in TW are in a comparable range for both diffusers (Annex 3). In addition, the clear dependency between airflow rate

and f_S observed for the disc diffusers cannot be observed for *Plate 1*, in contrast to *Plate 2* (see Figure 21-B). Here, the f_S-value increases with increasing airflow rate without reaching a noticeable peak, which is consistent with the results of the tests with 32 disc diffusers. However, as before with the disc diffusers, the operational range for *Plate 2* (25 – 35 m³/h/plate) specified by manufacturer was not fully reached due to the limited blower capacity. Therefore, it can be expected, similar to the tests with the 32 disc diffusers, that with increasing airflow rate f_S would first increase further, reach a maximum and then decrease again. If the f_S value is plotted against the airflow rate, this is confirmed, as we will show below.

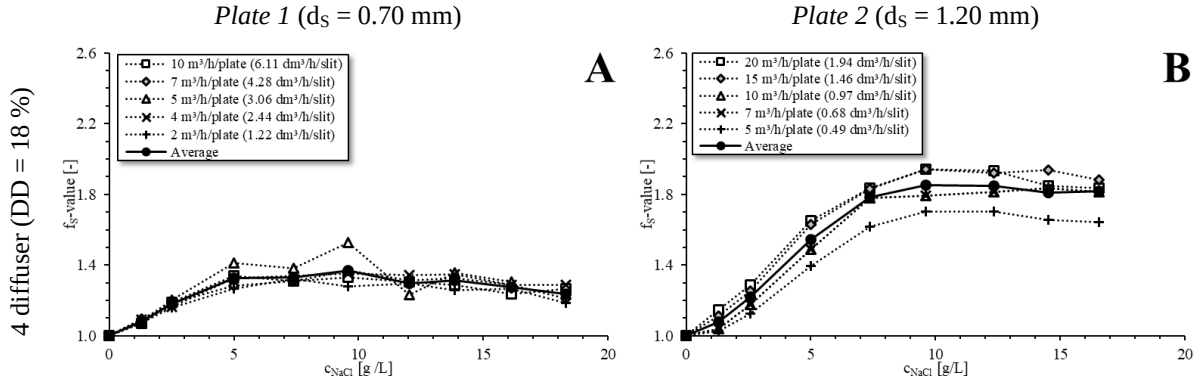

Figure 21: f_S-values as function of c_{NaCl} from plate diffusers for different $q_{A,Plate}$ and $q_{A,Slit}$

Results from tube diffuser

In Figure 22 f_S-values from test series with tube diffusers are plotted against c_{NaCl} for different airflow rates. For both tube diffusers, f_S increases up to 10 g/L NaCl as with the disc diffusers until $f_{S,max}$ is reached. Therefore, the results confirm the CCC_{NaCl} determined in the lab-scale experiments once again. The present data show that the average $f_{S,max}$ of *Tube 1* (2.1) is 10 % higher than that of *Tube 2* (1.9), regardless of the number of installed diffusers. No effect of the number of installed diffusers (or diffuser density) on f_S in case of tube diffusers was detected. In comparison, k_La_{20}-values in *TW* are comparable for both diffusers (Annex 4). Thus, the higher f_S values could be reached with the diffusers with smaller slits, which corresponds to the results of disc diffusers.

At a salt concentration of 13 g/L NaCl and a $Q_{A,VAT}$ = 1 $Nm^3/m^3/h$, a $SOTR_{VAT}$ of 156 and 182 g/m³/h could be achieved with 6 and 10 *Tube 1* diffusers respectively. This corresponds to an increase by 7 % (146 g/m³/h) and 9 % (167 g/m³/h) using *Tube 2* diffusers. Compared to $SOTR_{VAT}$ in TW it is an increase of 79 % (6 tube diffusers: 87 g/m³/h) and 84 % (10 tube diffusers: 99 g/m³/h). Therefore, for tube diffusers $SOTR_{VAT}$ can always be increased by a higher number of installed diffusers independent of $q_{A,tube}$. However, as in *TW*, it is expected that the increase of $SOTR_{VAT}$ is minimal when *DD* exceeds a specific value. Behnisch et al. (2020) observed in TW only minor improvement in oxygen transfer for tube diffusers, when *DD* exceeds 35 %.

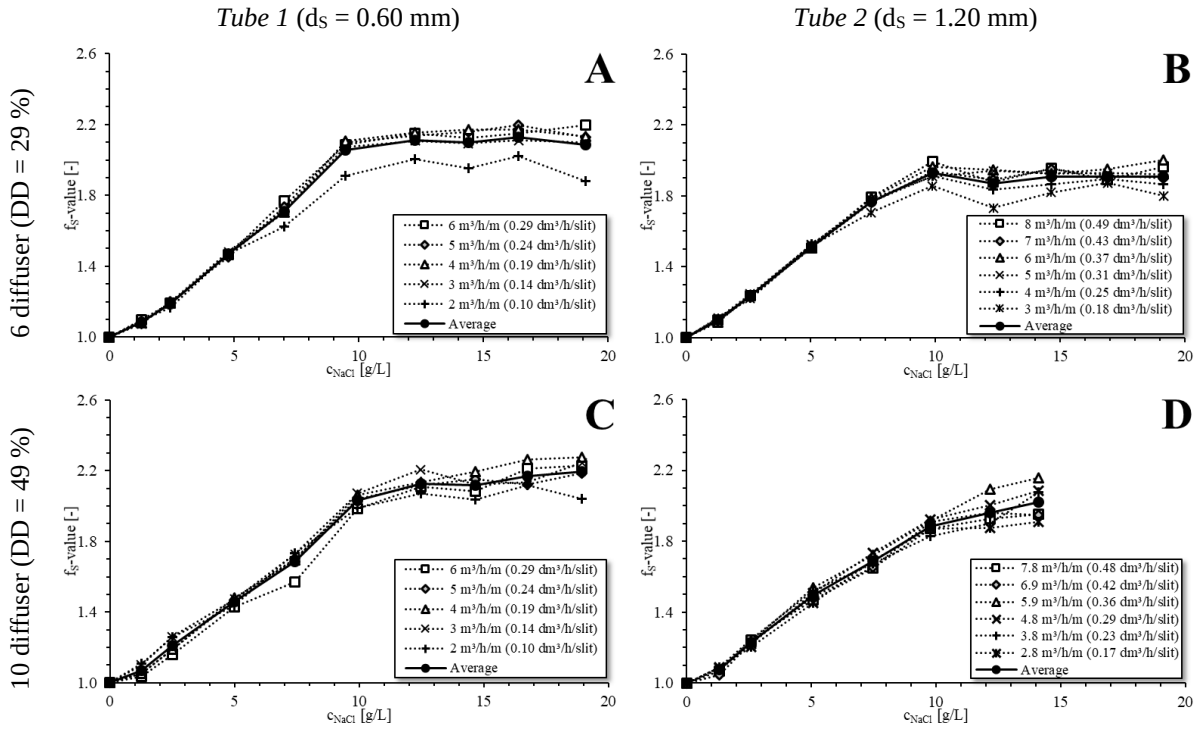

Figure 22: f_S-values as function of c_{NaCl} from tube diffusers for different $q_{A,Tube}$ and $q_{A,Slit}$

Dependency of f_S on airflow rate

To illustrate the dependency of $f_{S,max}$ and airflow rate for the different diffuser types, f_S as a function of the airflow rate is plotted in Figure 23. For a simplified presentation, only results of measurements are shown, where c_{NaCl} is higher than CCC_{NaCl} and f_S is constant. The airflow rate is given as the airflow rate per slit and slit length ($q_{A,dS} = q_{A,Slit} \cdot (d_S)^{-1}$). This enables a comparison between the different diffusers, which have different membrane design properties (i.e. d_S, *SD*, number of slits). It should be noted, however, that this does not take into account the elasticity of the slits, which expand depending on different material properties of the membrane (e.g. deflection, flexibility, thickness) with increasing $q_{A,Slit}$ (Loubière and Hébrard 2003). However, the expansion is very small despite high airflow rates as shown in experiments with multi orifice diffuser membranes (Painmanakul et al. 2004). Therefore, the expansion of the slits with rising airflow rate is ignored here.

Figure 23 illustrates the difference between the individual diffusers. While for tube diffusers $q_{A,dS}$ is very low (0.1 - 0.5 dm³/h/mm) and for disc diffusers and *Plate 2* moderate (up to 2 dm³/h/mm), $q_{A,dS}$ for *Plate 1* is very high (1.7 - 9 dm³/h/mm). The reason for this is the combination of very low number of slits of *Plate 1* (low SD) with relatively high $q_{A,Plate}$ values. Therefore, for a better illustration of the results of the tube and disc diffusers as well as *Plate 2* diffuser, in Figure 23 the range $q_{A,dS}$ from 0 to 2 dm³/h/mm is shown enlarged.

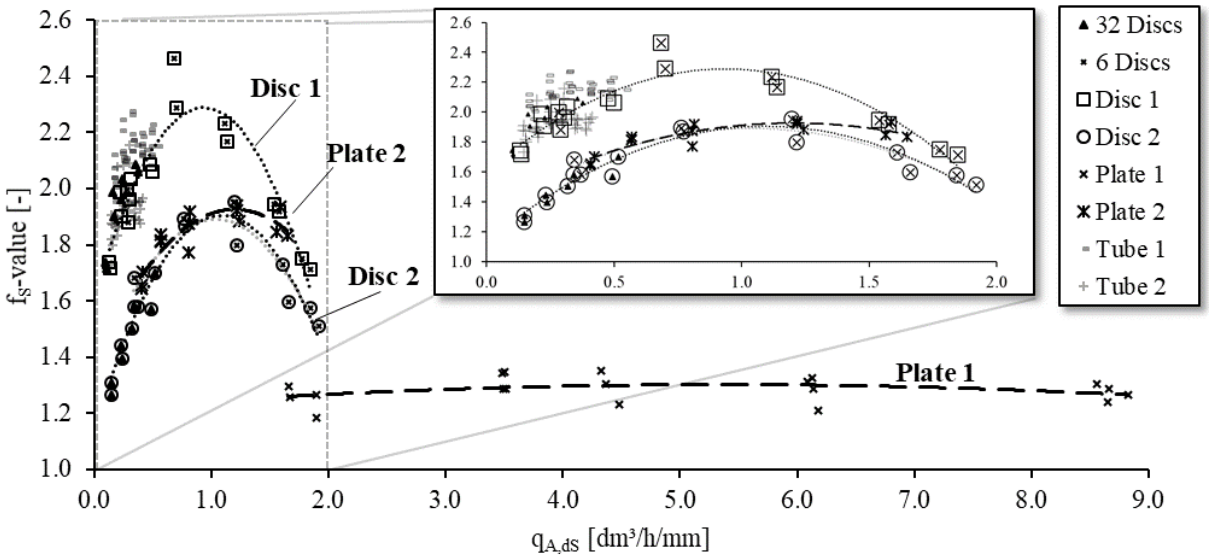

Figure 23: f_S-value as a function of the airflow rate per slit and slit length ($q_{A,dS}$) for different diffuser types and $c_{NaCl} > CCC_{NaCl}$

As mentioned before, Figure 23 shows, that there is no dependency between f_S and airflow rate for tube diffusers within the considered range of airflow rate. A slight effect on f_S can be seen for *Plate 1*. In contrast, the effect is very strong for disc diffusers and *Plate 2*. For both disc diffusers as well as for *Plate 2*, the highest f_S values were reached at ~1 dm³/h/mm. If the airflow rate changes, f_S decreases again. Sander et al. (2017) attribute the dependency between f_S-value and airflow rate to the fact, that at low airflow rates, coalescence also occurs less frequently in TW because of the isolated bubble rise behaviour. Baz-Rodríguez et al. (2014) also observed no dependence between k_La and c_{Salt}, when gas hold-up or airflow rate is very low and the bubbles are relatively far from each other. The decrease of f_S at very high airflow rates is explained by an increase in initial bubble size (Sander et al. 2017). Several experiments show, that the initial bubble size increases with rising airflow rate (Loubière and Hébrard 2003; Painmanakul et al. 2004; Hasanen et al. 2006). Since the bubble size remains constant during the entire ascent in a coalescence inhibited system (Baz-Rodríguez et al. 2014; Behnisch et al. 2018), the oxygen transfer and thus f_S decreases.

When looking at the results of *Plate 1*, it has to be taken into account, that the *SD* of *Plate 1* is very low (0.88 slits per cm²) compared to *Plate 2* (5.5 slits per cm²) and *Disc 1* and *Disc 2* (15.5 and 10 slits per cm²). This results in distances between the slits (P_R/d_S and P_S/d_S; see Table 7) being up to nine times larger than for the other diffuser types. To prevent coalescence close to the diffuser (in TW), Painmanakul et al. (2004) recommend a distance between the slits in relation to the bubble size of 1.0 (i.e. $P_R/d_{32,min}$ and $P_S/d_{32,min} > 1.0$). The $d_{32,min}$ value of *Plate 1* was not measured. If we assume a $d_{32,min}$ between 1 and 2 mm, this ratio will be exceeded by more than four to nine times in case of *Plate 1*. Therefore, no or less coalescence occurs also in TW. In addition, $q_{A,dS}$ increases very rapidly with increasing $q_{A,Plate}$ and so does the initial bubble size. Both effects lead to the fact that the coalescence behaviour as well as the bubble size distribution might differ fundamentally from the other diffusers. However, the slight influence of airflow rate on f_S for *Plate 1* and the lower *CCC* cannot be explained finally on the basis of the present results. Therefore, further experiments are necessary.

For the missing dependency of f_S on airflow rate for tube diffusers, there are in our opinion three possible explanations, which we will discuss in more detail below:

- The material: Unlike the plate and disc diffusers made of EPDM, the tube diffusers are made of silicon. However, the material properties only influence the initial bubble size (Loubière and

Hébrard 2003) but should not affect the coalescence behaviour of the rising bubble. Hence, the missing dependency of f_S values on airflow rate cannot be explained by the membrane material.

- Low $q_{A,dS}$ values: The number of slits per tube diffuser is much higher than for the other two diffuser types. Therefore, maximum $q_{A,dS}$ for tube diffusers (0.49 dm³/h/mm) is very low compared to disc diffusers (1.9 dm³/h/mm) and Plate 2 diffuser (1.6 dm³/h/mm). Initial bubble size should therefore change only slightly. The decrease of f_S observed for disc diffusers and Plate 2 with increasing airflow rate is therefore missing. In contrast to the maximum $q_{A,dS}$, the achieved minimum $q_{A,dS}$ compares well with values for disc and tube diffusers (~ 0.14 dm³/h/mm). The missing decrease of f_S with decreasing airflow rate can therefore not be explained by different $q_{A,dS}$ values.
- The coalescence behaviour: As described previously, for disc diffusers f_S decreases at low airflow rates because coalescence also occurs less frequently in TW due to the isolated bubble rise behaviour. The slits of tube diffusers are on the side of the diffuser and therefore the bubble formation occurs tangentially to the diffuser membrane and not vertically, as for disc and plate diffusers. Furthermore, this arrangement of the slits makes the cross-section of the assumed flow channel along the rising bubble swarm much thinner than with disc and plate diffusers (Figure 18). While the cross section of the flow channel for discs and plates roughly corresponds to the perforated membrane area, this is not the case for tubes. Here, the cross section of the flow channel corresponds to the projected surface area of the tube diffuser (A_P = 665 cm² per diffuser), which is much smaller than the active (perforated) membrane area (A_A = 1,450 cm² per diffuser). If the number of slits is related to A_P of the tube diffuser, the resulting quasi-slit-densities (26 and 33 slits/cm²) are more than twice as high as the SD of disc and plate diffusers. Therefore, it is obvious that for tube diffusers, even at relatively low airflow rates, the bubbles do not ascent isolated and coalescence continuously in TW. This results in high f_S values even at low airflow rates.

Dependency of f_S on diffuser density

After discussing the effect of airflow rate on f_S, we check if there is any influence of the number of installed diffusers (or DD) on f_S. According to results from Figure 22-A and Figure 22-C as well as Figure 22-B and Figure 22-D there is no effect of the number of installed diffusers on f_S in case of tube diffusers. Regardless of the number of installed diffusers, the same $f_{S,max}$ was achieved as CCC_{NaCl} was reached. In case of disc diffusers, a comparison between the different diffuser densities is more difficult, because of the overlapping influence of the airflow rate. Considering individual results of the disc diffusers in Figure 23, the same f_S could be achieved with both 6 and 32 disc diffusers for the same disc diffuser and the same $q_{A,dS}$ (or $q_{A,Disc} = (q_{A,dS}) \cdot d_S \cdot$ slits per diffuser). Hence, for 32 disc diffusers, the increase of f_S with increasing $q_{A,dS}$ is identical to that for 6 disc diffusers. Due to the high number of diffusers and limited blower capacity, the range of tested airflow rate with 32 disc diffusers is significantly below the tests with 6 disc diffusers or the given specified operating range from manufacturers. If $q_{A,dS}$ and $q_{A,Disc}$ continue to increase, a similar dependency between f_S and $q_{A,dS}$ (or $q_{A,Disc}$) will most likely result as was shown for the tests with 6 disc diffusers. Therefore, no influence of diffuser density on f_S for disc diffusers as well as for tube diffusers was detectable. For plate diffusers only one diffuser density was tested. A comparison is therefore not possible. The result that diffuser density has no effect on f_S promotes the notion, that bubbles only coalesce with bubbles from the same diffuser or adjacent slits and not with bubbles from other diffusers. This confirms the observations of Hasanen et al. (2006) and Behnisch et al. (2018), that coalescence occurs mainly close to the diffuser.

Summary of the effects on f_S

The results shown above correspond to the results from Part I of this paper: Both c_{Salt} as well as the design of the diffuser membrane (see Table 7) have an influence on k_La or f_S in SW (Behnisch et al. 2018). Hence, at high c_{Salt} diffusers with smaller detaching bubbles show higher f_S and k_La values. Additionally, we could show that the type of the diffuser also influences the oxygen transfer in SW. For tube diffusers, f_S only depends on c_{Salt}, while for disc and plate diffusers f_S also depends on $q_{A,Disc}$ and $q_{A,Plate}$ respectively. Except *Plate 1*, for all diffusers $f_{S,max}$ was reached when $c_{Salt} \geq$ CCC. Furthermore, diffuser density does not seem to affect f_S.

Additional design considerations

Other factors also have to be taken into account for design of aeration systems in SW. An important parameter is c_S, which decreases with increasing c_{Salt} (Annex 1). Due to the lower concentration gradient between gas and liquid phase and reduced molecular diffusivity, k_L is expected to decrease, resulting in a lower f_S and k_La. When looking at the results of plate and tube diffusers (Figure 21 and Figure 22), we did not observe a significant decrease in f_S after reaching its peak value in the considered concentration range. Because of the lower range of tested salt concentration, a clear conclusion is not possible for disc diffusers. Nevertheless, we do not expect a significant decrease of f_S for disc diffusers with further increasing c_{Salt}. This is confirmed by the results of Baz-Rodríguez et al. (2014), who found no dependence of k_La, a and k_L on c_{Salt} when coalescence is completely inhibited. They show that the reduction of the molecular diffusivity with increasing c_{Salt} and the effect on k_L is marginal. According to these authors, the main effect on k_L is the slip velocity, which is substantially influenced by the bubble size (i.e. d_{32} or a). However, the reduced c_S also decrease $SOTR_{VAT}$ and *SSOTE* as shown in Figure 24-A. Similar to f_S, *SSOTE* increases with increasing c_{NaCl} until a maximum is reached. *SSOTE* of up to 15 %/m could be reached. Diffusers with the smaller slits (*Tube 1*, *Disc 1*) always exhibit higher values than diffusers with larger slits (*Tube 2*, *Disc 2*). In TW SSOTE increases with increasing diffuser density (Behnisch et al. 2020). When comparing the results of 6 and 10 *Tube 1* diffusers, the same can be observed in SW. When reaching the peak value, *SSOTE* slightly decreases as a result of the reduced c_S. The decrease averages about 0.7 %/m for c_{NaCl} = 20 g/L compared to the peak value at $c_{NaCl} = CCC_{NaCl}$. Nevertheless, SW *SSOTE* still outperforms *SSOTE* values that can be achieved in TW with conventional fine-bubble diffusers (8.5 – 9.8 %/m), even at very high diffuser densities (Behnisch et al. 2020).

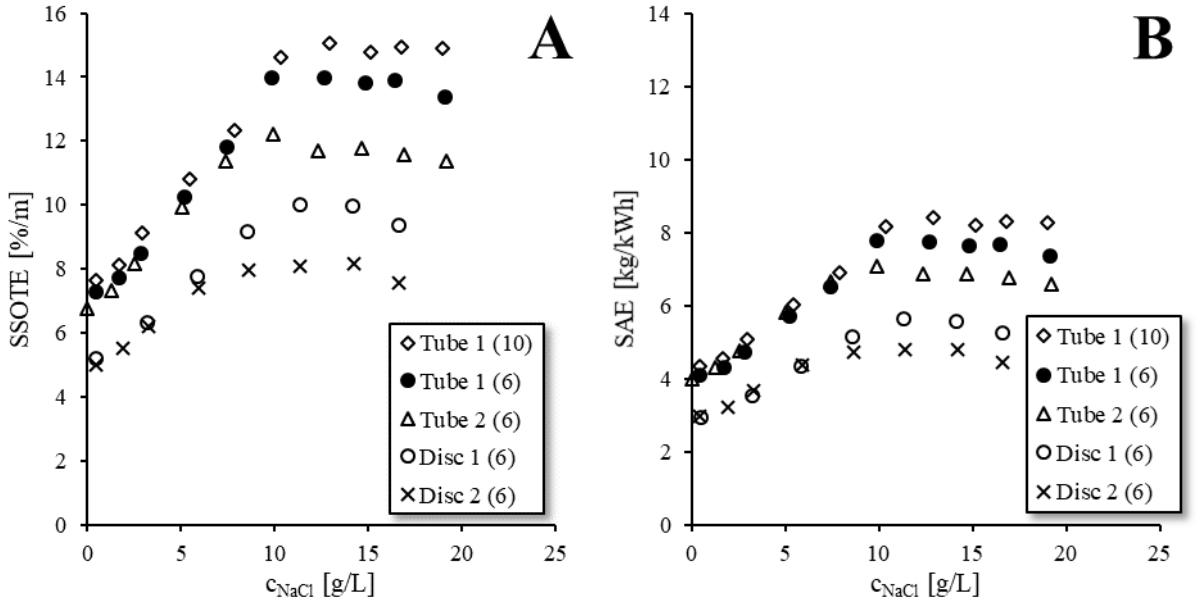

Figure 24: Average *SSOTE* values as function of c_{NaCl} (A); Average *SAE* values as function of c_{NaCl} (B) calculated with isochoric power formula (η = 0.60)

Another factor that must be considered in the design of aeration systems is the total air supply pressure (p_T), which includes the hydrostatic pressure resulting from depth of submergence (p_h), pressure drop of pipes and valves (p_s) and pressure drop of diffusers (p_d) (Krampe 2011). The p_h increases with increasing c_{Salt} due to the increment of water density. Nevertheless, in practice this increase can be neglected. The density of water rises marginally by 1.6 % with an increase in c_{NaCl} from 0 g/L (997 kg/L at 20 °C) to 20 g/L (1.013 kg/L at 20 °C). The p_S is not affected by c_{Salt}. Also no dependence against c_{Salt} was found for p_d (Annex 5). Nevertheless, when improving the oxygen transfer in SW by installing diffusers with smaller slits, p_d increases. In our tests, for tube and disc diffusers the difference in p_d between the diffuser with the smaller slits and those with the larger slits was on average 2.2 kPa (at the same q_A, see Annex 5). Thus, in SW a higher f_S tends to go hand in hand with a higher p_d and therefore p_T. The increased p_T results in a higher power requirement (P) for the blowers.

When calculating P, we must differentiate between isochoric compression and adiabatic compression. Positive displacement blowers (as used here) are widely used on WWTP. Since they compress a fixed volume of air in an enclosed space to a higher pressure, they operate using the isochoric compression principle (Mueller et al. 2002). P can be calculated according to the following formula: $P = Q_A \cdot p_T / \eta$; being η the overall efficiency of the blower. For our calculation, we assumed a typical η of 0.60 (Bell and Abel 2011). Then we calculated the standard aeration efficiency (*SAE=SOTR*/*P*).

With *SAE*, we are able to illustrate the interaction between increased energy demand due to increased p_T through the smaller slits and the improved oxygen transfer. The average *SAE* is shown in Figure 24-B as a function of c_{NaCl}. Since identical Q_A were set for each diffuser type, its influence on *SAE* is eliminated and the average values are sufficient for a comparison. Figure 24-B shows, that SAE in TW ranges between 3.0 and 4.4 kg/kWh and thus within an expected range for such kind of operation conditions (Behnisch et al. 2020). With increasing c_{Salt} *SAE* increases and reaches its peak value similar to *SSOTE*. *SAE* for the diffusers with smaller slits (*Tube 1*, *Disc 1*) are comparable or higher than for the diffusers with larger slits (*Tube 2*, *Disc 2*). Hence, with *Tube 1* (smaller slits) *SAE* of up to 8.4 kg/kWh could be achieved.

Contrary to positive displacement blowers, with turbo blowers internal air compression takes place (= adiabatic compression). Turbo blowers are generally designed for large airflow rates and are therefore

used especially on large WWTP. *P* depends upon the inlet pressure (p_0), air density (ρ) and inlet temperature (T_0) (Mueller et al. 2002). Depending on design and operation conditions, overall efficiencies for turbo blowers of up to 0.85 are possible (Bell and Abel 2011). In order to consider these types of blowers as well, we calculated *SAE* again using the adiabatic power formula (EPA 1989). All results and the formula with the assumed operating conditions are shown in Figure 25. Due to the higher overall efficiency (using a constant η of 0.80) and the chosen operation conditions (T_0 = 20 °C; p_0 = 101.3 kPa; ρ = 1.2 kg/m³), on average 52 % higher SAE values of up to 12.8 kg/kWh were achieved compared to positive displacement blowers. However, it has to be taken into account, that the presented power requirement values are only based on theoretical calculations. Since overall efficiency and the power requirement will change under varying operation conditions, lower *SAE* values are likely to be achieved in practice. Apart from that, the previous conclusions remain valid. Higher *SAE* values were achieved with diffusers with smaller slits.

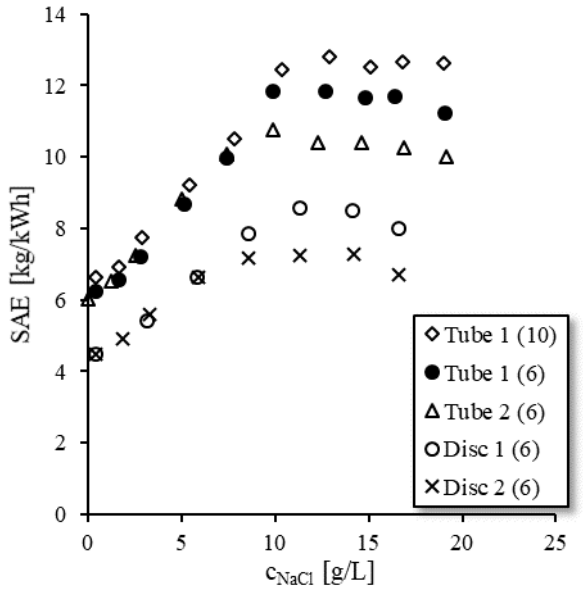

Adiabatic power formula according to Metcalf et al. (2014):

$$P = \frac{Q_A \cdot \rho \cdot R \cdot T_0}{28.97 \cdot \frac{k-1}{k} \cdot \eta} \cdot \left[\left(\frac{p_0 + p_T}{p_0} \right)^{\frac{k-1}{k}} - 1 \right]$$

With:

P = power requirement [kW]

Q_A: airflow rate [m³/s]

ρ: air density (=1.20 kg/m³ with T = 20 °C)

R: universal gas constant = 8.314 J/(mol·K)

T_0: absolute inlet temperature (=293 K)

p_0: absolute inlet pressure (=101.3 kPa)

p_T: air supply pressure [kPa]

k: specific heat ratio (=1.395)

28.97: molecular weight of dry air

η: overall efficiency (= 0.80 for turbo blowers)

Figure 25: Average *SAE* values with η =0.80 (left) calculated with adiabatic power formula (right)

In summary, the *SAE* results show, that independent of the used blower type and despite the higher pressure drop, in SW a higher efficiency of the aeration system is achieved using the diffusers with smaller slits. However, it is questionable whether this can be applied to all diffusers. Whether a diffuser with smaller slits in SW ensures a more efficient aeration depends largely on the difference in oxygen transfer as well as on pressure drop compared to the diffuser with larger slits. Additionally, further measurements need to show whether a higher SAE-value can also be achieved in activated sludge. The activated sludge could have an influence on the coalescence behaviour in the aerated tank. Diffusers with smaller slits could also lead to increased fouling. Therefore, further experiments are already planned to answer these questions.

Conclusion

In the present work, the experiments presented in Part I of this paper (Behnisch et al. 2018) were continued to investigate the oxygen transfer of fine-bubble aeration systems and their influencing factors in saline water. In Part I data from bubble size distribution were combined with results from oxygen transfer tests to investigate the impact of the design of the diffuser membrane. Within Part II the effect

of different salts as well as the effects of diffuser type and density on oxygen transfer of fine-bubble aeration systems in saline water is presented.

First, we determined the critical coalescence concentration (*CCC)* for various salts for the first time using conventional fine-bubble diffusers, for which we developed a new analytical approach. When *CCC* is reached, coalescence is completely inhibited and k_La_{20} and f_S remain constant. Regardless of salt type, the reached $f_{S,max}$ values were the same. With the new analytical approach, the *CCC* is determined by evaluating the oxygen transfer rate at different salt concentrations. The new method is much faster and easier to use than bubble size measurement and provides valid results. In the future, this will make it possible to investigate the coalescence behaviour for any aeration system and (mixed) salt solution quickly and easily. Furthermore, since salt and salt mixture in wastewater changes and depends on the origin of the used water, we recommend that in the future not only the total salt concentration should be considered in wastewater analytics but also its composition from different salts (e.g. by ion analysis).

Second, we carried out oxygen transfer tests with three different types of diffusers at different diffuser densities in a pilot scale test tank at a water depth of 3.8 m and at different NaCl concentrations. The effect of the design of the diffuser membrane observed in Part I was confirmed. Except *Plate 1*, diffuser membranes with smaller detaching bubbles show higher f_S values. Furthermore, our results show that there is a clear influence of the diffuser type. While f_S for tube diffusers only depends on the salt concentration, the other diffuser types show a clear influence of the airflow rate per slit and slit length ($q_{A,dS}$). For disc diffusers and Plate 2, the highest f_S values were achieved at $q_{A,dS} \sim 1.0$ dm³/h/mm. If $q_{A,dS}$ changes, f_S and k_La will decrease again. This complicates the operation of an aeration system. When using tube diffusers, this problem can be avoided. To achieve a high oxygen transfer in saline water, the slit density of the diffuser membrane can be further increased. In tap water, the slit density is usually up to 15 slits per cm² to prevent coalescence close to the diffuser. Under saline conditions ($c_{Salt}>CCC$), the coalescence is inhibited and the slit density can be increased further. This also prevents high $q_{A,dS}$ and thus an increase in initial bubble size.

Third, despite the reduced oxygen saturation concentration in saline water, extremely high *SSOTE* values compared to tap water of up to 15 %/m were achieved during the tests in the pilot scale test tank. *SSOTE* are much higher than is possible with conventional fine-bubble diffusers in tap water. Using isochoric power formula (valid for positive displacement blowers) calculated *SAE* values of up to 8.4 kg/kWh show, that by using diffusers with smaller slits, the energy efficiency of the aeration system will improve in saline water despite the increased pressure drop. If even more efficient blowers (e.g. turbo blowers) were used, theoretically (using adiabatic power formula) even higher *SAE* of up to 12.8 kg/kWh values could be achieved. However, it is not yet known whether the use of diffusers with smaller slits also improves aeration in activated sludge tanks. The coalescence behaviour in the aerated tank as well as the fouling of the diffusers could be influenced by the activated sludge. Therefore, further investigations are already planned.

Acknowledgements

We thank the German Federal Ministry of Education and Research (BMBF) for funding the research project WaReIp ‘Water-Reuse in Industrial parks’ (Grant No. 02WAV1409A).

References of Paper III

ASCE/EWRI 18-18, 2018: *Standard Guidelines for In-Process Oxygen Transfer Testing* (ASCE/EWRI 18-18).

EN 12255-15, 2003: *Wastewater treatment plants - Part 15: Measurement of the oxygen transfer in clean water in aeration tanks of activated sludge plants*.

EPA (1989): *Design Manual - Fine Pore Aeration Systems*. (EPA/625/1-89/023). Washington, DC, USA: U.S. Environmental Protection Agency.

Baz-Rodríguez, S. A.; Botello-Álvarez, J. E.; Estrada-Baltazar, A.; Vilchiz-Bravo, L. E.; Padilla-Medina, J. A.; Miranda-López, R. (2014): *Effect of electrolytes in aqueous solutions on oxygen transfer in gas-liquid bubble columns*. In: *Chemical Engineering Research and Design*, (92) 2014, 2352–2360.

Behnisch, J.; Ganzauge, A.; Sander, S.; Herrling, M. P.; Wagner, M. (2018): *Improving aeration systems in saline water: measurement of local bubble size and volumetric mass transfer coefficient of conventional membrane diffusers*. In: *Water Science and Technology* 78 (3-4), 860–867.

Behnisch, J.; Schwarz, M.; Wagner, M. (2020): *Three decades of oxygen transfer tests in clean water in a pilot scale test tank with fine-bubble diffusers and the resulting conclusions for WWTP operation*. In: *Water Practice and Technology* 15 (4), 910–920.

Bell, K. Y.; Abel, S. (2011): *Optimization of WWTP aeration process upgrades for energy efficiency*. In: *Water Practice and Technology* 6 (2)

Cho, Y.S; Laskowski, J.S (2002): *Effect of flotation frothers on bubble size and foam stability*. In: *International Journal of Mineral Processing* 64 (2-3), 69–80.

Craig, V. S.J.; Ninham, B. W.; Pashley, R. M. (1993): *Effect of electrolytes on bubble coalescence*. In: *nature* 364 (6435), 317–319.

Firouzi, M.; Howes, T.; Nguyen, A. V. (2015): *A quantitative review of the transition salt concentration for inhibiting bubble coalescence*. In: *Advances in colloid and interface science* 222, 305–318.

Grau, R. A.; Laskowski, J. S.; Heiskanen, K. (2005): *Effect of frothers on bubble size*. In: *International Journal of Mineral Processing* 76 (4), 225–233.

Hasanen, A.; Orivuori, P.; Aittamaa, J. (2006): *Measurements of local bubble size distribution from various flexible membrane diffusers*. In: *Chemical Engineering and Processing*, 2006 (45), 291–302.

He, H.; Chen, Y.; Li, X.; Cheng, Y.; Yang, C.; Zeng, G. (2017): *Influence of salinity on microorganisms in activated sludge processes: A review*. In: *International Biodeterioration & Biodegradation* 119, 520–527.

ISO 5814, 2012: *Water quality - Determination of dissolved oxygen - Electrochemical probe method*.

Krampe, J. (2011): *Assessment of diffuser pressure loss on WWTPs in Baden-Württemberg*. In: *Water science and technology* 62 (12), 3027–3033

Lefebvre, O.; Moletta, R. (2006): *Treatment of organic pollution in industrial saline wastewater: A literature review*. In: *Water research* (40), 3671–3682.

Lessard, R. R.; Zieminski, S. A. (1971): *Bubble coalescence and gas transfer in aqueous electrolytic solutions*. In: *Industrial & Engineering Chemistry Fundamentals* 10 (2), 260–269.

Loubière, K.; Hébrard, G. (2003): *Bubble formation from a flexible hole submerged in an inviscid liquid*. In: *Chemical Engineering Science* 58 (1), 135–148.

Loubière, K.; Hébrard, G.; Guiraud, P. (2003): *Dynamics of Bubble Growth and Detachment from Rigid and Flexible Orifices*. In: *The Canadian Journal of Chemical Engineering* 81 (3-4), 499–507.

Marrucci, G.; Nicodemo, L. (1967): *Coalescence of gas bubbles in aqueous solutions of inorganic electrolytes*. In: *Chemical Engineering Science* 22 (9), 1257–1265.

Metcalf; E.; Tchobanoglous, G.; Abu-Orf, M.; Stensel, H. D.; Bowden, G. et al. (2014): *Wastewater engineering. Treatment and resource recovery*. 5. ed. New York, NY: McGraw-Hill.

Mueller, J. A.; Boyle, W. C.; Pöpel, H. J. (2002): *Aeration. Principles and practice*, Vol. 11. CRC Press, Boca Raton, FL.

Painmanakul, P.; Loubiere, K.; Hebrard, G.; Buffiere, P. (2004): *Study of different membrane spargers used in waste water treatment: characterisation and performance*. In: *Chemical Engineering and Processing: Process Intensification* 43 (11), S. 1347–1359.

Prince, M. J.; Blanch, H. W. (1990): *Transition electrolyte concentrations for bubble coalescence*. In: *AIChE J.* 36 (9), 1425–1429.

Quinn, J. J.; Sovechles, J. M.; Finch, J. A.; Waters, K. E. (2014): *Critical coalescence concentration of inorganic salt solutions*. In: *Minerals Engineering* 58, 1–6.

Rusydi, A. F. (2018): *Correlation between conductivity and total dissolved solid in various type of water: A review*. In: *IOP Conf. Ser.: Earth Environ. Sci.* 118, 12019.

Sander, S. (2018): *Optimierung der Bemessung feinblasiger Druckbelüftungssysteme bei erhöhten Meersalzkonzentrationen* (*Optimisation of the design of fine-bubble aeration systems at increased sea salt concentrations*). Darmstadt (IWAR Schriftenreihe, 243).

Sander, S.; Behnisch, J.; Wagner, M. (2017): *Design of fine-bubble aeration systems for municipal WWTPs with high sea salt concentrations*. In: *Water Science and Technology* 75 (7). 1555-1563

Sovechles, J. M.; Waters, K. E. (2015): *Effect of ionic strength on bubble coalescence in inorganic salt and seawater solutions*. In: *AIChE J.* 61 (8), 2489–2496.

Wagner, M.; Pöpel H. J.; Kalte, P. (1998): *Pure oxygen desorption method – A new and cost-effective method for the determination of oxygen transfer rates in clean water*. In: *Water Science and Technology* 38 (3). 103-109

Wagner, M.; Stenstrom, M. K. (2014): *Aeration and mixing. In: Activated Sludge – 100 Years and Counting* (D. Jenkins & J. Wanner, eds.). IWA Publishing, London, England, 131-153.

Zlokarnik, M. (1980): *Koaleszenzphänomene im System gasförmig/flüssig und deren Einfluss auf den O2-Eintrag bei der biologischen Abwasserreinigung (Coalescence phenomena in the gas/liquid system and their influences on* oxygen *uptake in biological waste water treatment)*. In: *Korrespondenz Abwasser, Abfall* 27 (11). 728-734

4.5 Paper IV

Title: **Oxygen transfer of fine-bubble aeration in activated sludge treating saline industrial wastewater**

First author: Behnisch, J., M.Sc.

Co-authors: Schwarz, M., M.Sc.

Trippel, J., M.Sc.

Engelhart, M., Prof. Dr.-Ing.

Wagner, M., Prof. Dr.-Ing. habil.

Abstract: Aeration is usually the most energy-intensive part of the activated sludge process, accounting for 50 % to 80 % of total requirement. To achieve high efficiency, designers and operators of WWTP must therefore consider all influencing factors including salinity. With increasing salinity oxygen transfer increases compared to tap water (TW), due to the inhibition of bubble coalescence. Previous saline water (SW) experiments show, that by using small slits diffuser membrane design oxygen transfer and aeration efficiency increase further. In this study, we present a modified approach for considering salt-effect on oxygen transfer and assess the transferability of SW results to saline activated sludge (sAS) conditions. Therefore, we operated a pilot activated sludge plant over 269 days with saline industrial wastewater influent. Oxygen transfer of disc-diffusers with two different membrane designs was measured continuously via off-gas method. Salt concentration (c_{Salt}) measured via ion-analyses ranges between 4.9 and 11 g/L. Despite high c_{Salt} fluctuation, COD elimination was >90% all the time. Our results confirm previous SW results. Oxygen transfer in sAS is up to three times higher compared to non-saline conditions. Aeration-efficiency shows, that despite higher-pressure drop, diffusers with smaller slits are to be recommended in order to improve aeration in sAS.

Keywords: Saline industrial wastewater; Diffuser membrane design; Critical Coalescence Concentration; Transition Concentration; disc diffuser

1. Introduction

The oxygen transfer of fine-bubble aeration systems is enhanced by high salt concentrations (c_{Salt}; g/L) due to the inhibition of bubble coalescence. In former studies, we assess the different factors influencing the oxygen transfer in saline water (SW) [1–3]. In the present study, we investigate the transferability of these SW test results to process conditions in saline activated sludge (sAS).

High c_{Salt} are quite common in industrial wastewater. Additionally, the global trend towards saving freshwater by increased (industrial)-wastewater reuse or by using seawater for toilet flushing, will raise the volume of saline wastewater that needs to be biologically treated [3,4]. The most prevalent process for aerobic biological wastewater treatment is the activated sludge process. Aeration is usually the most energy intensive part of the activated sludge process accounting for 50 to 80 % of the total energy requirement [5]. Therefore, a deeper understanding of the effects on oxygen transfer of increased c_{Salt} is crucial to enhance the energy efficiency of activated sludge process.

Aeration in aerobic biological wastewater treatment is essential to satisfy the oxygen demand of microorganisms in activated sludge [5]. Today, mainly fine bubble aeration systems are used in wastewater treatment plants (WWTP). Thereby, compressed air is injected via diffusers installed at the bottom of the aeration tank. The oxygen is transferred from the ascending small bubbles into the liquid phase. The oxygen transfer is described by the volumetric mass transfer coefficient (k_La; 1/h), which represents the product of the liquid-side mass transfer coefficient (k_L; m/h) and the liquid/gas interfacial area (a; m²/m³). Many different factors influence k_La. In order to describe these effects, usually k_La under process conditions is set in relation to k_La in tap water (TW) at standard conditions (20 °C water temperature; 0 mg/L dissolved oxygen concentration; 101.3 kPa atmospheric pressure; see Table 10). Depending on the aerated medium, the quotients are labelled differently. In the following we distinguish between α (for aerating non-saline activated sludge), f_S (for aerating saline water) and αf_S (for aerating saline activated sludge).

Table 10: Design parameters

Medium	Definition		
non-saline activated sludge (AS)	$\alpha = \frac{k_L a_{non\ saline\ activated\ sludge}}{k_L a_{tap\ water}}$	[-]	(23)
Saline water (SW)	$f_S = \frac{k_L a_{Saline\ water}}{k_L a_{tap\ water}}$	[-]	(24)
saline activated sludge (sAS)	$\alpha f_S = \frac{k_L a_{saline\ activated\ sludge}}{k_L a_{tap\ water}}$	[-]	(25)

In non-saline activated sludge (AS), k_La is inhibited by dissolved and suspended ingredients and the biomass itself, which is why α is usually < 1.0. The prediction of α in dependence of different parameters (e.g. wastewater ingredients, process parameters) is the objective of many studies [6–8]. Since the wastewater composition is subject to daily fluctuations, common practice in design of aeration systems currently ensures necessary flexibility determining minimum α_{min} and maximum α_{max} [9]. Mean α (α_{mean}) is adopted to evaluate aeration efficiency.

In SW, k_La increases with increasing c_{salt} due to the inhibition of bubble coalescence. Hence, f_S takes values greater than 1.0 and increases linearly with increasing c_{salt}. The increase in f_S depends on airflow rate, type of diffuser and design of diffuser membrane [2]. When c_{Salt} reaches a certain concentration, which is specific for each salt and mixed salt solution, the coalescence is fully inhibited and f_S reaches its maximum ($f_{S,max}$) [1]. This is termed the critical coalescence concentration (CCC) [10].

In sAS, the inhibiting effects of wastewater and AS ingredients as well as the enhancing effect of increased salt concentration affect k_La. Therefore, depending on the balance between inhibiting (described by α) and enhancing (described by f_S) effects, αf_S can assume values >1.0 or <1.0. Sander et al. [3] ran oxygen transfer tests with iron hydroxide flocs to simulate activated sludge with different NaCl concentrations. They show that the net effect can be expressed via multiplicative linking of α and f_S:

$$\alpha f_S = \alpha \cdot f_S \quad [-] \quad (26)$$

Our previous studies show that in SW $f_{S,max}$ as well as maximum k_La is higher with small slits membrane design than with large slits [1]. For disc diffusers k_La increases by 10 %, when using the small slits diffuser membrane design compared to diffusers with the large slits design [2]. However, the improved k_La is accompanied by an increased pressure drop of the diffusers (due to the smaller slits) and therefore by a higher energy requirement for air supply. Nevertheless, model calculations based on SW test results show that the aeration efficiency improves due to the higher oxygen transfer [2].

However, it is questionable whether this also applies to process conditions in sAS. The activated sludge or wastewater ingredients could influence the coalescence behaviour in the aeration tank as well as the fouling of the diffusers. Therefore, in the present study we will investigate whether the use of diffusers with smaller slits also improves aeration in sAS. For this purpose, we operated a pilot scale activated sludge tank with a water volume of 2.25 m³ and depth of submergence of the diffusers of 3.5 m over 269 days with industrial wastewater influent and measured the oxygen transfer continuously by the off-gas method. Time of operation is divided into four measurement phases. In each phase, we installed a new diffuser. With the corresponding TW results, αf_S was calculated. In parallel, we recorded the pressure drop of the diffusers and the overall performance of the pilot plant.

We use the results to assess a modified design approach for considering salt effect on oxygen transfer. The new design approach enables a more precise design and thus a more energy efficient operation of an aeration system at high salt concentrations. The current design approach described by Sander et al. [3] is only applicable for municipal wastewater with high sea salt concentration. Therefore, it cannot be used for industrial wastewater of the present study, which shows another salt mixture than sea salt. Furthermore, the influence of the diffuser membrane design is not taken into account in the current design approach so far. Our modified design approach normalizes the effect of different salts and mixed salt solutions on k_La. Therefore, it is applicable for each coalescence inhibiting salt or mixed salt solution. Additionally, we show how the influence of the membrane design can be assessed by conducting simple SW tests with the diffusers used for aerating sAS.

2. Material and Methods

2.1. Modified design approach for considering salt effect on k_La

In order to design an aeration system as efficiently as possible, the individual influences must be considered as precisely as possible. The f_S value includes the salt effect on k_La (see Table 10). Sander et al. [3] found a correlation between f_S of disc diffusers and concentration of sea salt ($c_{SeaSalt}$; g/L):

$$\begin{aligned} f_S &= k \cdot c_{Sea\ Salt} + 1 && \text{when } c_{Sea\ Salt} \leq CCC_{Sea\ Salt} && [-] \\ f_S &= f_{S,max} && \text{when } c_{Sea\ Salt} > CCC_{Sea\ Salt} && [-] \end{aligned} \quad (27)$$

where *k* is an empirical parameter between 0.08 and 0.16 depending on the airflow rate per disc diffuser ($q_{A,Disc}$; m³/Disc/h). However, this approach is only valid for sea salt and does not consider the different

CCC of different salts or salt mixtures. Therefore, we propose to normalize salt effect by including the dimensionless c_{Salt}/CCC_{Salt} ratio:

$$f_S = k_N \cdot \frac{c_{Salt}}{CCC_{Salt}} + 1 \qquad \text{when } c_{Salt} \leq CCC_{Salt} \qquad [-]$$
$$f_S = f_{S,max} = k_N + 1 \qquad \text{when } c_{Salt} > CCC_{Salt} \qquad [-] \qquad (28)$$

The normalised k-value (k_N; -) describes the slope of the linear increase of f_S until $c_{Salt}/CCC_{Salt} = 1.0$ and f_S reaches $f_{S,max}$. Since only the diffuser membrane design and $q_{A,Disc}$ affects $f_{S,max}$ or bubble diameter, but not the salt type [2,11–13], it is reasonable that solutions of different salts and salt mixtures with the same c_{Salt}/CCC_{Salt} ratio and aerated with the same diffuser would present similar f_S values. Other studies already show the advantages of using a dimensionless concentration as independent parameter for analyses of hydrodynamics and oxygen transfer with different salt solutions in bubble columns [13–15].

Because the salt type has no effect on $f_{S,max}$, k_N can be derived by equation (28) by measuring $f_{S,max}$ of the diffuser used for aerating sAS in any salt solution. For $f_{S,max}$ determination we recommend to use NaCl, because it is easy to handle and cheap. It must be noted, that $f_{S,max}$ is affected by diffuser type and design of diffuser membrane. For disc and plate diffusers $f_{S,max}$ is also affected by $q_{A,Disc}$ or the airflow rate per plate ($q_{A,Plate}$; m³/Plate/h), respectively. Therefore, the test conditions should be the same as process conditions (same diffuser and in case of plate and disc diffusers the same $q_{A,Disc}$ or $q_{A,Plate}$, respectively).

Behnisch et al. [2] measured f_S values of different diffusers in a NaCl solution and checked whether there is a scale effect. They concluded, that for measuring $f_{S,max}$ a sufficient reactor volume as well as blower capacity is necessary, to ensure that the full range of airflow rate of diffusers can be set during the tests. Neither diffuser density nor water depth show an influence on f_S [2, 16]. From equation (28) and with known $f_{S,max}$ value and $c_{Salt}/CCC_{Salt} = 1.0$ results:

$$k_N = f_{s,max} - 1.0 \qquad [-] \qquad (29)$$

Because of the influence of air-flow rate on $f_{S,max}$ in case of plate and disc diffusers, for these diffuser types the k_N value is identical for each salt and mixed salt solution, as long as the airflow rate remains constant. For tube diffusers k_N is constant all the time, because there is no influence of the airflow rate on f_S within the operation range specified by the manufacturer [2].

To consider the salt effect with equation (28), CCC of the given salt solution or wastewater must be determined. An analytical approach is described by Behnisch et al. [2]. They measured CCC of different salts in lab-scale as well as in pilot scale setup by evaluating the oxygen transfer at different salt concentrations and show, that there is no scale effect in determining CCC. Therefore, CCC measuring can be carried out in a small bubble column. For measuring the coalescence behaviour of saline wastewater, Zlokarnik [17] proposed to use biologically treated wastewater. Otherwise, the wastewater ingredients would falsify the results. If biologically treated wastewater is not available, we recommended to use a salt mixture with a similar salt composition for the tests.

2.2. Pilot plant

Figure 26 shows a scheme of the pilot scale activated sludge test plant. The inflowing industrial wastewater consisted of a mixed effluent combining the wastewater generated by the various production lines of an industrial site. The main product of the industrial site is colour effect pigments, which are used e.g. in paints for cars.

The influent was collected from grit chamber effluent of a WWTP treating the wastewater of the industrial site. It was stored for approximately 3 h in a 0.6 m³ tank before it entered the aerated biological reactor (B1). The storage tank was equipped with online probes (CPS16D, CLS50D, Endress + Hauser, Switzerland) for pH (-) and electrical conductivity (EC; mS/cm). 24-h composite samples were taken from influent before it entered B1. The 24-h composite samples were analysed by standard kit (Merck-Spectroquant, Merck KGaA) for total COD concentration (COD_t), filtrated COD (COD_f), ammonia, nitrate, nitrite and phosphorous. Despite the small storage tank, the influent to B1 was subject to strong concentration fluctuations, as can be seen from the high standard deviation values of analysed chemical parameters: 334 ± 295 mg/L COD_t; 119 ± 237 mg/L COD_f; 3.5 ± 5.8 mg N/L of Ammonia and 1.0 ± 1.84 mg P/L of phosphorous. The influent contained neither nitrate nor nitrite. In contrast to the chemical parameters, EC was relatively stable at 10.1 ± 1.1 mS/cm.

B1 was a completely closed cylindrical tank with a diameter of 0.88 m, a water depth of 3.7 m and a water volume (V_{B1}) of 2.25 m³. The reactor was equipped with one disc diffuser at the bottom of the tank with a depth of submergence of 3.5 m. A recirculation pump assisted in the mixing of the tank and pumps 2.5 m³/h from the bottom to the top of B1 continuously. Several online probes (CUS51D, CPS16D, CLS50D and COS61D, Endress + Hauser, Switzerland) in the reactor measured total suspended solids (TSS), pH, EC and dissolved oxygen concentration (DO) respectively. All probes were checked and cleaned every two days. TSS-probe was regularly compared with laboratory analysis. To increase the salt concentration in B1, a highly concentrated NaCl-solution could be dosed from fully mixed tank B3.

The activated sludge was separated from the treated wastewater in the secondary clarifier (B2) and returned to B1. A 24h-composite sample of the clarified effluent was taken and analysed in the same way as the sample from the influent. The sludge retention time (SRT; d) was set at approx. 11 d by daily withdrawal of 0.2 m³ (Q_{WAS}; m³/d) waste activated sludge (WAS) from B1. Taking sludge direct from the fully mixed aerated reactor has the advantage that the sensitive and time-consuming measurement of TSS of WAS is not necessary. Therefore, TSS in B1 and TSS of Q_{WAS} is the same and SRT can easily be calculated according to:

$$SRT = \frac{V_{B1} \cdot TSS}{Q_{WAS} \cdot TSS} = \frac{V_{B1}}{Q_{WAS}} \quad [d] \qquad (30)$$

Inoculum biomass was taken from an industrial nitrifying activated sludge plant. EC of inoculum was 8.7 mS/cm. Thus, the biomass was already acclimatised to increased salt concentrations. Daily withdrawal of WAS started 26 days after inoculation. After another 100 days of start-up period, off-gas measurements were initiated and took 143 days.

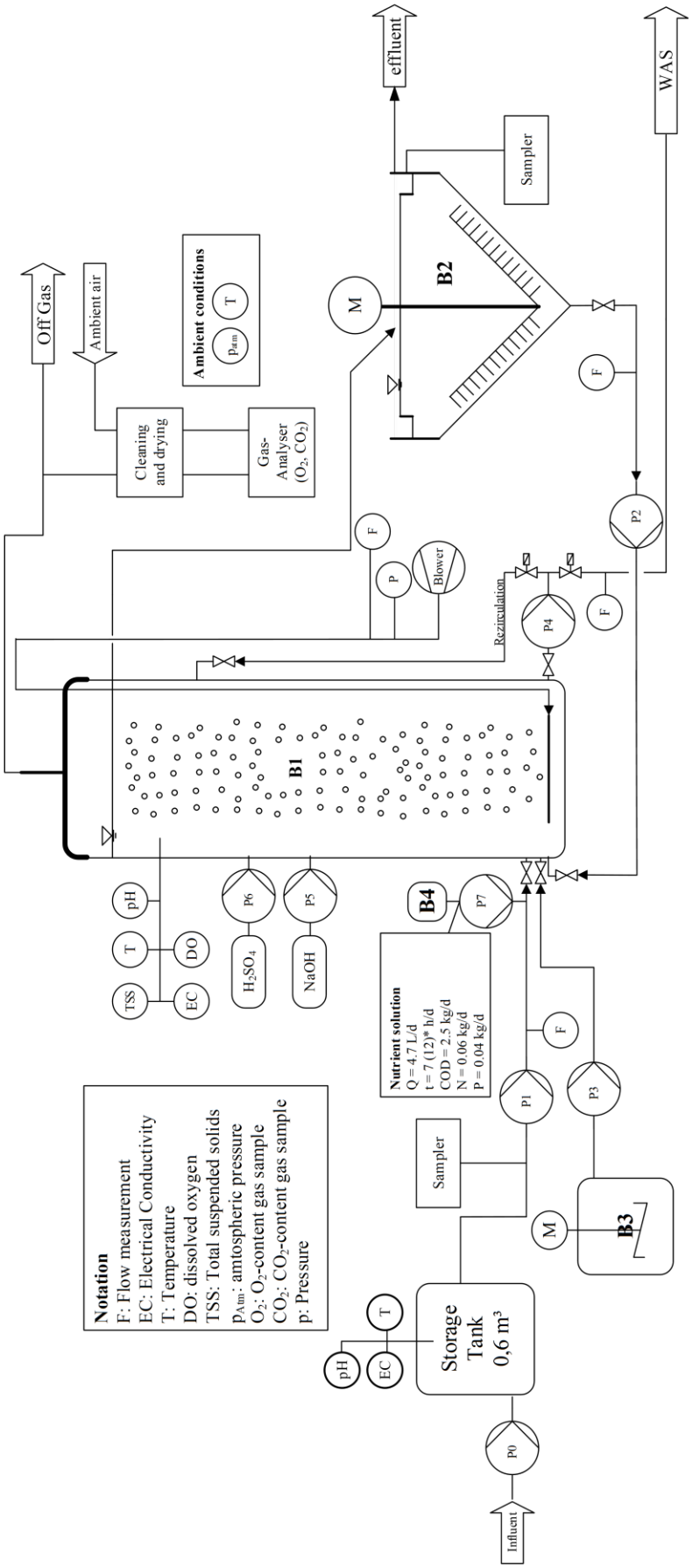

Figure 26: Scheme of the pilot scale activated sludge plant with off gas testing equipment

2.3. Disc diffuser

The used disc diffusers have two different membrane designs (Figure 27). As previously shown [1,2], the membrane design influences the oxygen transfer in SW. The two different diffuser membrane designs differ in length of the slits (d_S), distance between slits (P_S), distance between rows (P_R) and slit density (SD). The slit density is defined as the number of slits per activated (perforated) membrane area (A_A). The diffuser density (DD) is the total membrane area (including non-perforated area) per area of the tank floor of B1. All installed diffusers are 28.5 cm in diameter, resulting in a DD = 10 %.

Membrane design		**A**	**B**
Material		EPDM*	EPDM*
disc diameter	[cm]	28.5	28.5
active membrane area (A_A)	[cm²]	324	306
slit length (d_S)	[mm]	0.75	1.25
P_R/d_S	[-]	4.07	2.44
P_S/d_S	[-]	2.44	1.80
slit density (SD)	[slits/cm²]	15.5	10
slits per diffuser	[-]	5,028	3,063

* Ethylene-Propylene-Dien-Terpolymere

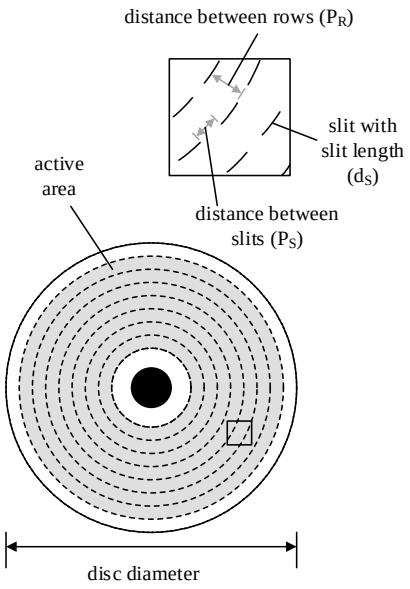

Figure 27: Membrane design properties of the disc diffusers

2.4. Desorption method in tap water

Before inoculation, oxygen transfer tests in TW with all tested disc diffusers in B1 were conducted by means of the desorption method [18]. With this method, the oxygen concentration is increased 15 – 20 mg/L beyond the oxygen saturation concentration by aerating with pure oxygen gas or oxygen enriched air [19]. By switching to aeration with ambient air, the oxygen concentration starts to decrease again until the saturation concentration is reached. From the curve of decreasing oxygen concentration, the k_La is calculated by nonlinear regression.

Because oxygen probes in B1 are not suitable for use at very high DO values (> 20 mg/L), four electrochemical oxygen probes (COS51D, Endress + Hauser, Switzerland) were installed at different heights in B1 during TW oxygen transfer tests. The resulting k_La values were standardized to 20 °C water temperature and a c_{Salt} of 1 g/L ($k_La_{20,1000}$) according to EN 12255-15 [18]. Airflow rate (Q_A) was measured at standard temperature and pressure (0 °C; 101.3 kPa; 0 % humidity) with a thermal flow sensor (t-mass A 150, Endress + Hauser, Switzerland).

2.5. Off-gas and pressure drop measurement in saline activated sludge

The k_La in saline activated sludge was measured by the off-gas method [6,7,20,21]. For this purpose, gas samples of off-gas and ambient air were collected continuously in parallel and analysed for volumetric fraction of O_2 and CO_2 in a gas analyser (X-Stream X2, Emerson, USA) which was calibrated weekly. Before entering the analyser, gas samples were cleaned and dried (CSS-V2, M&C TechGroup, Switzerland). According to equation (25), αf_S results from the ratio of k_La in sAS to k_La in TW. As

before during oxygen transfer tests in TW, Q_A was measured at standard conditions with a thermal flow sensor (t-mass A 150, Endress + Hauser, Switzerland). The total air supply pressure (p_T; kPa) was measured by manometer (PMC21, Endress + Hauser, Switzerland) installed downstream of the blower. Pressure drop of the disc diffusers (p_D; kPa) was calculated with the following equation [22]:

$$p_D = p_T - p_h - p_s \quad \text{[kPa]} \qquad (31)$$

being p_h the hydrostatic pressure resulting from depth of submergence (= 3.5 m) and p_S the pressure of pipes and valves (= 0,3 kPa).

Due to the high oxygen transfer and the relatively weak pollution of the influent, the DO in B1 was between 7 and 8 mg/L. This is too high when using the off-gas method, where DO is limited to 50 % of the oxygen saturation concentration due to the increasing uncertainty of the results [20]. Therefore, Q_A had to be reduced to the minimum airflow rate of the used diffusers given by the manufacturer (= 1.5 m³/h). Nevertheless, DO was still too high. Therefore, we increased the oxygen uptake rate (OUR) by dosing a high nutrient solution from an additional tank (B4). The nutrient solution consists of glycerol as carbon source, ammonium hydrogen carbonate as nitrogen source and dipotassium phosphate as phosphorus source. Glycerol is considered to be readily biodegradable and has almost no influence on oxygen transfer even at relatively high concentrations of up to 10 vol.-% [23]. The maximum glycerol concentration was less than 0.3 vol.-%. An influence of the nutrient solution on the oxygen transfer can therefore be excluded. The nutrient solution was only dosed during a few hours of the day (mostly at night). In the absence of dosing, DO increased > 50 % of saturation concentration and data collected during this time were discarded.

2.6. Description of test Phases

An overview for the different test phases together with the individual notation of the disc diffusers are given in Table 11. The period of oxygen transfer measurement took 143 days and consisted of four Phases (I – IV). For operational reasons, the off-gas measurement had to be interrupted for 45 days between Phase II and III. The operation of the pilot plant continued during this time. In Phase II and Phase III a disc diffuser with diffuser membrane design Type A, and in Phase I and IV a disc diffuser with diffuser membrane design Type B was installed (see chapter 2.3). In each Phase, a new diffuser was installed. In the following, the notation of the different disc diffusers includes the number of the test Phase (I, II, III and IV) and the length of slits (0.75 mm and 1.25 mm); e.g. *Disc I (1.25)* means the Disc diffuser from Phase I with a slit length of 1.25 mm. Besides the different membrane designs, the type of additional salt dosage varied between the test phases. In Phase I and II, the salt was dosed as a shock load. The influent was turned off and salt dosage from B3 started for 48 h. After salt dosage, the influent restarted. During the time, withdrawing of WAS and dosage of the nutrient solution continued. In Phase III and IV, the dosage of salt was carried out continuously. In order to reduce the required amount of NaCl, the influent flow rate was reduced to 110 L/h during time of NaCl dosage.

Table 11: Overview of the test phases

Test Phase:	**Phase I**	**Phase II**	**Phase III**	**Phase IV**
Notation disc diffuser:	Disc I (1.25)	Disc II (0.75)	Disc III (0.75)	Disc IV (1.25)
diffuser membrane design type	B	A	A	B
additional salt dosage	shock wise	shock wise	continuously	continuously

2.7. Measurement of salt concentration

The salt concentration was measured by ion analyses according to APAH [24]. For this purpose, samples from B1 were regularly taken and were filtrated to 0.45 µm. The samples were analysed for major anions (Na^+, K^+, Mg^{2+}, Ca^{2+}, Fe^{2+}, P^+) and cations (Cl^-, SO_4^{2-}) by ionic chromatography (IC; 930 Compact IC Flex, Metrohm, Switzerland) and inductively coupled plasma optical emission spectrometry (ICP-OES; Spectro Arcos, Spectro Analytical Instruments, Germany) according to ISO 10304-1 [25] and ISO 11885 [26]; carbonate hardness (MQuant 1.10648.0001; Merck KGaA) and electric conductivity (CLS50D, Endress + Hauser, Switzerland). Since such analyses can easily yield incorrect results due to impurities or measurement errors, we carried out anion-cation-balance of every sample. 79 % of our analysed samples show an anion-cation-difference of less than ±5 % and therefore fulfil the criterion for acceptance according to APAH [24]. Results that missed the criterion of acceptance were discarded.

3. Results

In the following, first we will present the results of the ion analyses of the industrial wastewater. With the given results we show, which ions are present in the industrial wastewater and prove the linearity between EC and c_{Salt}. Then, we show how k_N, f_S and CCC can be found exemplarily for the present disc diffusers and industrial wastewater salt mixture in order to assess salt effect on oxygen transfer. The results of previous tap water oxygen transfer tests are shown in chapter 3.3. To give an overview of the overall operation performance of the pilot plant, the most important operation parameters are listed and discussed in chapter 3.4. In chapter 3.5, the results of off-gas and pressure drop measurement are discussed in context of EC, airflow rate and COD F/M ratio. The calculated α values are discussed in chapter 3.6. To assess whether a small slit design is recommended in saline conditions, we finally compare standard oxygen transfer rate in process water ($SOTR_{PW}$; kg/h) and the aeration efficiency (AE; kg/kWh) of both diffuser membrane designs in chapter 3.7.

3.1. Analysed ions and salt concentration in activated sludge

On average, the sum of anions ($\Sigma c_{eq,anions}$) and cations ($\Sigma c_{eq,cations}$) in the industrial wastewater were 120 meq/L (milliequivalent per litre). The main components of $\Sigma c_{eq,cations}$ were Chloride (78 mol-%) and Sulphate (17 mol-%); and of $\Sigma c_{eq,anions}$ it was Sodium (90 mol-%). The c_{Salt} is calculated by summing the mass concentration of all analysed ions [24].

Figure 28 shows c_{Salt} as a function of EC. A linear trend line was derived and plotted as dotted line. The coefficient of determination (R^2) of 0.99 indicated a very good linear dependency between EC and c_{Salt}. With the given equation from Figure 28, it is possible to calculate c_{Salt} (in g/L) in real time and on-site by measuring EC (in mS/cm):

$$c_{Salt} = 0.61 \cdot EC + 0.23 \qquad \text{[g/L]} \qquad (32)$$

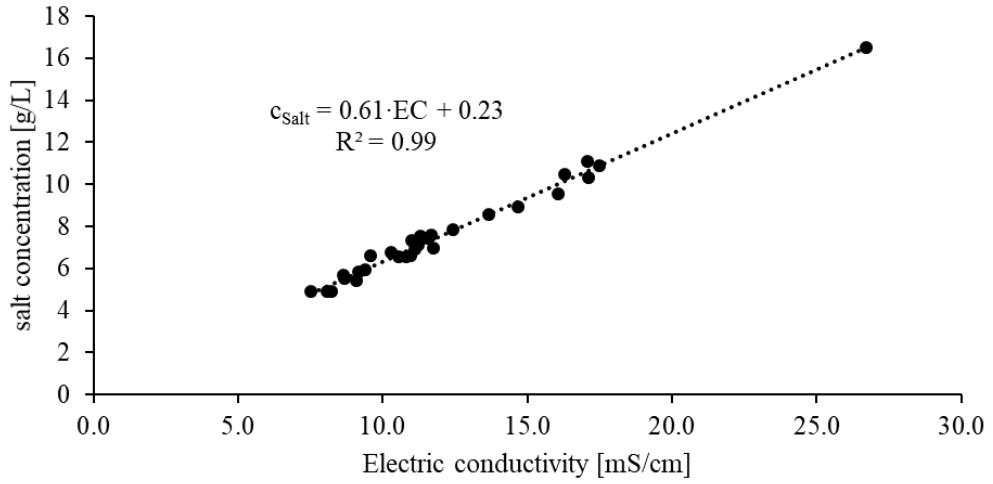

Figure 28: salt concentration (c_{Salt}; g/L) as a function of electric conductivity (EC; mS/cm)

3.2. Determination of k_N and measuring CCC of saline industrial wastewater

The modified equation for considering the salt effect on k_La is described in chapter 2.1. In the following, we will show how to find k_N for the used diffusers and wastewater conditions based on experimental results in SW, which are described in detail in Behnisch et al. [2]. With k_N and measured CCC, we are able to calculate the f_S value in dependence of salt concentration measured on site in sAS.

In a previous study [2], we measured $f_{S,max}$ of the disc diffusers described in chapter 2.3. The tests were conducted in NaCl solution (0 g/L– 15 g/L) in a pilot scale test tank (water volume 17.1 m³; depth of submergence 3.65 m) with different airflow rates. The results are shown in Figure 29-a) as a function of $q_{A,Disc}$ for both membrane designs. The influence of $q_{A,Disc}$ on $f_{S,max}$ is obvious. The highest $f_{S,max}$ is reached in the middle of the operation range of the diffusers. The $f_{S,max}$ for the corresponding $q_{A,Disc}$ can be calculated using the specified regression functions. With the known $f_{S,max}$ value, the k_N value can be derived from equation (29). The k_N values for both diffuser membrane designs as a function of $q_{A,Disc}$ are shown in Figure 29-b). The k_N value ranges between 0.6-1.3 and between 0.2-0.8 for membrane design A and design B, respectively. The airflow rate during off-gas measurement was constant at $q_{A,Disc}$ = 1,5 m³/Disc/h. The corresponding k_N value is 1.1 for diffuser membrane design A and 0.7 for diffuser membrane design B, respectively. The f_S value calculated according to equation (28) is plotted as a function of the dimensionless c_{Salt}/CCC_{Salt} ratio in Figure 30. With $q_{A,Disc}$ = 1.5 m³/Disc/h, $f_{S,max}$ is 2.1 for diffuser membrane design A and 1.7 for membrane design B, respectively.

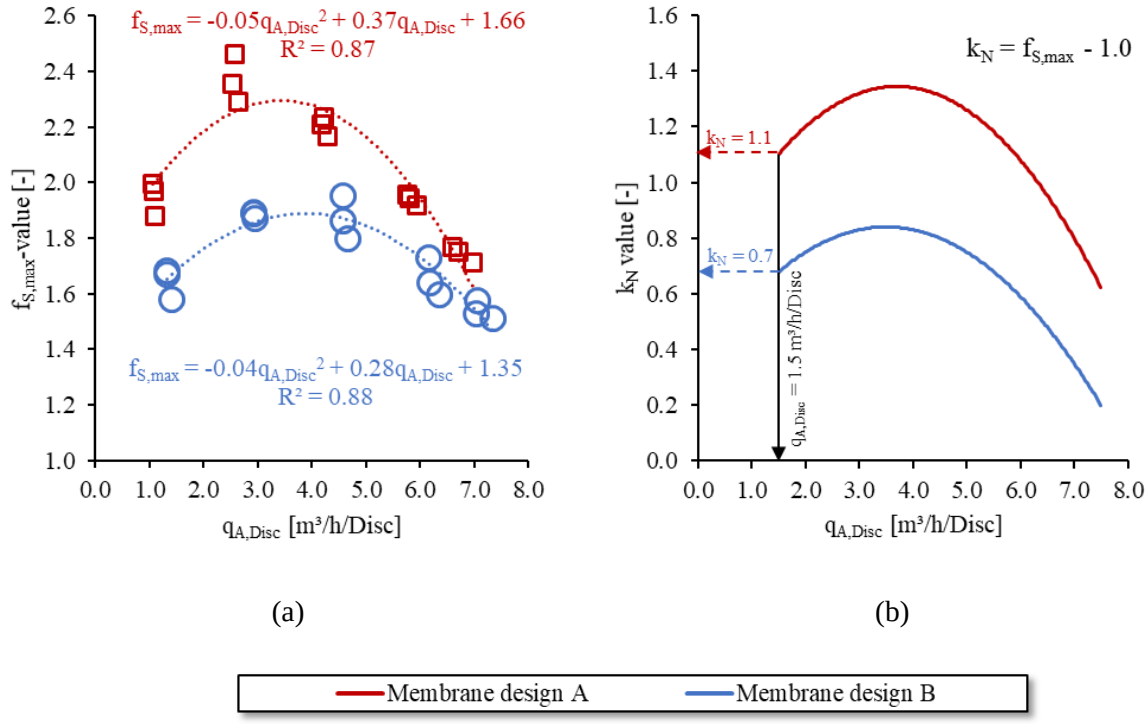

Figure 29: $f_{S,max}$ measured in NaCl solution in a pilot scale test tank for both membrane designs as a function of $q_{A,Disc}$ [2] (a); k_N calculated according to equation (29) for both diffuser membrane designs as a function of $q_{A,Disc}$ (b)

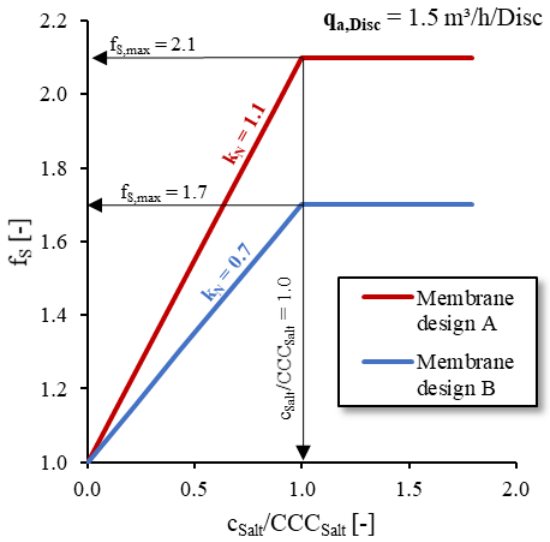

Figure 30: f_S as a function of the dimensionless c_{Salt}/CCC_{Salt} ratio for both diffuser membrane designs for an airflow rate per disc diffuser of 1.5 m³/h/Disc

The CCC of the industrial wastewater was measured according to the analytical approach described in Behnisch et al. [2]. Accordingly, oxygen transfer tests were performed at different airflow rates and salt concentration as well as f_S were calculated. The point at which the fitted lines for zone of linear increase and zone of constant f_S meet defines CCC. The CCC measurement was taken in a 250 l bubble column in the lab of the Technical University of Darmstadt. The transport of a sufficient amount of biological treated saline industrial wastewater was not possible and furthermore the industrial wastewater shows only small fluctuations in salt concentration (see chapter 2.2). Therefore, we used an artificial salt solution consisting of a salt mixture of NaCl and Na_2SO_4 in a ratio of 5:2. The salt solution in the bubble

column therefore show similar ion composition ($\Sigma c_{eq,Cl-}/\Sigma c_{eq,cations}$ = 0.75; $\Sigma c_{eq,SO42-}/\Sigma c_{eq,cations}$ = 0.25) as found in average in industrial wastewater (see chapter 3.1). The artificial salt solution makes it possible to determine f_S at different salt concentrations. We measured a CCC of 9.2 g/L. In previous study with same disc diffuser measured CCC of various single salt solutions, CCC ranges between 6.0 g/L and 15.7 g/L [2].

With the given k_N and CCC value, we are able to consider the salt effect on k_La on-site as a function of the salt concentration. Thereby, the good linear dependency of EC and c_{Salt} (see Figure 28) makes it possible to measure c_{Salt} in real time very quickly and easily.

3.3. Tap water oxygen transfer tests

To calculate αf_S, we have to know k_La in TW. Therefore, oxygen transfer tests in TW with all disc diffusers were conducted in B1 before inoculation with sAS (see chapter 2.4). The measured k_La values as a function of the airflow rate per aerated reactor volume ($Q_{A,VAT}$; m³/m³/h) are shown in Figure 31-a). When $Q_{A,VAT}$ = 1.0 m³/m³/h, the average k_La is 6.0 h^{-1} and 5.9 h^{-1} for membrane design A and B, respectively. It can be seen, that there is no significant difference between the diffusers as well as the different membrane designs. Also in our previous oxygen transfer tests in TW with same disc diffusers in different reactors of varying volume, we do not determine significant difference in k_La [1,2].

The tap water oxygen transfer tests were conducted without B1 intern recirculation. To assess the effect of recirculation on k_La, the tests with Disc II (0.75) were repeated with recirculation. During the tests, recirculation pump (P4) ran at 100 % of its capacity (6.5 m³/h), which is much more than in the later tests with sAS (2.5 m³/h). The results are shown in Figure 31-b). It can be seen that the recirculation has no effect on k_La.

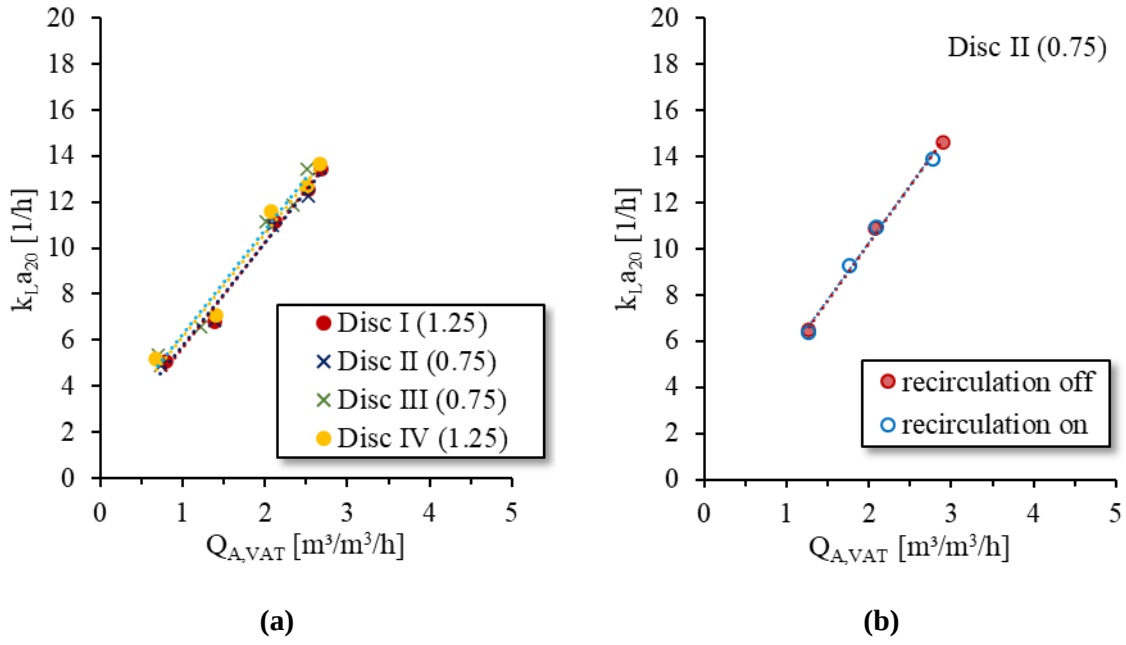

Figure 31: Results of oxygen transfer tests in TW (a); Results of oxygen transfer tests in TW with Disc II (0.75) with and without recirculation (b)

3.4. Overall performance of the pilot plant

An overview of the most important operating parameters of the pilot plant in the individual test phases can be taken from Table 12. The wastewater temperature (T; °C) of about 21 °C in Phase I and II is somewhat lower than in Phase III and IV (~ 25 °C). This can be explained by the fact that Phase I and

Phase II were carried out in spring, while Phase III and Phase IV were run in the summer months. The mean COD F/M ratio of approx. 0.25 gCOD/g TSS/d is comparable in all experimental phases. Only Phase IV shows a slightly higher load. During this phase, the industrial wastewater inflow contained an exceptionally high organic load for a few days. The COD F/M ratio and the SRT of 11 d corresponds to a nitrifying municipal WWTP [8]. The TSS in B1 was between 7 g/L and 4.4 g/L with a volatile content of 62 % to 75 %. In Phase I and II the influent flow (Q_{In}; L/h) was about 200 L/h. To reduce the required amount of added salt, the inflow in Phase III and IV was reduced to 110 L/h. The total COD elimination (η_{COD}; %) was stable above 90 % in all Phases. The COD concentration in the effluent, both COD_t and COD_f, was permanently below 50 mg/L. Only in Phase IV there was a slight increase, which can also be attributed to the unusually high and intermittent loading of the plant. The sludge volume index (SVI; mL/g) during operation decreased from 119 mL/g in Phase I to 47 mL/g in Phase IV, which is very low.

Table 12: Operating parameters of the pilot plant for individual test phases I to IV

		Phase I	**Phase II**	**Phase III**	**Phase IV**
Temperature	°C	20.6 ±1.2	20.9 ±1.9	24.8 ±1.8	25.9 ±1.5
COD F/M ratio*	g/g/d	0.23 ±0.08	0.24 ±0.07	0.22 ±0.09	0.30 ±0.16
TSS	g/L	6.95 ±0.63	7.01 ±0.43	5.73 ±0.90	4.43 ±0.65
volatile content	%	62 ±1	65 ±1	66 ±7	75 ±1
Q_{In}	L/h	195 ±15	194 ±16	117 ±44	107 ±19
η_{CSB}	%	95 ±2	95 ±2	92 ±2	91 ±5
SVI	mL/g	119 ±12	89 ±5	46 ±7	47 ±6
$COD_{t,eff}$	mg/L	39.5 ±8.4	42.2 ±13	32.5 ±9.9	63.2 ±91.6
$COD_{f,eff}$	mg/L	22.7 ±7.5	27.5 ±12.7	17.6 ±4.2	42.7 ±66.7

*= (daily COD load influent + daily COD load nutrient solution)/(TSS · VB_1)

3.5. Off-gas measurement and pressure

Figure 32 shows $Q_{A,VAT}$, αf_S, EC, p_d, as 15 min averages and the COD F/M ratio as 24 h average for each individual test phase. Not shown are all αf_S values where DO was above 50 % of oxygen saturation concentration or other circumstances (e.g. maintenance of equipment) prevent oxygen transfer measurement by off gas method. In the following we discuss them individually.

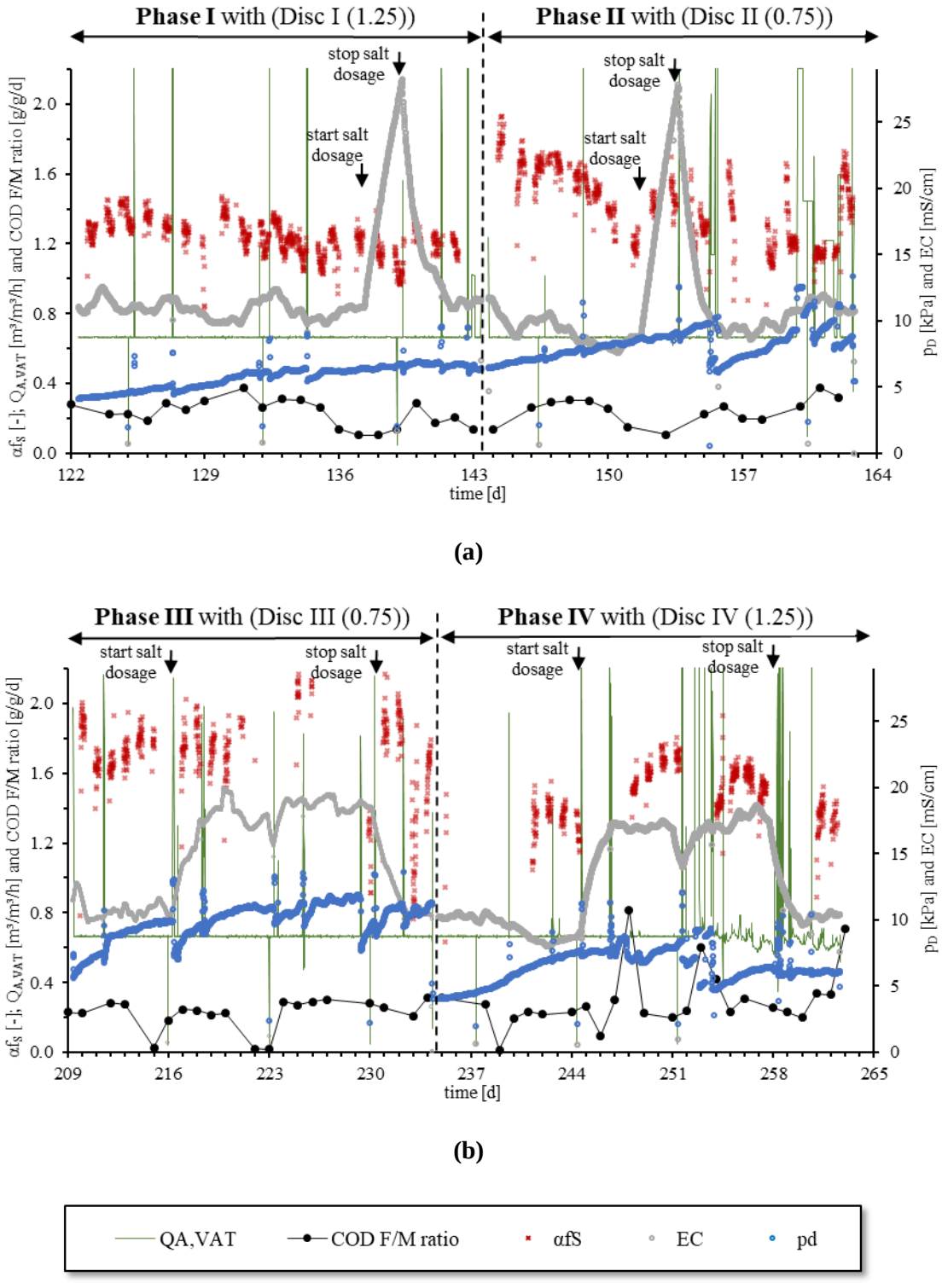

Figure 32: $Q_{A,VAT}$, αf_S, EC, p_d, as 15 min averages and the COD F/M ratio as 24 h for Phase I and II (a); and Phase III and IV (b)

3.5.1. EC, $Q_{A,VAT}$ and COD F/M ratio

In Figure 32, the times when salt was added from B3 are clearly recognisable by the rapidly rising EC. The EC in the reactor out of the salt dosing times ranges between 7.7 and 12.1 mS/cm and corresponds to that of the inflowing industrial wastewater. According to equation (32), this corresponds to a c_{Salt} between 4.9 and 7.6 g/L, which is much lower than the measured CCC of 9.2 g/L (see chapter 3.2). This means that without additional salt dosing the coalescence is not fully inhibited. When salt dosing in Phase I and Phase II started, EC increased 2.5 times in less than 2 d and drops sharply again after salt dosage stops and inflow restarted. In Phase III and Phase IV, salt was dosed continuously for about 14 days. EC reached a mean value of 17.7 mS/cm (= 11 g/L) in 62 h after salt dosage started. When the salt dosage stopped, EC reduced to the original value by dilution with the influent. As shown before (Table 12), the average COD F/M ratio is comparable in all phases. Only in Phase IV, the average ratio increases slightly due to high COD load in the influent on day 248, 253, 254 and 263. $Q_{A,VAT}$ averaged 0.7 m³/m³/h in all phases (corresponds to a Q_A = 1.5 m³/h or $q_{A,Disc}$ = 1.5 m³/h/Disc). It increases only for maintenance, when taking a sample from B1 for TSS measurement or to satisfy the oxygen demand when COD load in the influent was very high. This can be seen in Figure 32 from the peaks in the otherwise very stable profile of $Q_{A,VAT}$.

3.5.2. Pressure drop p_D

Figure 32 shows, that in all phases, p_D increases during time of operation. In Phase I p_D rises from 4.1 to 6.3 kPa during 21 d of operation and thus by an average of 0.07 kPa per day. At the beginning of Phase II, p_D of the newly installed Disc II (0.75) is 6.4 kPa. Then p_D increases rapidly by 0.82 kPa per day and reaches 9.8 kPa after only 12 days of operation. After a brief increase in $Q_{A,VAT}$, p_D drops to 6.2 kPa. However, when $Q_{A,VAT}$ is reduced to the previous value, p_D rises again rapidly. This decrease in p_D after a short-term increase in $Q_{A,VAT}$ can also be observed in Phase III and partly also in Phase IV. This can be explained by the fact, that the biofilm on the surface and in the slits of the diffuser is removed by the increased airflow rate. The p_D is therefore temporarily reduced until new biofilm is formed. The formation of biofilm and the clogging of slits is improved by the present low airflow rate [27].

At the beginning of Phase III, p_D is 5.6 kPa. A rapid increase in p_D follows, which can only be interrupted for a short time by briefly increasing the airflow rate. At the end of Phase III, however, p_D appears to be relatively stable at about 10 kPa. With the beginning of Phase IV and the change to Disc IV (1.25), p_D drops to 4.1 kPa. This corresponds to the starting p_D value of Disc I (1.25) in Phase I. After a slow increase, p_D reaches a relatively stable value of about 7.7 kPa. After the brief increase of airflow rate as response of the high organic load on days 253 and 254, p_D drops again to 4.7 kPa, rises slightly and remains stable at 5.9 kPa.

In all phases, no influence of EC or salt concentration on p_D could be observed. Neither does the increase in p_D change with the shock wise increase in salt concentration in Phase I and II, nor does it change with the temporarily elevated concentrations in Phase III and IV. In addition, no effect on p_D could be observed with the decrease of EC or salt concentration.

In summary, we observed a partly strong increase of p_D during aerating saline activated sludge. Only at the end of Phase III and IV after about 14 days of operation, p_D was stable with 10 kPa (Disc III (0.75)) and 7.7 kPa (Disc IV (1.25)). Membrane design A shows a higher p_D due to the smaller slits than membrane design B all the time. The reason for the rising p_D is most probably the growing biofilm on the surface and in the slits of the membrane diffuser, as is to be expected when aerating activated sludge. Especially the low airflow rate enhances the growth of the biofilm [27]. Furthermore, we observed no influence of EC or salt concentration on p_D. This confirms former results of p_D measurements in SW [2,16]. In SW the difference in p_D for the two membrane designs was on average 2.0 kPa and therefore in the same magnitude as observed here in sAS.

3.5.3. αf_s

The high αf_S values of > 1.0 in all phases (see Figure 32) show the positive effect of increased salt concentrations on oxygen transfer. In non-saline conditions (f_S= 1.0), for a nitrifying WWTP an α of 0.6 to 0.85 would be expected [8]. Our results show that the αf_S in sAS with the given diffusers is up to three times higher. The partially high fluctuations of αf_S within only few hours result from the multitude of oxygen transfer inhibiting effects, which change with the changing influent wastewater characteristics. Various studies show an inverse relationship of oxygen transfer and high organic influent concentration [7,28,29]. In our tests, however, the organic load was determined only once a day on the basis of a 24 h composite sample. A comparison of these data with a 24 h αf_S mean value cannot be made either, as the αf_S could not be recorded during the entire day due to the reasons already explained in chapter 2.5. Dynamic modelling of α is therefore not possible due to the lack of data.

To assess the effect of c_{Salt} on αf_S, Figure 33 shows αf_S values as a function of c_{Salt}/CCC_{Salt} ratio, separated by membrane design. The EC measured in B1 is plotted on the second abscissa. With empty circle symbols, the αf_S values measured during the time of salt dosing are additionally highlighted.

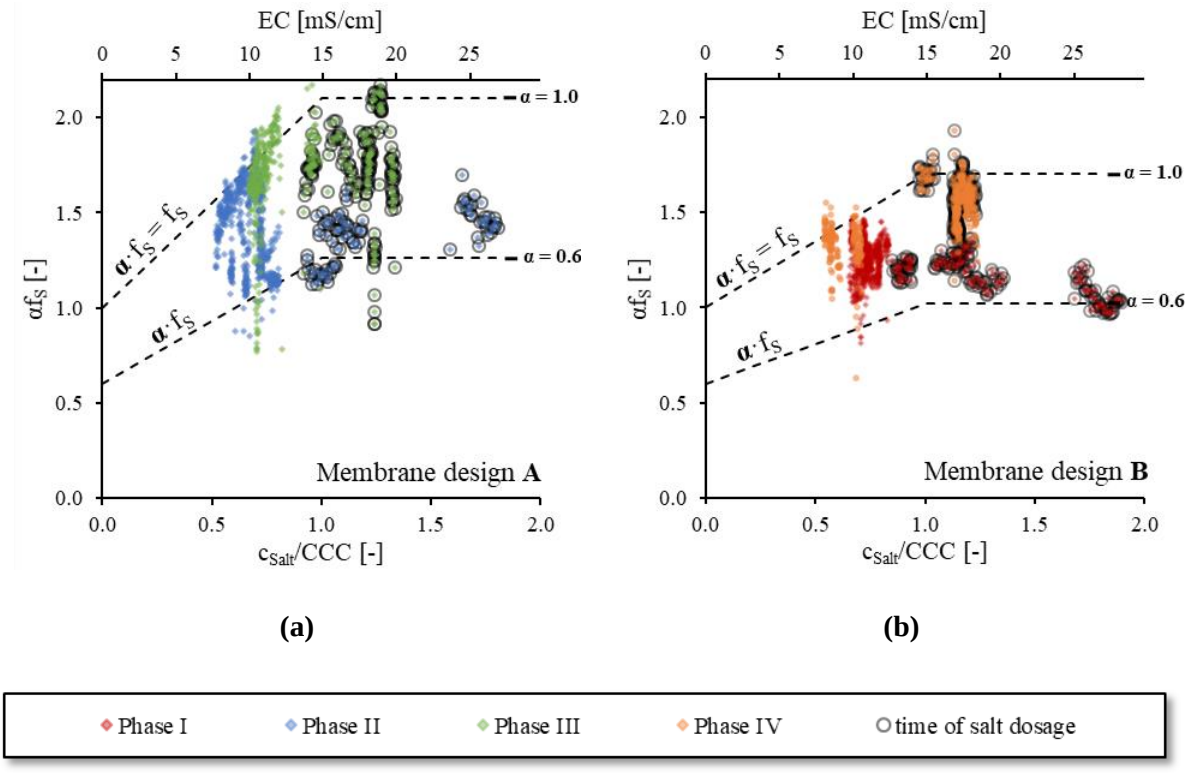

Figure 33: αf_S as a function of c_{Salt}/CCC_{Salt} for diffuser membrane design A (a) and diffuser membrane design B (b)

The upper dashed line shows the mean f_S progression calculated for the respective diffuser membrane design as described in chapter 3.2. Since the airflow rate was kept constant during the tests, f_S is only influenced by membrane design and c_{Salt}. Therefore, the calculated progression of f_S represents the limit below the range of αf_s is to be expected. Measured αf_S values closely to the calculated progression of f_S indicate, that α is ~ 1.0 and the oxygen transfer is not inhibited by wastewater ingredients. Corresponding to the dispersion of the f_S values around the specific regression functions in SW (see Figure 29-a)), αf_S values fluctuate around the calculated f_S progression.

With decreasing α, αf_S decreases. Assuming a minimum α for the current operation conditions (see Table 12) of 0.6 [8], the lower limit of the expected range of αf_S can be calculated (lower dashed line). 90 %

of measured αf_S values are within the expected range. Therefore, with the method presented in 2.1 and the given design recommendations for α, we were able to correctly predict the range of αf_S and f_S in sAS as a function of salt concentration.

When comparing the results of Figure 33-a) and –b), it became obvious that αf_S was higher for diffusers with diffuser membrane design A than with diffuser membrane design B. Averaging all αf_S values of a membrane design yields a mean value of 1.6 for membrane design A and 1.4 for membrane design B, respectively. This represents a relative improvement of 14 % in oxygen transfer with membrane design A compared to membrane design B. If only the results of the phases with the same type of salt addition (shock or continuous) are compared, a similar improvement of 13 % (Phase I vs. II) or 14 % (Phase III vs. IV) is found. During the tests in SW with the same diffuser membrane designs [1,2], an improvement of a comparable magnitude was found (+ 10 %).

Therefore, the present results confirm the previous SW results [2] and oxygen transfer increases significantly in sAS in a similar proportion to that in SW and improves further when an optimized diffuser membrane design is used. The AS in the aerated reactor at present TSS concentration up to 7 g/L and the wastewater ingredients do not apparently affect the coalescence behaviour of the ascending gas bubbles. Thus, when designers of aeration systems for activated sludge process faced with the question of which diffuser or which diffuser membrane design show the higher oxygen transfer in sAS, this can be assessed by relatively simple experiments in SW as described in Behnisch et al. [1]. However, it must be investigated in the future to what extent these findings can be transferred to other biological treatment processes, which are also aerated by fine-bubble aeration systems. Coalescence could be affected due to higher concentrated AS, such as present in membrane bioreactors. In other treatment processes, the biomass growths on inorganic carrier material or form granules. These could influence the ascend of the gas bubbles and therefore the coalescence behaviour. Further experiments are therefore necessary.

3.6. α value

With the known f_S for the respective membrane design (see chapter 3.2), α was calculated according to equation (14). Figure 34 shows α as a function of c_{Salt}/CCC_{Salt} ratio separated by membrane design. The EC measured in B1 is plotted on the second abscissa. Values measured during salt dosage are highlighted with empty circles. According to design recommendation for aeration systems in nitrifying WWTP [8], an α between 0.60 (= α_{min}) and 0.85 (= α_{max}) is expected for the given treatment operation conditions (see Table 12). The limits of expected range of α are marked as dashed lines. Less than 2 % of the measured α values are below the expected range. This shows that α_{min} value was estimated correctly and agrees with data from literature.

Contraryily, about 45 % of values are above α_{max}. High α values are not uncommon in WWTP. However, an increase of α of up to ~1.0 is usually only for a short time a day in periods of low-income load, e.g. at night or in the early morning. In the present case, the high α values can be explained by the fact, that the industrial wastewater is permanently slightly polluted. Surfactants and other possible oxygen transfer inhibiting constitutions was not explicitly measured, but elevated concentration of such substances is usually accompanied by increased organic concentration in the influent [8,27, 30]. An increased concentration of such substances in the influent is therefore most unlikely. Even the nutrient solution and its ingredients, which is dosed in order to achieve a sufficiently high OUR in the reactor (see chapter 2.5), have almost no influence on the oxygen transfer [23]. Therefore, if the wastewater is more polluted, extended times with lower α and αf_S can be expected.

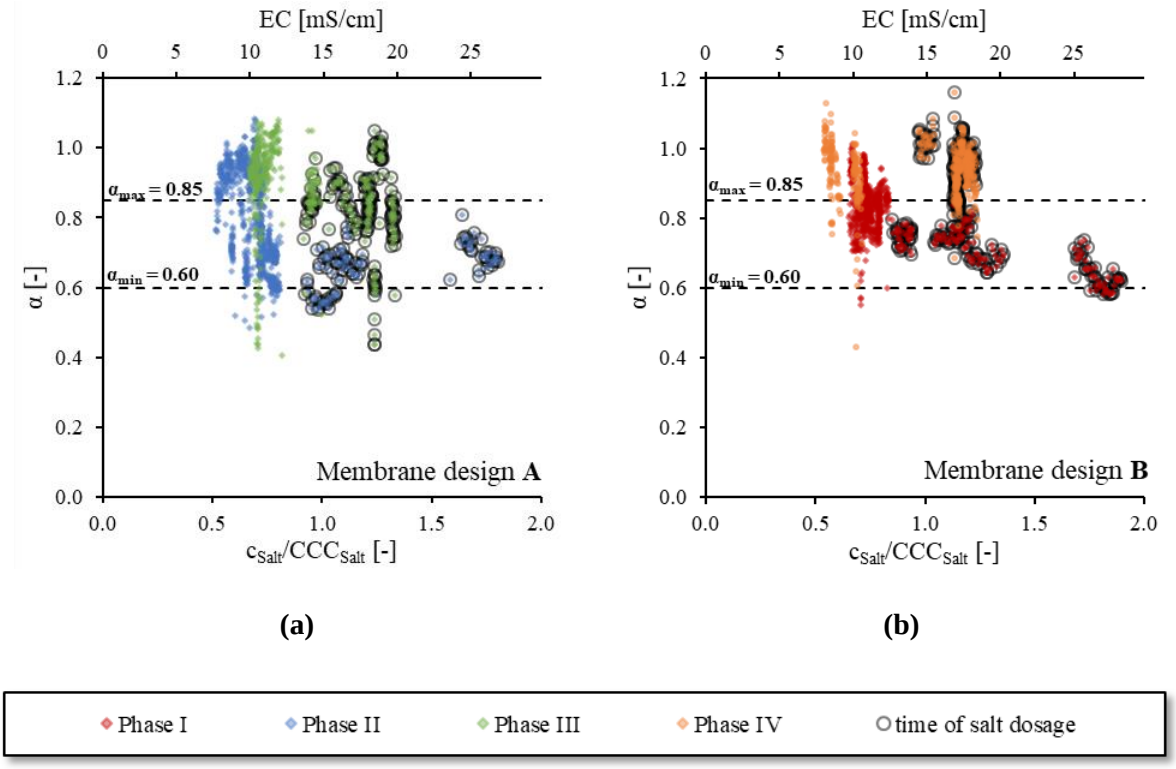

Figure 34: α as a function of EC for diffuser membrane design A (a) and diffuser membrane design B (b)

In Phase I and II the salt was dosed by shock load over 48 h. During the salt dosage the inflow of industrial wastewater and thus possibly inhibiting ingredients was stopped. Only the dosage of nutrient solution was continued. Since the ingredients of the nutrient solution do not inhibit oxygen transfer and the TSS concentration was kept constant by continuing the WAS removal, we expected that α will rise towards 1.0. The opposite happened. In Phase I, α even decreases slightly with increasing EC (see Figure 34-b)). This was not observed in Phases III and IV with continuous salt dosage.

A possible explanation is that the salt shock causes the microorganisms to produce oxygen transfer inhibiting substances [6, 8, 29, 30]. Since the influent was stopped during salt dosage, these substances accumulate in the system (i.e. reactor B1 and B2) and thereby enhance the effect. When the salt dosing was stopped and the inflow restarted, these substances were diluted and α rose to the value before salt dosing. This explanation is consistent with observations from other studies. It is a well-known fact, that microorganisms secrete more extracellular polymeric substances (EPS) to adapt to adverse environmental conditions [31]. Ng et al. [32] found an increase in organic dissolved substances with rising salt concentration. Jia et al. [33] measured an increase in EPS concentration with both increasing and decreasing salt concentration. Baquero-Rodríguez et al. [34] state, that especially the solved fraction of EPS (SMP) inhibits the oxygen transfer.

We could not investigate this phenomenon further. However, when designing aeration systems, it should be noted, that the oxygen transfer can be inhibited if the salt concentration fluctuates, not because of variation in f_s but because of secondary effects. Strong fluctuations in concentration can be prevented, for example, by an equalisation tank upstream of the aeration tank.

3.7. Performance comparison of both diffuser membrane designs

Results presented in chapter 3.5.3 show, that installing diffusers with small slits membrane design increases oxygen transfer up to 14 % in sAS compared to large slits membrane design. However, small

slits result in a rising pressure drop (see chapter 3.5.2) and a corresponding increased power requirement of the blowers (P). Therefore, using diffusers with small slits membrane design in saline conditions causes advantages and disadvantages. It is questionable at which c_{Salt}/CCC ratio the use of small slits membrane design improves aeration. To answer this question, we compare the performance of both diffuser membrane designs.

For performance comparison we calculate based on the TW results (see chapter 3.3), the given equations for calculating f_S (see chapter 3.2) for corresponding membrane design and a fixed α the standard oxygen transfer rate in process water ($SOTR_{PW}$; kg/h), standardized at DO = 0 mg/L, atmospheric pressure = 101.3 kPa and T = 20 °C:

$$SOTR_{PW} = \frac{V \cdot \alpha \cdot f_S \cdot k_L a_{20} \cdot \beta \cdot c_{S,20}}{1.000} \quad \text{[kg/h]} \qquad (33)$$

where V is the aerated water volume (m³), β is the ratio of oxygen saturation concentration in process conditions to standard conditions (-) and $c_{S,20}$ is the oxygen saturation concentration at standard conditions (mg/L). Since the α of the present experiments are exceptionally high due to the low wastewater contamination (see chapter 3.6), and to get representative results, for $SOTR_{PW}$ calculation we assume a fixed α of 0.75, which is a typically mean value for nitrifying WWTP [8].

The aeration efficiency (AE) is suitable to illustrate the interaction between increased energy requirements and improved oxygen transfer. It is defined as the ratio $SOTR_{PW}$ to P [18].

$$AE = \frac{SOTR_{PW}}{P} \quad \text{[kg/kWh]} \qquad (34)$$

Positive displacement blowers (PD) are commonly used for air supply on WWTP's. For this type of blower P can be calculated using the isochoric power formula [34]:

$$P = \frac{Q_A \cdot (p_h + p_D + p_S)}{\eta} \quad \text{[kW]} \qquad (35)$$

where Q_A is the airflow rate (m³/s), p_h is the hydrostatic pressure resulting from depth of submergence (kPa), p_D is the pressure drop of diffusers (kPa), p_S is the pressure of pipes (kPa) and valves and η the overall efficiency of the blower (-). The p_h increases with increasing c_{Salt} due to the increment of water density. Nevertheless, this increase is marginal and can be neglected [2]. The p_D depends on the membrane design (see chapter 3.5.2). The p_S is affected neither by c_{Salt} nor by diffuser membrane design. Assuming a typically η for PD blowers of 0.60 [35], and using p_D results shown in 3.5.2 (Design A: 10 kPa; Design B: 7.7 kPa), for Q_A = 1.5 m³/h a P of 32 W and 30 W is calculated for diffuser membrane design A and design B, respectively.

Figure 35 shows $SOTR_{PW}$ per aerated water volume ($SOTR_{PW}$/V; m³/m³/h) as a function of c_{Salt}/CCC ratio. AE is plotted on the second ordinate. For both diffuser membrane designs $SOTR_{PW}$/V and AE increase with increasing c_{Salt}/CCC ratio and reach their maxima when c_{Salt}/CCC = 1.0. When c_{Salt}/CCC > 1.0 $SOTR_{PW}$/V and AE decrease again due to the constant f_S (see Figure 30) with a simultaneous decrease in oxygen saturation concentration.

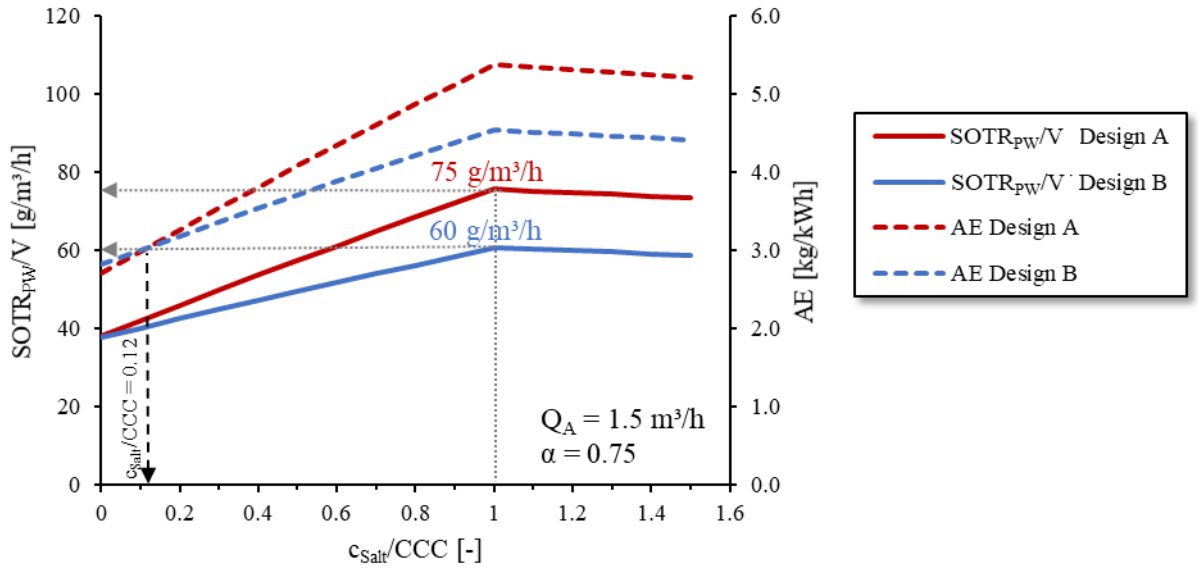

Figure 35: $SOTR_{PW}$ in activated sludge (α = 0.75) per aerated water volume V ($SOTR_{PW}$/V) and AE for both diffuser membrane designs as a function of c_{Salt}/CCC at a fixed airflow rate of 1.5 m³/h

The high $SOTR_{PW}$/V values of up to 75 g/m³/h reached for membrane design A and 60 g/m³/h for membrane design B when c_{Salt}/CCC = 1.0 show the improved aeration due to the increased salt concentration. In TW with fine bubble aeration systems and corresponding $Q_{A,VAT}$ a mean $SOTR_{PW}$/V of 60 g/m³/h is typical [36]. Despite consideration of k_La inhibition by α = 0.75, this value is reached and even clearly exceeded in the case of diffuser membrane design A.

When c_{Salt}/CCC = 0, $SOTR_{PW}$/V is identical for both diffuser membrane designs due to similar TW k_La values (see chapter 3.3). However, due to the higher-pressure drop of membrane design A and the corresponding higher power requirement for air supply, AE of membrane design A is lower than of membrane design B. This means that in non-saline conditions the use of diffusers with smaller slits decreases the energy efficiency of aeration systems. Therefore, in non-saline conditions it is more efficient to use diffusers with larger slits and therefore lower pressure drop.

Because of increasing coalescence inhibition and the corresponding increase in f_S with rising c_{Salt}/CCC ratio, $SOTR_{PW}$/V and AE increases more rapidly for membrane design A than for membrane design B. When c_{Salt}/CCC > 0.12, AE of membrane design A exceeds AE of membrane design B. That means that with given diffusers (f_S, p_D) and a fixed Q_A of 1.5 m³/h, the aeration improves by using diffusers with membrane design A than with membrane design B as soon as c_{Salt}/CCC > 0.12.

However, in the present $SOTR_{PW}$ and AE calculation, we used for simplification a fixed airflow rate (Q_A = 1.5 m³/h) as set during the sAS oxygen transfer tests. Since f_S increases differently for different diffuser membrane designs, this results in different $SOTR_{PW}$ values with increasing c_{Salt}/CCC ratio as described before. To match the same $SOTR_{PW}$/V with both diffuser membrane designs, Q_A could be adjusted. Since both f_S and p_D changes with changing Q_A, this would require the recalculation of $SOTR_{PW}$ and P.

4. Conclusion

In previous studies, we assess the different factors influencing the oxygen transfer in saline water. In the present study, we investigate whether the saline water results are transferable to saline activated sludge aeration. For this purpose, we operate a pilot scale activated sludge plant (water volume = 2.25 m³; depth of submergence = 3.5 m) over 269 days with industrial wastewater influent. Oxygen transfer was assessed continuously by off-gas method. Salt concentration and different operation parameters were measured to evaluate their impact on overall plant performance.

1. We present a modified design approach for considering salt effect on oxygen transfer. This enables a more precise design and therefore a more energy efficient operation of aeration systems at high salt concentrations. The current design approach is only applicable to municipal wastewater with high sea salt concentration. By normalizing the salt effect on oxygen transfer, our modified design approach can be used for each coalescence inhibiting mixed salt solution. Furthermore, we exemplify how the influence of membrane design can be taken into account by performing very simple laboratory tests in NaCl solution.

2. The diffuser membrane design has a significant influence on oxygen transfer in saline activated sludge. The oxygen transfer improves up to 14 % by installing diffusers with small slits diffuser membrane design compared to oxygen transfer of diffusers with large slits membrane design. This corresponds to our previous saline water results and thus confirms the transferability from saline water to saline activated sludge conditions. Overall, the oxygen transfer in saline activated sludge is more than doubled compared to non-saline nitrifying WWTP. The $SOTR_{PW}$ in activated sludge per aerated tank volume reaches up to 75 g/m³/h and thus even exceeds corresponding TW conditions. Using isochoric power formula calculated aeration efficiency of up to 5.4 kg/kWh (small slit design) and 4.5 kg/kWh (large slit design) show, that also the energy efficiency improves in saline activated sludge using small slits membrane design despite the increased pressure drop.

3. The pressure drop of the diffusers in saline activated sludge was not affected by salt concentration. The difference in pressure drop between diffuser membrane designs was in the same magnitude as in saline water experiments. Nevertheless, pressure drop increases during operation for both diffuser membrane designs, as is to be expected when aerating activated sludge. The increment results from biofilm formation on the surface and in the slits of membrane diffuser. By brief increase of airflow rate, biofilm could be removed and pressure drop reduced temporarily.

4. The lowest α values were measured during shock wise salt dosing and stopped influent flow. A possible explanation is, that that activated sludge secretes more EPS and dissolved organic substances to adapt to rapidly changing salt concentrations and these substances inhibit the oxygen transfer and increase diffuser fouling as well. We could not investigate this phenomenon further in the present study, which is why further experiments with a longer observation period should be carried out.

Author Contributions: Conceptualization, J.B.; methodology, J.B. and M.W.; validation, J.B., M.S., J.T., M.E., M.W.; formal analysis, J.B.; data curation, J.B.; writing—original draft preparation, J.B.; writing—review and editing, J.B., M.S., J.T., M.E., M.W.; visualization, J.B.; supervision, M.E., M.W.; project administration, J.B., M.W.; funding acquisition, J.B., M.W. All authors have read and agreed to the published version of the manuscript.

Funding: We thank the German Federal Ministry of Education and Research (BMBF) for funding the research project WaReIp ‘Water-Reuse in Industrial Parks’ (Grant No. 02WAV1409A).

Data Availability Statement: Measurement data presented in this study is available on request from the corresponding author.

Conflicts of Interest: The authors declare no conflict of interest. The funders had no role in the design of the study; in the collection, analyses, or interpretation of data; in the writing of the manuscript, or in the decision to publish the results.

5. References of Paper IV

1. Behnisch, J.; Ganzauge, A.; Sander, S.; Herrling, M.P.; Wagner, M. Improving aeration systems in saline water: measurement of local bubble size and volumetric mass transfer coefficient of conventional membrane diffusers. *Water Science and Technology* **2018**, *78*, 860–867, doi:10.2166/wst.2018.358.
2. Behnisch, J.; Schwarz, M.; Trippel, J.; Engelhart, M.; Wagner, M. Improving aeration systems in saline water (Part II): Effect of different salts and diffuser type on oxygen transfer of fine-bubble aeration systems. *Water Science and Technology* **2021**, *83*, 2278–2792.
3. Sander, S.; Behnisch, J.; Wagner, M. Design of fine-bubble aeration systems for municipal WWTPs with high sea salt concentrations. *Water Science and Technology* **2017**, 75, 1555–1563.
4. Bauer, S.; Dell, A.; Behnisch, J.; Linke, H.J.; Wagner, M. Sustainability requirements of implementing water-reuse concepts for new industrial park developments in water-stressed regions. *Journal of Water Reuse and Desalination* **2020**, *10*, 490–499, doi:10.2166/wrd.2020.028.
5. Wagner, M.; Stenstrom, M.K. *Aeration and mixing. In: Activated Sludge – 100 Years and Counting;* Jenkins, D.; Wanner, J.; Ed; IWA Publishing: London, England, 2014.
6. Henkel, J. *Oxygen Transfer Phenomena in Activated Sludge*. Ph.D. Thesis, Technical University of Darmstadt, Darmstadt, 2010.
7. Leu, S.-Y.; Rosso, D.; Larson, L.E.; Stenstrom, M.K. Real-Time Aeration Efficiency Monitoring in the Activated Sludge Process and Methods to Reduce Energy Consumption and Operating Costs. *Water Environment Research*, 2009, 81, 2471–2481.
8. Günkel-Lange, T. *Sauerstoffzufuhr und α-Werte feinblasiger Belüftungssysteme beim Belebungsverfahren - Abhängigkeiten und Bemessungsempfehlungen (Oxygen-transfer and α-value of fine bubble aeration in activated sludge – Dependences and design approaches)*. Ph.D. Thesis, Technical University of Darmstadt, 2013
9. DWA. *Design of wastewater treatment plants in hot and cold climates*: *DWA Topics T4/2016, corrected version May 2019;* German Association for Water, Wastewater and Waste: Hennef, 2019, ISBN 978-3-88721-616-0.
10. Cho, Y.S.; Laskowski, J.S. Effect of flotation frothers on bubble size and foam stability. *International Journal of Mineral Processing* **2002**, *64*, 69–80, doi:10.1016/S0301-7516(01)00064-3.
11. Quinn, J.J.; Sovechles, J.M.; Finch, J.A.; Waters, K.E. Critical coalescence concentration of inorganic salt solutions. *Minerals Engineering* **2014**, *58*, 1–6, doi:10.1016/j.mineng.2013.12.021.
12. Marrucci, G.; Nicodemo, L. Coalescence of gas bubbles in aqueous solutions of inorganic electrolytes. *Chemical Engineering Science* **1967**, *22*, 1257–1265, doi:10.1016/0009-2509(67)80190-8.
13. Baz-Rodríguez, S.A.; Botello-Álvarez, J.E.; Estrada-Baltazar, A.; Vilchiz-Bravo, L.E.; Padilla-Medina, J.A.; Miranda-López, R. Effect of electrolytes in aqueous solutions on oxygen transfer in gas-liquid bubble columns. *Chemical Engineering Research and Design*, 2014, 92, 2352–2360.
14. Ribeiro Jr., C.P.; Mewes, D. The influence of electrolytes on gas hold-up and regime transition in bubble columns. *Chemical Engineering Science* **2007**, *62*, 4501–4509, doi:10.1016/j.ces.2007.05.032.
15. Botello-Álvarez, J.E.; Baz-Rodríguez, S.A.; González-García, R.; Extrada-Baltazar, A.; Padilla-Medina, J.A.; González-Alatorre, G.; Navarrete-Bolanos, J.L. Effect of Electrolytes in Aqueous Solution on Bubble Size in Gas-Liquid Bubble Columns. *Industrial & Engineering Chemistry Research*, 2011, 50, 12203–12207.

16. Sander, S. *Optimierung der Bemessung feinblasiger Druckbelüftungssysteme bei erhöhten Meersalzkonzentrationen (Optimisation of the design of fine-bubble aeration systems at increased sea salt concentrations)*. Ph.D. Thesis, Technical University of Darmstadt, Darmstadt, 2018.

17. Zlokarnik, M. Koaleszenzphänomene im System gasförmiger/flüssiger und deren Einfluß auf den O2-Eintrag bei der biologischen Abwasserreinigung (*Coalescence phenomena in the gas/liquid system and their influences on oxygen uptake in biological waste water treatment)*. *Korrespondenz Abwasser, Abfall* **1980**, *27*, 728–734.

18. EN 12255-15. *Wastewater treatment plants - Part 15: Measurement of the oxygen transfer in clean water in aeation tanks of activated sludge plants;* European Committee for Standardization, Brussels Belgium, 2003 (12255-15).

19. Wagner, M.; Pöpel, H.J.; Kalte, P. Pure oxygen desorption method - A new and cost-effective method for the determination of oxygen transfer rates in clean water. *Water Science and Technology* **1998**, *38*, 103–109.

20. ASCE/EWRI 18-18. *Standard Guidelines for In-Process Oxygen Transfer Testing;* American Society of Civil Engineers: Reston, Virginia, 2018 (18-18).

21. DWA-M 209. *Messung der Sauerstoffzufuhr von Belüftungseinrichtungen in Belebungsanlagen in Reinwasser und in Belebtschlamm (Worksheet – Measurement of oxygen transfer of aeration systems of activated sludge processe in clean water and activated sludge);* German Association for Water, Wastewater and Waste, Henef, 2007.

22. Krampe, J. Assessment of diffuser pressure loss on WWTPs in Baden-Württemberg. *Water Science and Technology* **2011**, *63*, 3027–3033, doi:10.2166/wst.2011.634.

23. Özbek, B.; Gayik, S. The studies on the oxygen mass transfer coefficient in a bioreactor. *Process Biochemistry* **2001**, *36*, 729–741, doi:10.1016/S0032-9592(00)00272-7.

24. American Public Health Association; American Water Works Association; Water Environment Federation. *Standard methods for the examination of water & wastewater*, 21st American Public Health Association (APHA): Washington, DC, USA, 2005.

25. ISO 10304-1. *Water quality - Determination of dissolved anions by liquid chromatography of ions - Part 1: Determination of bromid, chlorid, fluorid, nitrate, nitrite, phosphate and sulfate;* International Organization for Standardization: Geneva, Switzerland, 2009. (10304-1).

26. ISO 11885. *Water quality - Determination of selected elements by inductively coupled plasma optical emission spectrometry (ICP-OES);* International Organization for Standardization: Gemeva, Switzerland, 2007. (11885).

27. Rosso, D.; Stenstrom, M.K.; Garrido-Baserba, M. Aeration fundamentals, performance and monitoring. In *Aeration, Mixing, and Energy: Bubbles and Sparks*; Rosso, D., Ed.; IWA Publishing: London, UK, 2018, 31–61.

28. Jiang, P.; Stenstrom, M.K. Oxygen Transfer Parameter Estimation: Impact of Methodology. *Journal of Environmental Engineering* **2012**, *138*, 137–142, doi:10.1061/(ASCE)EE.1943-7870.0000456.

29. Germain, E.; Nelles, F.; Drews, A.; Pearce, P.; Kraume, M.; Reid, E.; Judd, S..J.; Stephenson, T. Biomass effects on oxygen transfer in membrane bioreactors. Water research **2017**, 41 (5), 1038–1044. DOI: 10.1016/j.watres.2006.10.020.

30. Schwarz, M.; Behnisch, J.; Trippel, J.; Wagner, M.; Engelhart, M. Oxygen Transfer in Two-stage Activated Sludge Process. *Water* **2021**, 13, 14: 1964. https://doi.org/10.3390/w13141964

31. He, H.; Chen, Y.; Li, X.; Cheng, Y.; Yang, C.; Zeng, G. Influence of salinity on microorganisms in activated sludge processes: A review. *International Biodeterioration & Biodegradation* **2017**, *119*, 520–527, doi:10.1016/j.ibiod.2016.10.007.

32. Ng, H.Y.; Ong, S.L.; Ng, W.J. Effects of Sodium Chloride on the Performance of a Sequencing Batch Reactor. *Journal of Environmental Engineering* **2005**, *131*, 1557–1564, doi:10.1061/(ASCE)0733-9372(2005)131:11(1557).

33. Jia, Y.; Wang, S.; Zhang, L.; Wang, X.; Guo, J. Effect of different salinity on sludge bulking by using sequencing batch reactor. *Transactions of Chinese Society of Agricultur Engineering* **2014**, 29, 112–119.

34. Baquero-Rodríguez, G.A.; Lara-Borrero, J.A.; Nolasco, D.; Rosso, D. A Critical Review of the Factors Affecting Modeling Oxygen Transfer by Fine-Pore Diffusers in Activated Sludge. *Water environment research: a research publication of the Water Environment Federation* **2018**, *90*, 431–441, doi:10.2175/106143017X15131012152988.

35. Mueller, J.A.; Boyle, W.C.; Pöpel, H.J. *Aeration*: *Principles and practice;* CRC Press: Boca Raton, FL, USA, 2002, ISBN 1-56676-948-5.

36. Bell, K.Y.; Abel, S. Optimization of WWTP aeration process upgrades for energy efficiency. *Water Practice and Technology* **2011**, *6*, wpt2011024.

37. Behnisch, J.; Schwarz, M.; Wagner, M. Three decades of oxygen transfer tests in clean water in a pilot scale test tank with fine-bubble diffusers and the resulting conclusions for WWTP operation. *Water Practice and Technology* **2020**, *15*, 910–920, doi:10.2166/wpt.2020.072.

5 Final Conclusions

The topic of this cumulative thesis is to investigate the influence of diffuser design on oxygen transfer of fine-bubble aeration systems in wastewater treatment at increased salt concentrations. Comprehensive experiments were carried out in tap water, saline water and saline activated sludge to show the differences in oxygen transfer and bubble size of fine-bubble diffusers at elevated salt concentrations. The main conclusions from the different experiments are summarized in the following.

The analyses of 306 oxygen transfer tests of 65 different fine-bubble diffusers, carried out in tap water in the same test tank under identical test conditions showed, that the average performance of modern fine-bubble aeration systems improves by 17 % in the last three decades. With an airflow rate per aerated tank volume ($Q_{A,VAT}$) of 1.0 m³/m³/h, an average standard oxygen transfer rate per aerated tank volume ($SOTR_{VAT}$) of 83 g/m³/h and standard aeration efficiency (SAE) of up to 5.6 kg/kWh is achieved.

The comparison of specific standard oxygen transfer efficiency (SSOTE) of tube, plate and disc diffusers showed, that in fully mixed aeration tanks and typically $Q_{A,VAT}$, the highest SSOTE of up to 10 %/m could be reached with tube diffusers. Furthermore, for all diffusers SSOTE increased the higher the depth of submergence or diffuser density was. However, only a minor improvement in SSOTE occurs if diffuser density exceeds 35 %.

Due to the improvement in performance of modern fine-bubble aeration diffusers in the last three decades, a new range of favourable SSOTE values indicated for different depth of submergence (3.8 m; 6 m; 8 m and 12 m) is proposed. Accordingly, at depth of submergence of 3.8 m, well designed and operated aeration systems can achieve in tap water SSOTE between 8.5 and 9.8 %/m. The proposed range of SSOTE can be used e.g. for first design calculation of new aeration systems, as benchmark to assess the performance of diffusers in tap water or to model the activated sludge process accordingly.

Nevertheless, in tap water no influence of the diffuser membrane design on oxygen transfer could be observed. Measuring bubble size and bubble size distribution via image analyses at different levels of the ascending bubble swarm originated by conventional disc diffusers with different membrane designs showed, that the smaller the slits of the diffuser membrane, the smaller are the bubbles close to the diffuser. However, the size of the bubbles increased rapidly along their ascent. For fine-slitted diffuser membrane design, bubble size increased about 93 % and reached the same size as bubbles generated by large-slitted membrane design. Therefore, the aeration performance in tap water is not improved by using fine-slitted diffuser membrane design. Instead, it leads to increased energy requirement for air-supply due to a higher pressure drop of fine-slitted diffusers.

With increasing salt concentration coalescence is increasingly inhibited and the oxygen transfer rises. The effect of salt on oxygen transfer is described by the f_S-value, which is defined as the ratio between volumetric mass transfer coefficient (k_La) in saline water and in tap water. To assess the effects of diffuser membrane design, diffuser type, diffuser density and salt type on oxygen transfer at elevated salt concentration, oxygen transfer tests with disc, plate and tube diffusers were conducted in a 250 L bubble column as well as in a 17,100 L pilot scale glass-steel-frame test tank.

The results showed, that due to the increasingly inhibited bubble coalescence f_S rises linearly with increasing salt concentration until a limit salt concentration is reached. This limit concentration is called the critical coalescence concentration (CCC). When CCC is achieved, coalescence is completely inhibited, and f_S reaches its maximum ($f_{S,max}$). The oxygen transfer tests showed, that despite the reduced oxygen saturation concentration at elevated salt concentration, SSOTE and SAE increase up to 15 %/m and 8.4 kg/kWh, respectively. With $Q_{A,VAT}$ = 1.0 m³/m³/h, maximum $SOTR_{VAT}$ was 182 g/m³/h, which represent an increase by more than 120 % compared to average tap water performance.

For measuring CCC, a new analytical approach was developed, within CCC is determined by evaluating the oxygen transfer at different salt concentrations. The new method is much faster and easier to use than bubble size measurement and provides valid results. In the future, this will make it possible to investigate the coalescence behaviour for any aeration system and (mixed) salt solution quickly and easily, as it was exemplified by measuring CCC of real industrial wastewater containing mixed salt solution.

Furthermore, with the new analytical approach, CCC of various single salt solutions for conventional fine-bubble aeration diffusers were determined for the first time ($MgCl_2$: 6.0 g/L or 0.063 mol/L; $CaCl_2$: 10 g/L or 0.08 mol/L; Na_2SO_4: 12.8 g/L or 0.085 mol/L; NaCl: 10.5 g/L or 0.18 mol/L; KCl: 15.7 g/L or 0.21 mol/L). The comparison of own CCC-results with results from literature confirmed the known correlation between primary bubble size and CCC: The smaller the primary bubbles the higher is CCC.

With oxygen transfer tests in various single salt solutions with the same diffuser it could be demonstrated, that $f_{S,max}$ is not affected by salt type. Therefore, once known $f_{S,max}$ of a diffuser can be transferred to any (mixed) salt solution. This confirms several experimental studies, which showed that in coalescence inhibited systems bubble size reaches always a fixed minimum value, regardless of salt type. This minimum bubble size equals the size of primary bubbles. The corresponding bubble diameter at their minimum size is also called quasi-static bubble diameter.

The decrease in bubble size could also be observed in the present experiments. Bubble size measurements showed, that due to the inhibition of coalescence in saline water, the mean bubble size of the bubble swarm aspire asymptotically to the observed primary bubble diameter or quasi-static bubble diameter, respectively. Due to the smaller primary bubbles fine-slitted diffusers offer in coalescence inhibited systems a larger interfacial area and thus oxygen transfer rises, as it could be confirmed via simultaneously conducted oxygen transfer tests. When using disc or tube diffusers with fine-slitted membrane design, $f_{S,max}$ enhances on average by 10 % compared to the corresponding diffusers with large-slitted membrane design.

Furthermore, results showed that there is a clear influence of the diffuser type. While f_S for tube diffusers only depends on the salt concentration, f_S of other diffuser types is affected by the airflow rate per slit and slit length ($q_{A,dS}$). The highest f_S values were achieved at $q_{A,dS} \sim 1.0$ dm³/h/mm. If $q_{A,dS}$ changes, f_S decreases again. Possible explanations were discussed, such as a change in bubble size with the changing airflow.

An effect of diffuser density on f_S could not be observed. This corresponds to the generally accepted concept, that bubbles only coalesce with bubbles from the same diffuser or adjacent slits and not with bubbles from other diffusers.

Based on the present results, a modified design approach for considering salt effect on oxygen transfer is proposed. The current design approach is only applicable to municipal wastewater with high sea salt concentration and do not consider the different CCC of various salt solutions as well as the diffuser design. The proposed design approach normalizes the salt effect on oxygen transfer by including the dimensionless c_{Salt}/CCC ratio. The slope of linearly increasing f_S as a function of c_{Salt}/CCC is described by the dimensionless k_N value. Accordingly, identically aerated solutions of different salts and salt mixtures with the same c_{Salt}/CCC_{Salt} ratio would present similar f_S values. Therefore, the new approach is applicable for each coalescence inhibiting mixed salt solution and enables an appropriate design of fine-bubble aeration systems at increased salt concentrations.

To assess the transferability of saline water results to saline activated sludge conditions and to evaluate the proposed design approach, a pilot scale activated sludge plant (water volume = 2.25 m³; depth of submergence = 3.5 m) was operated for 269 days with industrial wastewater influent. The TSS concentration was up to 7 g/L. Oxygen transfer was determined continuously by off-gas method. Salt

concentration and different operation parameters were measured to evaluate impact on overall plant performance. Previous oxygen transfer tests in tap water enable the calculation of αf_S, which is defined as the ratio of k_La in saline activated sludge to k_La in tap water.

With $Q_{A,VAT}$ = 0.7 m³/m³/h, average $SOTR_{VAT}$ in tap water was 60 g/m³/h. Similar to the previous tests in the bubble column or the pilot scale glass-steel frame tank, in tap water no effect of diffuser membrane design on oxygen transfer could be observed. Due to the oxygen transfer inhibiting substances in the wastewater and the activated sludge, a decrease in $SOTR_{VAT}$ would be expected. Indeed, average $SOTR_{VAT}$ was 60 g/m³/h and thus in the same magnitude as in tap water and rises further of up to 75 g/m³/h when using fine-slitted diffuser membrane design. Therefore, the positive effect of salt on oxygen transfer is obvious and overlaps the oxygen transfer inhibiting effects of ingredients in the activated sludge. Calculated aeration efficiencies using isochoric power formula of up to 5.4 kg/kWh (fine-slitted membrane design) and 4.5 kg/kWh (large-slitted membrane design) showed, that despite the increased pressure drop also the energy efficiency of aeration improves in saline activated sludge when using fine-slitted membrane design.

The pressure drop of the diffusers in saline water as well as in saline activated sludge was not affected by salt concentration. Nevertheless, it increases during operation in saline activated sludge for both diffusers membrane designs, as is to be expected when aerating activated sludge. The increment results from biofilm formation on the surface and in the slits of membrane diffusers. By brief increase of airflow rate, biofilm could be removed, and pressure drop reduced temporary. The difference in pressure drop between both diffuser membrane designs was about 2 kPa.

Based on the saline water as well as saline activated sludge experiments, it can be proposed that aeration devices used at elevated salt concentration should be designed with smaller slit lengths and higher slit density. Both enhance the formation of small primary bubbles. In coalescence inhibited systems, the smaller bubbles offer a larger interfacial area, which results in an increasing oxygen transfer.

6 Outlook

Within this work, multiple factors affecting oxygen transfer at elevated salt concentrations were assessed. However, this study has raised several questions. It is still not known, why airflow rate has no effect on f_S when using tube diffusers. To clarify this question, the coalescence behavior of tube diffusers should be focused on detail in further experiments. Measuring bubble size in the bubble swarm is difficult but analyzing high resolution images or videos taken with a high-speed camera of the ascending bubble swarm could be a first step. Since the results presented suggest that bubbles only coalesce with subsequent bubbles or bubbles from adjacent slits the length of tube diffusers should not have any influence. Therefore, using shortened tube diffusers could easily enable lab-scale experiments. Furthermore, bubble formation at non-horizontally oriented openings or slits is still largely unresearched. Here, laboratory tests with single bubbles could already give first hints and be a good start to further experiments of rising complexity. In addition, to better compare the results of tube diffusers with those of plates and discs, further oxygen transfer tests at elevated salt concentration should be conducted with other membrane designs and higher $q_{A,dS}$ values.

Within the present experiments used plate diffusers had lower slit density than the used tubes and disc diffusers, which results in very high $q_{A,dS}$ values. Since $q_{A,dS}$ has a significant influence on bubble formation and to confirm the present results, the tests with plate diffusers should be repeated with other membrane designs.

The results of oxygen transfer tests in saline activated sludge suggest that substances produced by the microorganisms as a result of salt shocks lead to an inhibition of the oxygen transfer. Firstly, these substances could be identified in lab-scale experiments. Secondly, oxygen transfer tests could be used to check whether these substances inhibit oxygen transfer. In addition, further long-term tests with diffusers with different membrane designs should be carried out in saline activated sludge to investigate the ageing of diffusers with different membrane designs and the associated increase in pressure drop.

Collection of all references

ASCE/EWRI (2006): Measurement of Oxygen Transfer in Clean Water (ASCE/EWRI 2-06). Reston, USA, American Society of Civil Engineers.

ASCE/EWRI (2018): Standard Guidelines for In-Process Oxygen Transfer Testing (ASCE/EWRI 18-18). Reston, USA, American Society of Civil Engineers.

Akita, K.; Yoshida, F. (1974): Bubble size, interfacial area, and liquid-phase mass transfer coefficient in bubble columns. In: *Industrial & Engineering Chemistry Process Design and Development* 13 (1), 84–91.

Amaral, A.; Bellandi, G.; Rehman, U.; Neves, R.; Amerlinck, Y.; Nopens, I. (2018): Towards improved accuracy in modeling aeration efficiency through understanding bubble size distribution dynamics. In: *Water research*, 131, 346–355.

American Public Health Association; American Water Works Association; Water Environment Federation (2005): Standard methods for the examination of water & wastewater, 21st Washington, DC, USA, American Public Health Association (APHA).

Bals, A. (2002): Grundlagen der Blasenbildung an Einzelporen und Lochplatten (Basics of bubble formation on single pores and perforated plates). In: *Chemie Ingenieur Technik*, 74 (3), 337–344.

Bassin, J.-P.; Kleerebezem, R.; Muyzer, G.; Rosado, A.-S.; van Loosdrecht, M. C. M.; Dezotti, M. (2012): Effect of different salt adaptation strategies on the microbial diversity, activity, and settling of nitrifying sludge in sequencing batch reactors. In: *Applied microbiology and biotechnology*, 93 (3), 1281–1294.

Baquero-Rodríguez, G.A.; Lara-Borrero, J.A.; Nolasco, D.; Rosso, D. A (2018): Critical Review of the Factors Affecting Modeling Oxygen Transfer by Fine-Pore Diffusers in Activated Sludge. In: *Water environment research*, 90 (5), 431–441.

Bauer, S.; Dell, A.; Behnisch, J.; Linke, H.J.; Wagner, M. (2020): Sustainability requirements of implementing water-reuse concepts for new industrial park developments in water-stressed regions. In: *Journal of Water Reuse and Desalination*, 10 (4), 490–499.

Baz-Rodríguez, S. A.; Botello-Álvarez, J. E.; Estrada-Baltazar, A.; Vilchiz-Bravo, L. E.; Padilla-Medina, J. A.; Miranda-López, R. (2014): Effect of electrolytes in aqueous solutions on oxygen transfer in gas-liquid bubble columns. In: *Chemical Engineering Research and Design*, 92 (11), 2352–2360.

Behnisch, J.; Ganzauge, A.; Sander, S.; Herrling, M.P.; Wagner, M. (2018): Improving aeration systems in saline water: measurement of local bubble size and volumetric mass transfer coefficient of conventional membrane diffusers. In: *Water Science and Technology*, 78(4), 860-867.

Behnisch, J.; Dell, A.; Linke, H.-J.; Wagner, M.; Bauer, S. (2020a): Pharmaindustrie (Pharmaceutical industry). In: *Taschenbuch der Industrieabwasserreinigung*. Rosenwinkel, K.-H.; Austermann-Haun, U.; Köster, S.; Beier, M. (*eds*). Essen, Germany, Vulkan-Verlag, 544 – 555.

Behnisch, J.; Schwarz, M.; Wagner, M. (2020b): Three decades of oxygen transfer tests in clean water in a pilot scale test tank with fine-bubble diffusers and the resulting conclusions for WWTP operation. In: *Water Practice and Technology*, 15 (4), 910–920.

Behnisch, J.; Schwarz, M.; Trippel, J.; Engelhart, M.; Wagner, M. (2021): Improving aeration systems in saline water (Part II): Effect of different salts and diffuser type on oxygen transfer of fine-bubble aeration systems. In: *Water Science and Technology*, *83 (11)*, 2278–2792.

Behnisch, J.; Schwarz, M.; Trippel, J.; Engelhart, M.; Wagner, M. (2022): Oxygen transfer of fine-bubble aeration in activated sludge treating saline industrial wastewater. In: *Water* 14(12), 1964

Bell, K. Y.; Abel, S. (2011): Optimization of WWTP aeration process upgrades for energy efficiency. In: *Water Practice and Technology*, 6 (2).

Botello-Álvarez, J. E.; Baz-Rodríguez, S. A.; González-García, R.; Estrada-Baltazar, A.; Padilla-Medina, J. A.; González-Alatorre, G.; Navarrete-Bolanos, J. L. (2011): Effect of electrolytes in aqueous solution on bubble size in gas–liquid bubble columns. In: *Industrial & Engineering Chemistry Research*, 50 (21), 12203-12207.

Burton, F. L.; Stensel, H.D.; Tchobanoglous, G. (2014): Wastewater engineering: Treatment and resource recovery. 5. ed. New York, USA: McGraw-Hill.

Busciglio, A., Vella, G., Micale, G., Rizzuti, L. (2008): Analysis of the bubbling behaviour of 2D gas solid fluidized beds: Part I. Digital image analysis technique. In: *Chemical Engineering Journal*, 140 (1), 398-413.

Campos, J.; Mosquera-Corral, A.; Sánchez, M.; Méndez, R.; Lema, J. M. (2002): Nitrification in saline wastewater with high ammonia concentration in an activated sludge unit. In: *Water research*, 36 (10), 2555–2560.

Canova, M.; Pinasseau, A.; Roth, J.; Roudier, S.; Zerger, B. (2018): Best available techniques (BAT) reference document for waste treatment. In: *Industrial Emissions Directive 2010/75/EU (integrated pollution prevention and control)*. European Commission Industrial Emissions Directive, Seville, Spain.

Chern, H.M.; Chou, S.R.; Shang, C.S. (2001): Effects of impurities on oxygen transfer rates in diffused aeration systems. In: *Water Research*, 35 (13), 3041-3048.

Cho, Y.S; Laskowski, J.S (2002): Effect of flotation frothers on bubble size and foam stability. In: *International Journal of Mineral Processing*, 64 (2-3), 69–80.

Craig, V. S.; Henry, C. L. (2010): Specific Ion Effects at the Air-Water Interface: Experimental Studies. In: *Specific ion effects*. Kunz, W. (*ed*). Singapore, World Scientific, 191–214.

Craig, V. S.J.; Ninham, B. W.; Pashley, R. M. (1993): Effect of electrolytes on bubble coalescence. In: *Nature*, 364 (6435), 317–319.

DeMoyer, C. D.; Gulliver, J. S.; Wilhelms, S. C. (2001): Comparison of Submerged Aerator Effectiveness. In: *Lake and Reservoir Management*, 17 (2), 139–152.

Dinçer, A. R.; Kargi, F. (2001): Performance of rotating biological disc system treating saline wastewater. In: *Process Biochemistry*, 36 (8-9), 901–906.

Dinkel, W.; Frechen, F.-B.; Garbowski, M.; Loebelt N. (2019): Mathematischer Modellansatz zur Abschätzung des volumetrischen Stoffübergangskoeffizienten. In: *GWF Wasser, Abwasser*, (5), 61–74.

Drogaris, G.; Weiland, P. (1983): Studies of coalescence of bubble pairs. In: *Chemical Engineering Communications*, 23 (1-3), 11–26.

DWA (2007): Messung der Sauerstoffzufuhr von Belüftungseinrichtungen in Belebungsanlagen in Reinwasser und in Belebtschlamm, DWA-M 209 (Measuring oxygen transfer of aeration systems in activated sludge process in clean water an in activated sludge, Advisory Leaflet DWA-M 209), German Association for Water, Wastewater and Waste (DWA), Hennef, Germany.

DWA (2011): Leitlinien zur Durchführung dynamischer Kostenvergleichsrechnungen – KVR Leitlinien (Dynamic Cost Comparison Calculations for selecting least-cost projects in Water Supply and Wastewater Disposal), 8th, German Association for Water, Wastewater and Waste (DWA), Hennef, Germany.

DWA (2015): Energiecheck und Energieanalyse – Instrumente zur Energieoptimierung von Abwasseranlagen, DWA-A 2016 (Energy check and energy analysis – Instruments for energy optimization of wastewater treatment plants, Worksheet DWA-A 216), German Association for Water, Wastewater and Waste (DWA), Hennef, Germany.

DWA (2017a): Systeme zur Belüftung und Durchmischung von Belebungsanlagen – Teil 1: Planung, Ausschreibung und Ausführung, DWA-M 229-1 (Aeration and Mixing in Activated Sludge Plants, Part 1: Planning, Invitation of Tenders and Accomplishment, Advisory Leaflet DWA-M 229-1), German Association for Water, Wastewater and Waste (DWA), Hennef, Germany.

DWA (2017b): System zur Belüftung und Durchmischung von Belebungsanlagen Teil 1: Planung, Ausschreibung und Ausführung, DWA-M 229-2. (Aeration and Mixing in Activated Sludge Plants, Part 2: Planning, tendering and execution, Advisory Leaflet DWA-M 229-2), German Association for Water, Wastewater and Waste (DWA), Hennef, Germany.

DWA (2019): Design of wastewater treatment plants in hot and cold climates. German Association for Water, Wastewater and Waste (DWA), Hennef, Germany.

Eckenfelder, W.W.; Barnhart, E.L. (1961): The effect of organic substances on the transfer of oxygen from air bubbles in water. In: *AIChE Journal*, 7 (4), 631-634.

Engelhart, M.; Wagner, M.; Behnisch, J.; Blach, T.; Schwarz, M. (2020): Abwassertechnik (Wastewater technology). In: *Handbuch für Bauingenieure*. Zilch, K.; Diederichs, C. J.; Beckmann, K. J.; Urban, W.; Gertz, C.; Malkwitz, A.; Moormann, Ch.; Valentin, F. (*eds*). Heidelberg Berlin, Germany, Springer, 1-60.

EN 12255-15, 2003: Wastewater treatment plants - Part 15: Measurement of the oxygen transfer in clean water in aeration tanks of activated sludge plants.

EPA (1989): Design Manual - Fine Pore Aeration Systems. US Environmental Protection Agency, Office of Research and Development, Center for Environmental Research Information.

Ferrer-Polonio, E.; Mendoza-Roca, J. A.; Iborra-Clar, A.; Alonso-Molina, J.L; Pastor-Alcañiz, L. (2015): Comparison of two strategies for the start-up of a biological reactor for the treatment of hypersaline effluents from a table olive packaging industry. In: *Chemical Engineering Journal*, 273, 595–602.

Firouzi, M.; Howes, T.; Nguyen, A. V. (2015): A quantitative review of the transition salt concentration for inhibiting bubble coalescence. In: *Advances in colloid and interface science*, 222, 305–318.

Germain, E.; Nelles, F.; Drews, A.; Pearce, P.; Kraume, M.; Reid, E.; Judd, S.J.; Stephenson, T. (2007): Biomass effects on oxygen transfer in membrane bioreactors. In: *Water research*, 41 (5), 1038–1044.

Gillot, S.; Capela-Marsal, S.; Roustan, M.; Héduit, A. (2005): Predicting oxygen transfer of fine bubble diffused aeration systems – model issued from dimensional analysis. In: *Water Research*, 2005 (39), 1379-1387.

Gillot, S.; Héduit, A. (2008): Prediction of alpha factor values for fine pore aeration systems. In: *Water Science and Technology*, 57 (8), 1265 – 1269.

Gnotke, O. (2005): Experimentelle und theoretische Untersuchungen zur Bestimmung von veränderlichen Blasengrößen und Blasengrößenverteilungen in turbulenten Gas-Flüssigkeits-Strömungen (Experimental and theoretical studies on the determination of variable bubble sizes and bubble size distributions in turbulent gas-liquid flows), Dissertation, Technical University of Darmstadt, Germany.

Grau, R. A.; Laskowski, J. S.; Heiskanen, K. (2005): Effect of frothers on bubble size. In: *International Journal of Mineral Processing*, 76 (4), 225–233.

Günkel-Lange, T. (2013): Sauerstoffzufuhr und α-Werte feinblasiger Belüftungssysteme beim Belebungsverfahren - Abhängigkeiten und Bemessungsempfehlungen (Oxygen transfer and α-values of fine-bubble aeration systems in the activated sludge process – Dependencies and design recommendations), Schriftenreihe IWAR 221, Dissertation, Technical University of Darmstadt, Germany.

Günther, H.-O.; Silem, A.; Beining, S. (2017): Behandlung von Abwasser aus der Rauchgaswäsche von Seeschiffen – Scrubberabwasser (Treatment of wastewater from flue gas scrubbing of seagoing vessels - scrubber wastewater). In: 6. *IndustrieTage Wassertechnik - Tagungsband*, 178–200.

Hasanen, A.; Orivuori, P.; Aittamaa, J. (2006): Measurements of local bubble size distribution from various flexible membrane diffusers. In: *Chemical Engineering and Processing*, 45 (4), 291–302.

He, H.; Chen, Y.; Li, X.; Cheng, Y.; Yang, Ch.; Zeng, G. (2017): Influence of salinity on microorganisms in activated sludge processes: A review. In: *International Biodeterioration & Biodegradation*, 119, 520–527.

Hebrard, G.; Zeng, J.; Loubiere, K. (2009): Effect of surfactants on liquid side mass transfer coefficients: A new insight. In: *Chemical Engineering Journal*, 148 (1), 132-138.

Hendricks, D. W. (2011): Fundamentals of Water Treatment Unit Processes. Physical, Chemical, and Biological, 1st, CRC Press.

Henkel, J. (2010): Oxygen transfer phenomena in activated sludge. Dissertation, Technical University of Darmstadt, Germany.

Henry, Ch. L.; Dalton, C. N.; Scruton, L.; Craig, V. S. (2007): Ion-Specific Coalescence of Bubbles in Mixed Electrolyte Solutions. In: *The Journal of Physical Chemistry C*, 111 (2), 1015–1023.

Higbie, R. (1935): The Rate of Absorption of a Pure Gas Into a Still Liquid During Short Periods of Exposure. In: *Transactions of American Institute of Chemical Engineers*, 31 (2), 365–389.

Huber, T.; Rische, T. (2017): Kreislaufverfahren zur Nutzung NaCl-haltiger Prozessabwässer (Circular process to use industrial waste water streams containing sodium chlorine), Final report, Ref.-No: NKa3-002031, Federal Ministry for the Environment, Nature Conservation, Nuclear Safety and Consumer Protection, Berlin, Germany.

ISO 5814: Water quality - Determination of dissolved oxygen - Electrochemical probe method, International Organization for Standardization, 2012.

ISO 10304-1: Water quality - Determination of dissolved anions by liquid chromatography of ions - Part 1: Determination of bromid, chlorid, fluorid, nitrate, nitrite, phosphate and sulfate, International Organization for Standardization, 2009.

ISO 11885: Water quality - Determination of selected elements by inductively coupled plasma optical emission spectrometry (ICP-OES), International Organization for Standardization, 2009.

Jia, Y.; Wang, S.; Zhang, L.; Wang, X.; Guo, J (2014): Effect of different salinity on sludge bulking by using sequencing batch reactor. In: *Transactions of Chinese Society of Agricultur Engineering*, 29 (19), 112–119.

Jiang, P.; Stenstrom, M.K. (2012): Oxygen Transfer Parameter Estimation: Impact of Methodology. In: *Journal of Environmental Engineering, 138 (2)*, 137–142.

Jolly, M.; Green, S.; Wallis-Lage, C.; Buchanan, A. (2010): Energy saving in activated sludge plants by the use of more efficient fine bubble diffusers. In: *Water and Environment Journal*, 24 (1), 58–64.

Kara, F.; Gurakan, G. C.; Sanin, F. D. (2008): Monovalent Cations and their Influence on activated sludge floc chemistry, structure, and physical characteristics. In: *Biotechnology and Bioengineering*, 100 (2), 231–239.

Kargi, F.; Dincer, A. R. (1997): Biological Treatment of Saline Wastewater by Fed-Batch Operation. In: *Journal of Chemical Technology & Biotechnology: International Research in Process, Environmental AND Clean Technology*, 69 (2), 167–172.

Kayser, R. (1967): Ermittlung der Sauerstoffzufuhr von Abwasserbelüftern unter Betriebsbedingungen (Measuring oxygen transfer of aeration devices under process conditions), Technische Hochschule Braunschweig, Braunschweig.

Krampe, J. (2011): Assessment of diffuser pressure loss on WWTPs in Baden-Württemberg. In: *Water Science and technology*, 62 (12), 3027–3033

Krause, S.; Cornel, P.; Wagner, M. (2003): Comparison of different oxygen transfer testing procedures in full-scale membrane bioreactors. In: *Water Science and Technology*, 47 (12), 169 – 176.

Khannous, L.; Souissi, N.; Ghorbel, B.; Jarboui, R.; Kallel, M.; Nasri, M.; Gharsallah, N. (2003): Treatment of saline wastewaters from marine-products processing factories by activated sludge reactor. In: *Environmental technology*, 24 (10), 1261–1268.

Krampe, J.; Krauth, K. (2003): Oxygen transfer into activated sludge with high MLSS concentrations. In: *Water Science and Technology*, 47 (11), 297-303.

Kumar, R.; Kuloor, N. K. (1970): The formation of bubbles and drops. In: *Advances in chemical engineering*, 8, 255–368.

Lay, W. C. L.; Liu, Y.; Fane, A. G. (2010): Impacts of salinity on the performance of high retention membrane bioreactors for water reclamation: A review. In: *Water research*, 44 (1), 21–40.

Lefebvre, O.; Moletta, R. (2006): Treatment of organic pollution in industrial saline wastewater: A literature review. In: *Water research*, 40 (20), 3671–3682.

Lessard, R. R.; Zieminski, S. A. (1971): Bubble coalescence and gas transfer in aqueous electrolytic solutions. In: *Industrial & Engineering Chemistry Fundamentals*, 10 (2), 260–269.

Leu, S.-Y.; Rosso, D.; Larson, L.E.; Stenstrom, M. K. (2009): Real-Time Aeration Efficiency Monitoring in the Activated Sludge Process and Methods to Reduce Energy Consumption and Operating Costs. In: *Water Environment Research*, 81 (12), 2471–2481.

Linarić, M.; Markić, M.; Sipos, L. (2013): High salinity wastewater treatment. In: *Water Science and Technology,* 68 (6), 1400–1405.

Loock, P. (2009): Veränderung der Leistungsfähigkeit feinblasiger Membranbelüftungselemente unter abwassertechnischen Betriebsbedingungen (Changing performance of fine-bubble aeration diffusers under process conditions), IWAR Schriftenreihe 202, Dissertation, Technical University of Darmstadt, Germany.

Loubière, K.; Hébrard, G. (2003): Bubble formation from a flexible hole submerged in an inviscid liquid. In: *Chemical Engineering Science,* 58 (1), 135–148.

Loubière, K.; Hébrard, G.; Guiraud, P. (2003): *Dynamics of Bubble Growth and Detachment from Rigid and Flexible Orifices*. In: *The Canadian Journal of Chemical Engineering,* 81 (3-4), 499–507.

Marrucci, G.; Nicodemo, L. (1967): Coalescence of gas bubbles in aqueous solutions of inorganic electrolytes. In: *Chemical Engineering Science,* 22 (9), 1257–1265.

McGinnis, D. F.; Little, J. C. (2002). Predicting diffused-bubble oxygen transfer rate using the discrete-bubble model. In: *Water research,* 36 (18), 4627–4635.

Mersmann, Al. (2013): Entstehen und mechanisches Zerstören von Schäumen (Formation and mechanical destruction of foams). In: *VDI-Wärmeatlas*. VDI-Gesellschaft Verfahrenstechnik und Chemieingenieurwesen (*ed*). Berlin Heidelberg, Germany, Springer, 1429-1438.

Metcalf; E.; Tchobanoglous, G.; Abu-Orf, M.; Stensel, H. D.; Bowden, G. et al. (2014): Wastewater engineering – Treatment and Resource recovery, 5th, New York, McGraw-Hill.

Moon, B.-H.; Seo, G.-T.; Lee, T.-S.; Kim, S.-S.; Yoon, C.-H. (2003): Effects of salt concentration on floc characteristics and pollutants removal efficiencies in treatment of seafood wastewater by SBR. In: *Water Science and Technology,* 47 (1), 65–70.

Moussa, M. S.; Sumanasekera, D. U.; Ibrahim, S. H.; Lubberding, H. J.; Hooijmans, C. M.; Gijzen, H. J.; van Loosdrecht, M. C M (2006): Long term effects of salt on activity, population structure and floc characteristics in enriched bacterial cultures of nitrifiers. In: *Water research,* 40 (7), 1377–1388.

Motarjemi, M.; Jameson, G. J. (1978): Mass transfer from very small bubbles - The Optimum Bubble size for aeration. In: *Chemical Engineering Science*, 33 (11), 1415–1423.

Mueller, J. A.; Boyle, W. C.; Pöpel, H. J. (2002): Aeration. Principles and practice, Volume 11, CRC Press.

Ng, H. Y.; Ong, S. L.; Ng, W. J. (2005): Effects of Sodium Chloride on the Performance of a Sequencing Batch Reactor. In: *Journal of Environmental Engineering,* 131 (11), 1557–1564.

Oren, A., (1999): Bioenergetic aspects of halophilism. In: *Microbiology and Molecular Biology Reviews*, 63 (2), 334-348.

Orsat, V.; Vigneault, C.; Raghavan, G. S. V. (1993). Air Diffusers Characterization using a Digitized Image Analysis System. In: *Applied Engineering in Agriculture*, 9 (1), 115–121.

Orvalho, S.; Stanovsky, P.; Ruzicka, M. C. (2021): Bubble coalescence in electrolytes: Effect of bubble approach velocity. In: *Chemical Engineering Journal,* 406, 125926.

Özbek, B.; Gayik, S. (2001): The studies on the oxygen mass transfer coefficient in a bioreactor. In: *Process Biochemistry*, 36 (8), 729–741.

Painmanakul, P.; Loubiere, K.; Hebrard, G.; Buffiere, P. (2004): Study of different membrane spargers used in waste water treatment: characterisation and performance. In: *Chemical Engineering and Processing: Process Intensification,* 43 (11), 1347–1359.

Painmanakul, P.; Loubiere, K.; Hebrard, G.; Mietton-Peuchot, M.; Roustan, M. (2005): Effect of surfactants on liquid-side mass transfer coefficients. In: *Chemical Engineering Science,* 60 (22), 6480-6491.

Panswad, T.; Anan, C. (1999): Impact of high chloride wastewater on an anaerobic/anoxic/aerobic process with and without inoculation of chloride acclimated seeds. In: *Water research,* 33 (5), 1165–1172.

Pöpel, H.J.; Wagner M. (1989): Sauerstoffeintrag und Sauerstoffertrag moderner Belüftungssysteme Teil 1: Druckbelüftung (Oxygen transfer and aeration efficiency of modern aeration systems Part 1: Fine-bubble aeration). In: *Korrespondenz Abwasser,* 5 (89), 453-457.

Polli, M.; Di Stanislao, M., Bagatin, R., Bakr, E. A., Masi, M. (2002): Bubble size distribution in the sparger region of bubble columns. In: *Chemical Engineering Science,* 57 (1), 197-205.

Prince, M. J.; Blanch, H. W. (1990): Transition electrolyte concentrations for bubble coalescence. In: *AIChE journal,* 36 (10), 1485–1499.

Pretorius, C.; Garrido-Baserba, M.; Rosso, D. (2018): Mixing in activated sludge systems. In: *Aeration, Mixing, and Energy: Bubbles and Sparks*. Rosso, D. (*ed*). London, England, IWA Publishing, 73 - 107

Quinn, J. J.; Sovechles, J. M.; Finch, J. A.; Waters, K. E. (2014): Critical coalescence concentration of inorganic salt solutions. In: *Minerals Engineering,* 58, 1–6.

Räbiger, N.; Schlüter, M. (2013): Bildung und Bewegung von Tropfen und Blasen (Formation and movement of dops and bubbles). In: *VDI-Wärmeatlas*. VDI-Gesellschaft Verfahrenstechnik und Chemieingenieurwesen (*ed*). Berlin Heidelberg, Germany, Springer, 1413–1428.

Rene, E. R.; Kim, S. J.; Park, H. S. (2008): Effect of COD/N ratio and salinity on the performance of sequencing batch reactors. In: *Bioresource technology,* 99 (4), 839–846.

Ribeiro Jr., C.P.; Mewes, D. (2007): The influence of electrolytes on gas hold-up and regime transition in bubble columns. In: *Chemical Engineering Science,* 62 (17), 4501–4509.

Rosso, D.; Iranpour, R.; Stenstrom, M. K. (2005): Fifteen Years of Offgas Transfer Efficiency Measurements on Fine-Pore Aeration: Key Role of Sludge Age and Normalized Air Flux. In: *Water Environment Research,* 77 (3), 266 – 273.

Rosso, D.; Huo, D.L.; Stenstrom, M.K. (2006): Effects of interfacial surfactant contamination on bubble gas transfer. In: *Chemical Engineering Science,* 61 (16), 5500-5514.

Rosso, D.; Stenstrom, M. K.; Garrido-Baserba, M. (2018): Aeration fundamentals, performance and monitoring. In: *Aeration, Mixing, and Energy: Bubbles and Sparks*. Rosso, D. (*ed*). London, England, IWA Publishing, 31–66.

Rosso, D.; Garrido-Baserba, M. (2018): Energy intensity of aeration. In: *Aeration, Mixing, and Energy: Bubbles and Sparks*. Rosso, D. (*ed*). London, England, IWA Publishing, 179–210.

Rodriguez-Valera, F.; Ruiz-Berraquero, F.; Ramos-Cormenzana, A. (1981): Characteristics of the heterotrophic bacterial populations in hypersaline environments of different salt concentrations. In: *Microbial Ecology,* 7 (3), 235-243.

Rusydi, A. F. (2018): Correlation between conductivity and total dissolved solid in various type of water: A review. In: *IOP conference series: earth and environmental science*, 118 (1), 012019.

Sardeing, R.; Painmanakul, P.; Hebrard, G. (2006): Effect of surfactants on liquid-side mass transfer coefficients in gas-liquid systems: A first step to modeling. In: *Chemical Engineering Science*, 61 (19), 6249-6260.

Sander, S.; Behnisch, J.; Wagner, M. (2016): Energy, cost and design aspects of coarse-and fine-bubble aeration systems in the MBBR IFAS process. In: *Water Science and Technology*, 75 (4), 890 – 897.

Sander, S.; Behnisch, J.; Wagner, M. (2017): Design of fine-bubble aeration systems for municipal WWTPs with high sea salt concentrations. In: *Water Science and Technology*, 75 (7), 1555–1563.

Sander, S. (2018): Optimierung der Bemessung feinblasiger Druckbelüftungssysteme bei erhöhten Meersalzkonzentrationen (*Optimisation of the design of fine-bubble aeration systems at increased sea salt concentrations*), IWAR Schriftenreihe 243, Dissertation, Technical University of Darmstadt, Germany.

Schraa, O.; Rieger, L.; Alex, J. (2017): Development of a model for activated sludge aeration systems: linking air supply, distribution, and demand. In: *Water Science and Technology*, 75 (3), 552–560.

Schröder, G.; Treiber, H. (2007). Technische Optik (Technical optics). Vogel Buchverlag, Würzburg, Germany.

Sovechles, J. M.; Waters, K. E. (2015): Effect of ionic strength on bubble coalescence in inorganic salt and seawater solutions. In: *AIChE Journal*, 61 (8), 2489–2496.

Schwarz, M.; Behnisch, J.; Trippel, J.; Wagner, M.; Engelhart, M. (2021): Oxygen Transfer in Two-stage Activated Sludge Process. In: *Water*, 13 (14), 1964.

Sheng, G. -P.; Yu, H. -Q.; Li, X. -Y. (2010): Extracellular Polymeric Substances (EPS) of Microbial Aggregates in Biological Wastewater Treatment Systems: A Review. In: *Biotechnology advances*, 28 (6), 882-894.

Statistisches Bundesamt (2018): Volume of wastewater discharged in Germany by economic sector in 2016 (in million cubic meters), German federal statistical agency, last check 09.11.2020.

Steinmetz, H. (1996): Einfluss von Abwasserinhaltsstoffen, Stoffwechselprozessen und Betriebsparametern von Belebungsanlagen auf den Sauerstoffeintrag in Abwasser-Belebtschlamm-Gemische (Impact of wastewater substances, bacterial metabolism and process parameters on oxygen transfer in activated sludge), Dissertation, Universität Kaiserslautern, Germany.

Sterger, O.; Köppke, K.-E. (2013): Abschlussbericht über die Errichtung einer Anlage zur anaeroben Behandlung hypersanliner Abwässer im Gemeinschaftsklärwerk Bitterfeld-Wolfen. (Final report on the construction of a plant for the anaerobic treatment of saline wastewater in the WWTP at Bitterfeld-Wolfen), 20144, Federal Environment Agency Dessau, Germany.

Stephenson, R. V.; Tekippe, R. J.; Coleman, P. F.; Conklin, A.; Crawford, G. V.; Jeyanayagam, S. S.; Johnson, B.R.; Reardon, R.D.; Sprouse, G. (2010): Suspended-Growth Biological Treatment. In: *Design of municipal wastewater treatment plants. Volume 2: Liquid Treatment Processes (5th)*. Krause, T. L.; Pincince, A. B. (*eds*). ASCE manuals and reports on engineering practice, No. 76.

Stolz, A. (2017): Extremophile Mikroorganismen (Extremophilic microorganisms). Berlin Heidelberg, Germany, Springer.

Uygur, A. (2006): Specific nutrient removal rates in saline wastewater treatment using sequencing batch reactor. In: *Process Biochemistry*, 41 (1), 61–66.

Wagner, M. (1991): Einfluss oberflächenaktiver Substanzen auf Stoffaustauschmechanismen und Sauerstoffeintrag (Influence of surfactants on mass- and oxygen transfer). IWAR Schriftenreihe 53, Dissertation, Technical University of Darmstadt, Germany.

Wagner, M. (1992): Die Belüftungstechnik in der Abwasserreinigung (Aeration technique in wastewater treatment). In: *Handbuch Wasserversorgungs- und Abwassertechnik*, 4, 479–501.

Wagner, M.; Pöpel, J. H. (1996): Surface active agents and their influence on oxygen transfer. In: *Water Science and Technology*, 34 (3), 249-256.

Wagner, M.; Pöpel, H. J. (1998): Oxygen Transfer and Aeration Efficiency – Influence of Diffuser Submergence, Diffuser Density and Blower Type. In: *Water Science and Technology*, 38 (3), 1-6.

Wagner, M.; Pöpel, H.J.; Kalte, P. (1998): Pure oxygen desorption method - A new and cost-effective method for the determination of oxygen transfer rates in clean water. In: *Water Science and Technology*, 38 (3), 103–109.

Wagner, J. (2002): Optimierung von Druckbelüftungssystemen in der Abwasserbehandlung (Optimization of fine-bubble aeration systems in wastewater treatment). Institut für Siedlungswasserwirtschaft und Abfalltechnik der Universität Hannover.

Wagner, M.; Loock, P. (2006): Betriebskosteneinsparung durch Optimierung von Belüftungseinrichtungen (Reducing operating costs through optimization of aeration system). In: *Conference documents - 78. Darmstädter Seminar - Abwassertechnik*, IWAR Schriftenreihe 172, Darmstadt, Germany.

Wagner, M.; Sander, S.; Günkel. T. (2011): Spannungsfeld Belüftung und Energie - eine Übersicht (Aeration and Energy – an overview). In: *Conference documents - 3. Infotag Abwassertechnik*, IWAR Schriftenreihe 172, Darmstadt, Germany.

Wagner, M.; Stenstrom, M. K. (2014): Aeration and mixing. In: *Activated Sludge - 100 Years and Counting*. Jenkins, D.; Wanner, J. (*eds*). London, England, IWA Publishing, 131–150.

Wang, J.-L.; Zhan, X.-M.; Feng; Y.-Ch.; Qian, Y. (2005): Effect of Salinity Variations on the Performance of Activated Sludge System. In: *Biomedical and Environmental Sciences*, 18 (1), 5–8.

Wang, R.; Zheng, P.; Ding, A-Q.; Zhang, M.; Ghulam, A.; Yang, Ch.; Zhao, H.-P. (2016): Effects of inorganic salts on denitrifying granular sludge: The acute toxicity and working mechanisms. In: *Bioresource technology*, 204, 65–70.

Woolard, C. R.; Irvine, R. L. (1995): Treatment of hypersaline wastewater in the sequencing batch reactor. In: *Water research*, 29 (4), 1159–1168.

Zlokarnik, M. (1980): Koaleszenzphänomene im System gasförmig/flüssig und deren Einfluss auf den O2-Eintrag bei der biologischen Abwasserreinigung (Coalescence phenomena in the gas/liquid system and their influences on oxygen transfer in biological waste water treatment). In: *Korrespondenz Abwasser, Abfall*, 27 (11), 728-734.

Annex

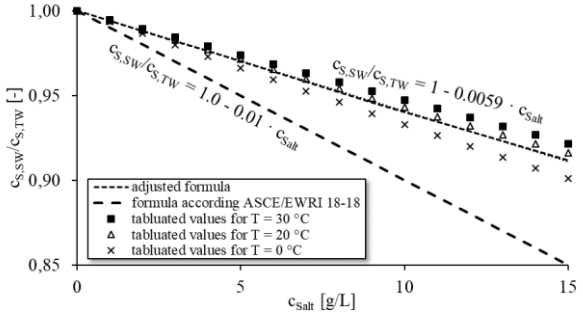

Annex 1 Comparison of calculated oxygen saturation concentration (c_S) for different salt concentrations (c_{Salt}) according to the given equation in ASCE/EWRI 18-18 and tabulated values in ISO 5814 for different water temperatures (T)

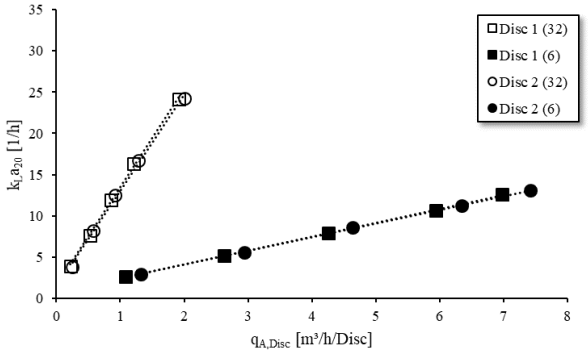

Annex 2 k_La_{20} as a function of $q_{A,Disc}$ for both disc diffusers and diffuser densities

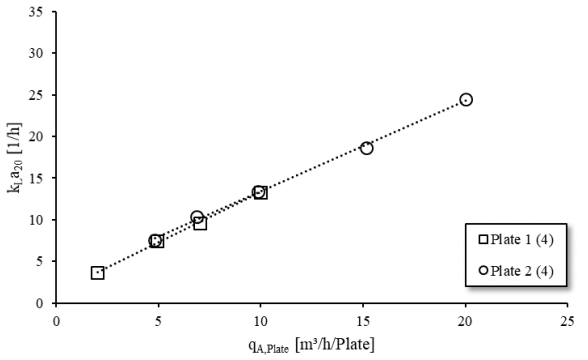

Annex 3 k_La_{20} as a function of $q_{A,Plate}$ for both plate diffusers

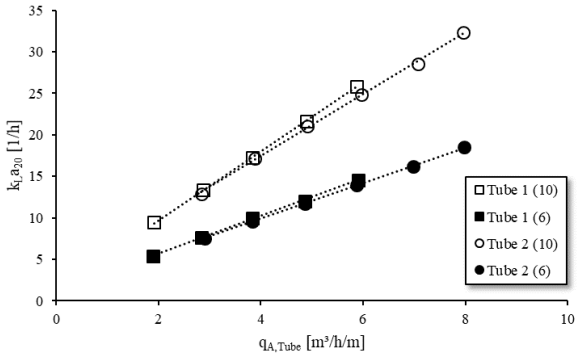

Annex 4 k_La_{20} as a function of $q_{A,Tube}$ for both tube diffusers and diffuser densities

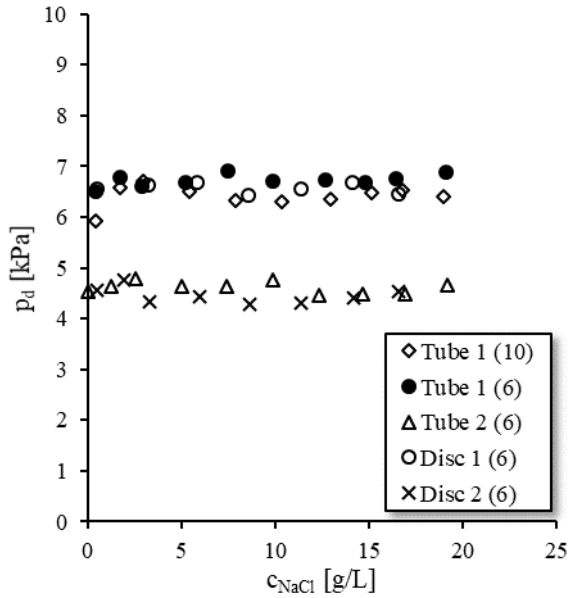

Annex 5 Average pressure drop of diffusers (p_d) as a function of salt concentration (c_{NaCl})